

## Catalysts for continuous homogeneous catalysis

**Citation for published version (APA):**

Ronde, N. J. (2004). *Catalysts for continuous homogeneous catalysis*. [Phd Thesis 1 (Research TU/e / Graduation TU/e), Chemical Engineering and Chemistry]. Technische Universiteit Eindhoven.  
<https://doi.org/10.6100/IR574585>

**DOI:**

[10.6100/IR574585](https://doi.org/10.6100/IR574585)

**Document status and date:**

Published: 01/01/2004

**Document Version:**

Publisher's PDF, also known as Version of Record (includes final page, issue and volume numbers)

**Please check the document version of this publication:**

- A submitted manuscript is the version of the article upon submission and before peer-review. There can be important differences between the submitted version and the official published version of record. People interested in the research are advised to contact the author for the final version of the publication, or visit the DOI to the publisher's website.
- The final author version and the galley proof are versions of the publication after peer review.
- The final published version features the final layout of the paper including the volume, issue and page numbers.

[Link to publication](#)

**General rights**

Copyright and moral rights for the publications made accessible in the public portal are retained by the authors and/or other copyright owners and it is a condition of accessing publications that users recognise and abide by the legal requirements associated with these rights.

- Users may download and print one copy of any publication from the public portal for the purpose of private study or research.
- You may not further distribute the material or use it for any profit-making activity or commercial gain
- You may freely distribute the URL identifying the publication in the public portal.

If the publication is distributed under the terms of Article 25fa of the Dutch Copyright Act, indicated by the "Taverne" license above, please follow below link for the End User Agreement:

[www.tue.nl/taverne](http://www.tue.nl/taverne)

**Take down policy**

If you believe that this document breaches copyright please contact us at:

[openaccess@tue.nl](mailto:openaccess@tue.nl)

providing details and we will investigate your claim.

# Catalysts for Continuous Homogeneous Catalysis

PROEFSCHRIFT

ter verkrijging van de graad van doctor aan de Technische  
Universiteit Eindhoven, op gezag van de Rector Magnificus,  
prof.dr. R.A. van Santen, voor een commissie aangewezen  
door het College voor Promoties in het openbaar te verdedigen  
op woensdag 21 april 2004 om 16.00 uur

door

Niek Johannes Ronde

geboren te Harderwijk

Dit proefschrift is goedgekeurd door de promotoren:

prof.dr. D. Vogt

en

prof.dr. G. van Koten

Copromotor:

dr. C. Müller

CIP-DATA LIBRARY TECHNISCHE UNIVERSITEIT EINDHOVEN

Ronde, Niek J.

Catalysts for Continuous Homogeneous Catalysis / by Niek J. Ronde. – Eindhoven:

Technische Universiteit Eindhoven, 2004

Proefschrift. – ISBN 90-386-2945-1

NUR 913

Subject headings: homogeneous catalysis / organometallic chemistry / hydroformylation /  
allylic substitution / membrane reactors / nanofiltration

Trefwoorden: homogene katalyse / organometaalchemie / hydroformylering / allylische  
substitutie / membraanreactoren / nanofiltratie

Omslag: Sneeuwkristal, Mineralien - und Fossilienverein Basel

<http://www.mineralien-basel.ch/schneekristalle.htm>

Ontwerp en vormgeving door Casper van Tilburg, tel. 06-41177459

Druk: *Universiteitsdrukkerij*, Technische Universiteit Eindhoven

# Table of Contents

|                         |  |            |
|-------------------------|--|------------|
| <i>Chapter 1</i>        | <b>General Introduction</b>  | <b>1</b>   |
|                         | 1.1 Introduction   |            |
|                         | 1.2 Reactors   |            |
|                         | 1.3 Membranes  |            |
|                         | 1.4 Dendrimer Supported Catalysts  |            |
|                         | 1.5 Dendritic Effects  |            |
|                         | 1.6 Unmodified or Non-dendritic Catalysts  |            |
|                         | 1.7 Aim and Scope of this Thesis   |            |
|                         | 1.8 References and Notes   |            |
| <i>Chapter 2</i>        | <b>Pincer Ligand Coupling via Nucleophilic Substitution</b>                        | <b>35</b>  |
|                         | 2.1 Introduction   |            |
|                         | 2.2 Results and Discussion   |            |
|                         | 2.3 Conclusions  |            |
|                         | 2.4 Experimental   |            |
|                         | 2.5 References and Notes   |            |
| <i>Chapter 3</i>        | <b>The Kinetics of the Allylic Amination Reaction</b>                              | <b>59</b>  |
|                         | 3.1 Introduction   |            |
|                         | 3.2 Results and Discussion   |            |
|                         | 3.3 Conclusions  |            |
|                         | 3.4 Experimental   |            |
|                         | 3.5 References and Notes   |            |
| <i>Chapter 4</i>        | <b>Continuous Allylic Substitution Reactions</b>                                   | <b>71</b>  |
|                         | 4.1 Introduction   |            |
|                         | 4.2 Results and Discussion   |            |
|                         | 4.3 Conclusions  |            |
|                         | 4.4 Experimental   |            |
|                         | 4.5 References and Notes   |            |
| <i>Chapter 5</i>        | <b>Immobilization of Diphosphine Ligands via Amine Coupling</b>                    | <b>87</b>  |
|                         | 5.1 Introduction   |            |
|                         | 5.2 Results and Discussion   |            |
|                         | 5.3 Conclusions  |            |
|                         | 5.4 Experimental   |            |
|                         | 5.5 References and Notes   |            |
| <i>Chapter 6</i>        | <b>Ligand Immobilization by Suzuki Coupling and Ullmann Diaryl Ether Synthesis</b> | <b>121</b> |
|                         | 6.1 Introduction   |            |
|                         | 6.2 Results and Discussion   |            |
|                         | 6.3 Conclusions  |            |
|                         | 6.4 Experimental   |            |
|                         | 6.5 References and Notes   |            |
| <i>Summary</i>          |  | <b>139</b> |
| <i>Samenvatting</i>     |  | <b>141</b> |
| <i>Dankwoord</i>        |  | <b>143</b> |
| <i>Curriculum Vitae</i> |  | <b>145</b> |



# 1

## General Introduction

### Abstract

---

In this chapter, a general introduction in the field of continuous homogeneous catalysis is given. Different types of reactors are discussed followed by an overview of commercially available nanofiltration membranes. Dendritic catalysts applied in homogeneous catalysis are discussed subsequently together with unmodified or non-dendritic catalysts.

---

## 1.1 Introduction

The selectivity and activity of homogeneous catalysts under mild reaction conditions is unbeaten by their heterogeneous counterparts. Unfortunately, the problem of separating the single-site-catalysts from the reaction media is still an important drawback which blocks large scale applications in industry. Only a few processes are applied nowadays in industry, such as the production of adiponitrile by Dupont, acetic acid by Monsanto and butanal by Celanese (former Ruhr Chemie).<sup>1</sup> In each case an individual solution was developed to solve the problem of catalyst separation and recovery. A general toolbox for this has to be filled. In Table 1, the advantages and disadvantages of homogeneous versus heterogeneous catalysis are shown. In this way the major problem of homogeneous catalysis becomes obvious.

**Table 1:** Homogeneous versus heterogeneous catalysis.

|                      | Homogeneous | Heterogeneous |
|----------------------|-------------|---------------|
| Activity             | +++         | -             |
| Selectivity          | +++         | +             |
| Catalyst Description | ++          | -             |
| Catalyst Recycling   | -           | +++           |
| TON                  | +           | +++           |
| Quantity of Catalyst | ++          | +++           |

A number of potential methods for homogeneous catalyst separation and recovery have been or are presently being developed, each with its own set of advantages and disadvantages.<sup>2,3</sup>

- two-phase catalysis
  - thermo-regulated two-phase
  - micellar two-phase
- heterogenization on inorganic or organic supports
- classical separation methods
  - precipitation
  - extraction
  - distillation
- supported liquid phase
- soluble supports
  - ultra- or nanofiltration

The separation of homogeneous catalysts by means of advanced filtration techniques (ultra- or nanofiltration) offers several advantages:

- the catalyst remains homogeneous
  - no to little mass-transfer limitations
  - high activity
- low energy consumption of the separation step
- simultaneous catalyst and product separation
- potential for continuous homogeneous catalysis

A prerequisite for the application of filtration methods is a significant difference in size of the catalyst and the reactants / products. Molecular enlargement, binding the homogeneous catalyst to soluble supports, is the method of choice. These supports can be dendrimers, hyper-branched polymers or even simple polymers, giving the opportunity to tailor the support according to the given process.

Abovementioned methods will be discussed in this chapter. A number of filtration and reactor units that have been used in published work will be described and an overview of the different membrane materials will be given. As generally catalytic reactions deal with organic substrates and are usually carried out in an organic solvent, the membranes have to be solvent resistant. Thermal stability can also be an issue depending on the process conditions.

## **1.2 Reactors**

All experimental setups described in literature for the separation of homogeneous catalysts by membrane filtration technology can be divided into two general classes: Dead-end filtration and cross-flow filtration. In the first type of units the product flow is perpendicular to the surface of the membrane, while the flow in the case of cross-flow-filtration is parallel to the membrane surface (see Figure 1).



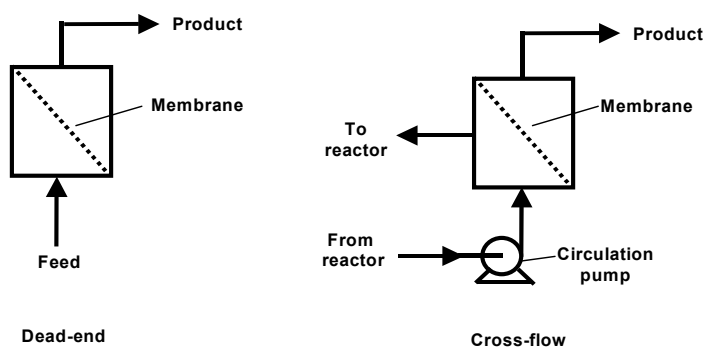


**Figure 1:** Principles of dead-end and cross-flow filtration

The dead-end setup is by far the easiest apparatus both in construction and use, reactor and separation unit can be combined and only one pump is needed to pump in the feed. A cross-flow setup, on the other hand, needs a separation unit next to the actual reactor and an additional pump to provide a rapid circulation across the membrane. The major disadvantage of the dead-end filtration is the possibility of concentration polarization, which is defined as an accumulation of retained material on the feed side of the membrane. This effect causes non-optimal membrane performance since losses through membrane defects, which are of course always present, will be amplified by a high surface concentration. In extreme cases concentration polarization can also lead to precipitation of material and membrane fouling. A membrane installed in a cross-flow setup, preferably applied with a turbulent flow, will suffer much less from this phenomenon because of the parallel flow along the membrane. In the following paragraphs, different types of reactors that have been reported in literature are discussed.

### 1.2.1 Dead-end Setups

The separation of homogeneous catalysts by means of membrane filtration has been pioneered by Wandrey and Kragl. Based on the enzyme-membrane-reactor (EMR),<sup>4,5</sup> that Wandrey developed and Degussa nowadays applies for the production of amino acids, they started to use polymer-bound ligands for homogeneous catalysis in a chemical membrane reactor (CMR).<sup>6</sup> For large enzymes, concentration polarization is less an issue, as the dimension of an enzyme is well above the pore-size of a nanofiltration membrane.

In collaboration with the Wandrey group, Vogt *et al.* developed a dead-end filtration reactor for application at high pressures (Figure 2). It was first used for the hydrovinylation of styrene.<sup>7,8</sup> In this reaction, ethylene is used as a solution in dichloromethane which is prepared separately in a stainless steel container (substrate solution 1). Using a second HPLC pump, styrene dissolved in dichloromethane was pumped into the reactor. The catalyst solution was introduced via an HPLC injection valve equipped with a loop of 2 mL. The products and unreacted compounds cross the membrane and leave the reactor on top where the pressure is regulated using a backpressure regulator (BPR). Details about the reaction can be found in paragraph 1.4.3. This dead-end reactor has also been used for hydrogenation reactions using polymer-stabilized Pd-nanoparticles, applying a H<sub>2</sub> solution.<sup>9</sup> This example clearly shows the limitations of the setup, as an internal gas phase is not permitted. The reactor is now used for the continuous allylic substitution reactions discussed in Chapter 4 of this thesis.

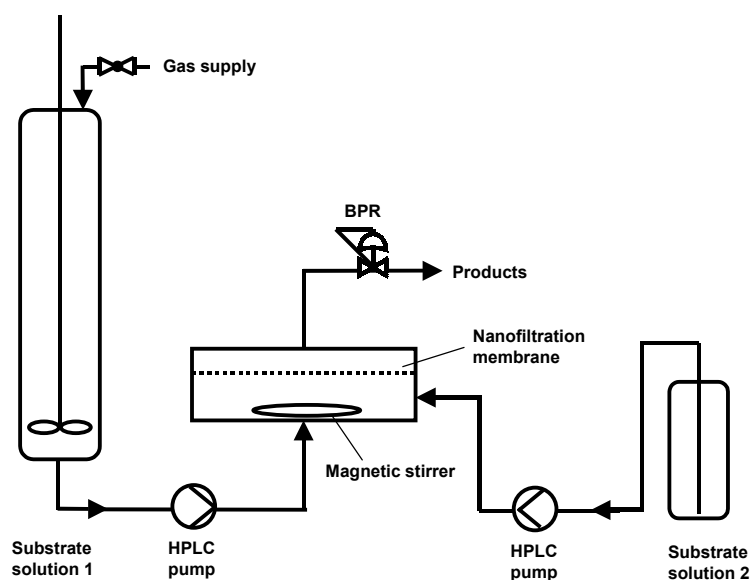


Figure 2: Dead-end reactor of Vogt *et al.*

A similar reactor setup was used by Keurentjes *et al.*<sup>10,11</sup> A Wilkinson catalyst with fluorinated ligands was applied in the hydrogenation of 1-butene in supercritical carbon dioxide. Tubular microporous silica membranes (ECN, Petten, The Netherlands) were used. The process started with the preformation of the catalyst, after which the reactor was pressurized up to 20 MPa. Substrate and hydrogen were fed continuously into the reactor. A trans membrane pressure was created by opening a needle valve on the permeate side, which started the continuous process (Figure 3). The process will be discussed in detail in paragraph 1.6.1.

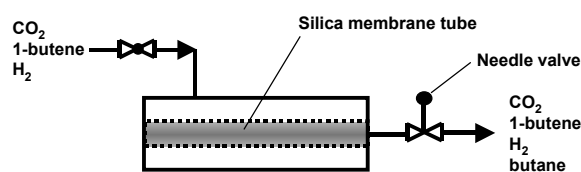


Figure 3: Dead-end reactor of Keurentjes *et al.*

Using unmodified Ru-BINAP and Rh-Et-DUPHOS catalysts Jacobs *et al.* performed hydrogenation reactions of dimethylitaconate (DMI) and methyl-2-acetamidoacrylate (MAA), respectively<sup>43,12</sup>. The continuous hydrogenation reactions were performed in a stirred 100 mL autoclave containing a MPF-60 membrane at the bottom, which also acts as a dead-end membrane reactor. The hydrogenation reactions will be discussed in paragraph 1.6.1.

Commercial dead-end filtration cells are available from Millipore<sup>13</sup> suitable for ultrafiltration (e.g. model 8003 and 8010) and from Schleicher & Schuell<sup>14</sup> applicable in ultra- and nanofiltration region.



Figure 4: High-Output Stirred Cell from Millipore.

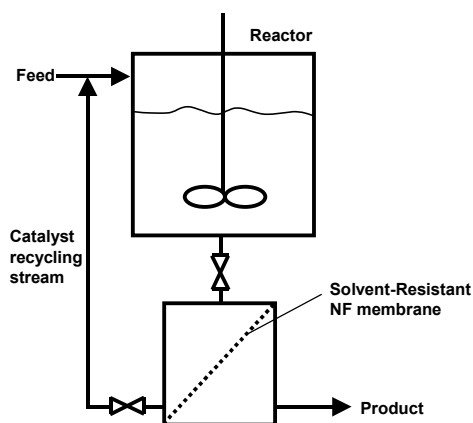


Figure 5: ULTRAN® - MaxiFlex from Schleicher & Schuell.

## 1.2.2 Cross-flow Reactors

A coupled reactor-separation system (Figure 4) was used by Livingston *et al.* in which they were able to perform a Heck reaction and to recycle the catalyst for 10 times using a semi batch method.<sup>15,16</sup> To prevent degradation of the membrane by the reaction mixture, the actual catalysis was performed in a separated stainless steel reactor. When the conversion reached more than 95%, the reactor was cooled to room temperature and the reaction mixture was

pumped through the solvent resistant nanofiltration membrane (SRNF) cell, where it was filtered until 85% of the initial volume had penetrated. The retained catalyst-rich solution was then transferred back into the reactor and diluted with fresh reactant solution, before a new catalysis cycle was performed (Figure 4). STARMEM membranes were used as well as Koch MPF-60 membranes (discussed in paragraph 1.3.2). The STARMEM membranes deteriorated in THF and were replaced after each cycle whereas the Koch membranes showed long-term stability.



**Figure 4:** Cross-flow reactor described Livingston *et al.*

A special type of cross-flow reactor was developed in the laboratories of Vogt (TU Eindhoven, The Netherlands) to handle continuous gas / liquid reactions. The challenge in the reactor design was to combine efficient gas-liquid mixing, liquid level control in the reactor, turbulent flow across the membrane, and efficient gas-liquid separation to avoid gas contacting the membrane, which would lead to a shunt of gas. The total internal volume should not exceed ca. 400 mL. The problems were solved by a combination of an IR level control, steering the feed pump and special geometric arrangements of sieves and using a level indicator controlling the feed pump (Figure 5). Furthermore ceramic membrane tubes are used to handle higher temperatures and to have less solvent influences.

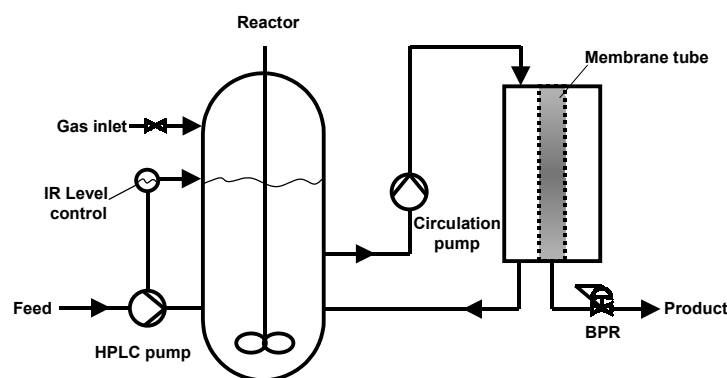


Figure 5: Cross-flow reactor of Vogt *et al.*

### 1.3 Membranes

In the 1970s the first papers were published combining membranes with reaction engineering. Before, membranes were used for water purification, food and dairy industry. Since this new application of membranes started, pioneered by Alan Michaels, membrane reactors were used first in combination with enzymes.<sup>4</sup> Later on, when membranes with smaller pores and resistance against organic solvents became available, membrane technology was also applied in homogeneous catalysis.<sup>17,18</sup> In following part, the different types of membrane filtration will be discussed. Furthermore, the advantages and disadvantages of the different materials of membranes will be explained. Finally an overview of the membranes used in literature will be given.

#### 1.3.1 Classification of Filtrations

In the field of membrane filtration, a distinction is made upon the size of the particles, which are retained by the membrane. That is: micro-, ultra-, nanofiltration and reversed osmosis. In Figure 6, a schematic picture of the classification of membrane processes is shown. The areas of importance for the application of homogeneous catalysts are ultra- and nanofiltration, depicted in gray.

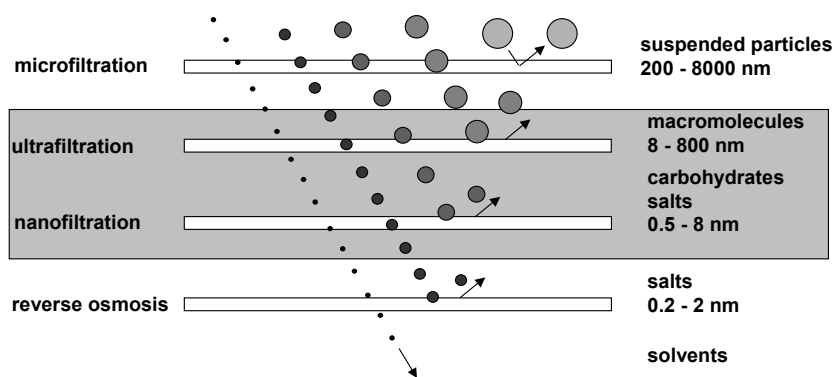


**Figure 6:** Classification of membrane processes.

To find a suitable membrane for a certain application, an important parameter is the molecular weight cut-off (MWCO). The MWCO is defined as the molecular weight at which 90% of the solutes are retained by the membrane. It should be taken into account that the pore size of many ultra- and nanofiltration membranes is greatly influenced by the solvent and by the temperature used under experimental conditions. This particularly concerns the polymeric membranes as will be discussed in the next paragraph.

### 1.3.2 Membrane Materials

There are basically two types of membranes, inorganic (ceramic) membranes and organic (polymer) membranes. Both types of membranes have their advantages and disadvantages as will be discussed in this section. The ideal membrane would have a very narrow pore size distribution, which is not influenced by solvent or temperature changes. Furthermore it should be stable under real reaction conditions, i.e. stable towards organic solvents, aggressive reagents and elevated temperatures. Additionally a sufficient flow under all circumstances and at a low trans membrane pressure is required.

The most widely applied commercial nanofiltration membrane is the MPF series of Koch Int.<sup>19</sup> (Figure 7). The series contains polymeric silicon-derived membranes in the MWCO range of 400-700 Da.<sup>20</sup> The membranes are supplied in a 50% ethanol / water mixture, and should under no circumstances be allowed to dry out. Before use, the membranes must be conditioned with the solvent of choice. Since these membranes are polymer-based, their MWCO is highly depended on the solvent used.<sup>21</sup>



**Figure 7:** A used nanofiltration membrane (Koch MPF-50).

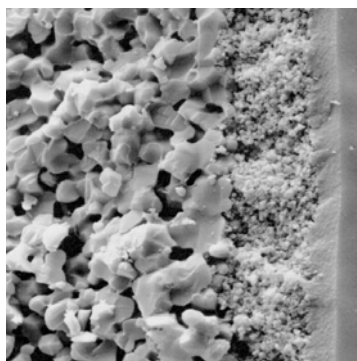


**Figure 8:** TEM picture of a ceramic membrane.

Another nanofiltration membrane often applied is the STARMEM™ series of MET.<sup>22</sup> These membranes have an active layer manufactured from polyimides and are available with MWCO's in the range of 200-400 Da. The membranes are supplied in dry form containing a conditioning agent, which can be easily washed out. In contrast to the MPF membranes, these membranes are not stable in chlorinated solvents or THF, but have higher temperature stability. Livingston *et al.* made a comparison study for these two membrane types together with the Desal-5 (Osmonics<sup>23</sup>) membrane.<sup>48</sup> More details about the polymeric membranes are given in Table 2.

**Table 2:** Commercially available nanofiltration membranes.

| Membrane   | MWCO | Manufacturer | Material        | Solvents  | Max temp (°C) |
|------------|------|--------------|-----------------|---|---------------|
| STARMEM120 | 200  | MET          | polyimide       | Tol, Xyl, EtOAc   | 60            |
| STARMEM220 | 220  | MET          | polyimide       | Tol, Xyl, EtOAc   | 60            |
| STARMEM228 | 280  | MET          | polyimide       | Tol, Xyl, EtOAc, C6   | 60            |
| STARMEM240 | 400  | MET          | polyimide       | Tol, Xyl, EtOAc, C6   | 60            |
| MPF-50     | 700  | Koch         | silicon derived | common org solvents,<br>limited stable in:<br>DMF, NMP, DMA, DMSO | 40            |
| MPF-60     | 400  | Koch         | silicon derived | Common org solvents,<br>limited stable in:<br>DMF, NMP, DMA, DMSO | 40            |
| Desal-5    | 350  | Osmonics     |                 |   | 50            |

Dense membranes are a special type of polymeric membranes. Jacobs *et al.* published on the use of polydimethylsiloxane (PDMS) dense membranes in the hydrogenation of dimethylitaconate and acetophenone using standard homogeneous catalysts (see further paragraph 1.6.1)<sup>44</sup>. The membranes were homemade from a PDMS solution in hexane, which was cross-linked in a vacuum oven at 100 °C. The membranes were able to almost completely retain unmodified Ru-BINAP (Figure 28) dissolved in isopropanol.

The only ceramic membranes of which results are published, are tubular microporous silica membranes provided by ECN (Petten, The Netherlands)<sup>11</sup>. The membrane consists of several support layers of  $\alpha$ - and  $\gamma$ -alumina, and the selective top layer at the outer wall of the tube is made of amorphous silica (Figure 8).<sup>24</sup> The pore size lies between 0.5 and 0.8 nm. The membranes were used in homogeneous catalysis in supercritical carbon dioxide see paragraph 1.6.1). No details about solvent and temperature influences are given but it is expected that these are less important than in the case of polymeric membranes.

In Table 3, a selection of membrane suppliers can be found, but none of them have been applied in catalysis so far. The membranes can be used for separation in the ultra- or nanofiltration range.

**Table 3:** Some ceramic ultra- and nanofiltration membranes.

| Manufacturer          | Pore size (nm) | Material support                 | Material active layer  |
|-----------------------|----------------|----------------------------------|--|
| ECN                   | 0.5 - 0.8      | $\alpha$ - and $\gamma$ -alumina | amorphous silica   |
| HITK <sup>25</sup>    | 30 - 1000      | $\alpha$ -alumina                | Al <sub>2</sub> O <sub>3</sub> , TiO <sub>2</sub> , ZrO <sub>2</sub> |
| Corning <sup>26</sup> | MF and UF      |                                  |  |

#### 1.4 Dendrimer Supported Catalysts

Since the first publication about dendritic structures by Vögtle *et al.*,<sup>27</sup> dendrimers attracted much attention. The synthesis and investigation of their structural properties became a new field in science. The application of dendrimers as support molecules for homogeneous catalysts was first reported by Van Koten *et al.* in 1994.<sup>28</sup> Dendrimers have the advantage of having perfect structures unlike polymeric structures and are therefore preferred in academic



research. Catalytic properties can be investigated using standard high-resolution analytical techniques in solution, whereas heterogeneously supported catalysts require more sophisticated techniques. In the next part the applications of dendritic supports in the recycling of homogeneous catalyst will be discussed.

### 1.4.1 Kharasch Addition Reaction

Building on the experience with enzyme catalysis in membranes reactors, Kragl and Van Koten performed one of the first continuous catalysis experiments using dendrimer supported homogeneous catalysts.<sup>36,37</sup> Zeroth and first generation carbosilane dendrimers were functionalized with 4, respectively 12 NCN pincer ligands (Figure 7). Nickel was introduced by lithiation followed by the reaction with  $\text{NiCl}_2(\text{PET}_3)_2$ . Both dendritic catalysts were tested on retention in a nanofiltration cell equipped with a Koch (former SELRO) MPF-50 membrane using  $\text{CH}_2\text{Cl}_2$  as solvent. The measured retention for zeroth generation catalyst was found to be 97.4%, while the first generation had a retention of 99.75%.

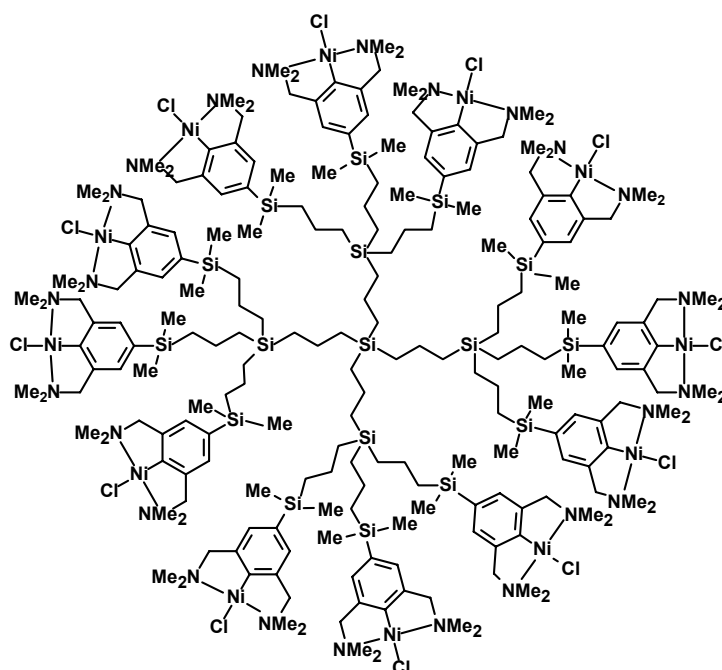


Figure 7:  $G_1$  carbosilane dendrimer with 12 NCN-pincer-Ni groups.

After reaching its maximum productivity (after ca. 8 hours.) the  $[G_1]\text{-Ni}_{12}$  showed a fast deactivation when applied in the continuous catalysis performed in a membrane reactor

(Figure 8). In spite of the non-quantitative retention, this cannot solely explain the observed fast deactivation. A model study revealed that this deactivation process probably takes place by the formation of insoluble Ni(III) species (see paragraph 1.5 for further details).

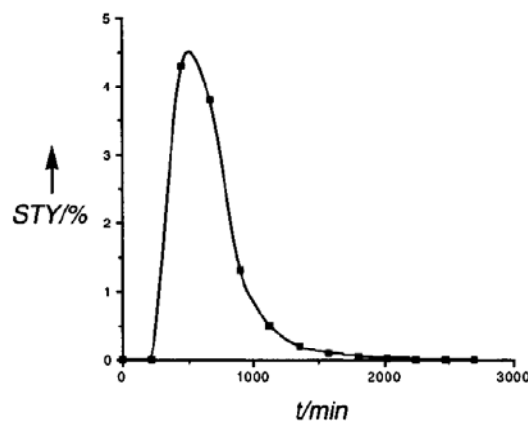


Figure 8: Continuous Kharasch addition.

### 1.4.2 Allylic Substitution Reaction

Another reaction performed in the dead-end reactor discussed before, is the allylic amination of 3-phenyl-2-propenyl-carbonic acid methyl ester with morpholine.<sup>29</sup> First and second generation commercially available DAB-dendrimers were functionalized with diphenylphosphine groups (Figure 9). Two different membranes were used, the Nadir UF-PA-5 (ultrafiltration) and the SELRO MPF-50 (nanofiltration), which gave retentions of 99.2% and 99.9% respectively for the second generation functionalized dendrimers.

The third generation dendritic catalyst was applied in continuous catalysis. The catalyst remained active for more than 100 residence times with a conversion ranging from 100% at the beginning to 80% at the end of the run (Figure 10). Leaching of palladium of only 0.07-0.14% per residence time was found. The authors give the formation of inactive palladium species as another possible reason for the drop in activity, next to the leaching of palladium. NMR data indeed indicate the formation of inactive palladium species such as ligand-PdCl<sub>2</sub> complex, possibly resulting from a decomposition of the complex by a reaction with dichloromethane.

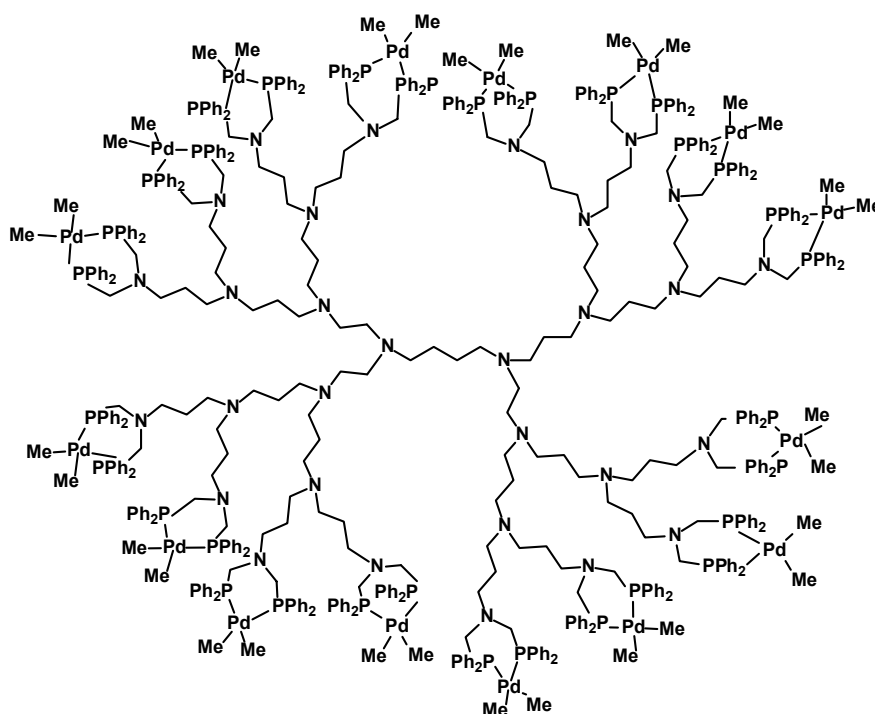


Figure 9: G<sub>2</sub> DAB dendrimer with 32 PPh<sub>2</sub> units.

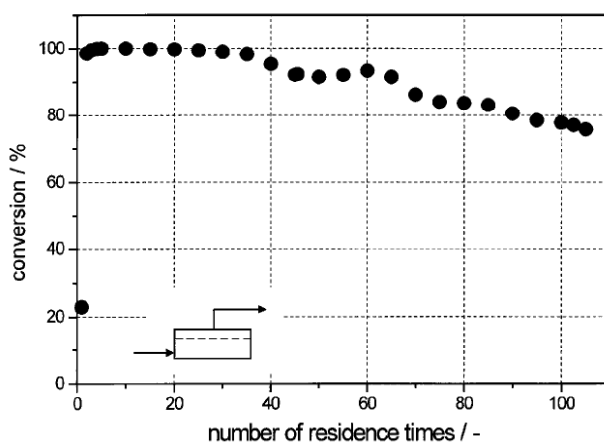
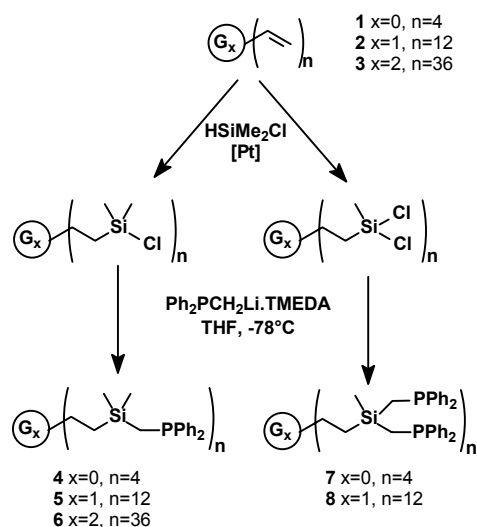


Figure 10: Continuous Allylic Amination.

Van Leeuwen *et al.* used several generations of carbosilane dendrimers with 4, 8, 24, and 36 diphenylphosphine end-groups (Figure 11) for the allylic alkylation reaction of allyl trifluoroacetate with sodium diethyl 2-methylmalonate.<sup>30</sup>



**Figure 11:** Synthesis of phosphine functionalized carbosilanes.

Application of the largest dendritic catalyst **8** (Figure 11) in a continuous process showed activity over 15 exchanged reactor volumes (Figure 12).

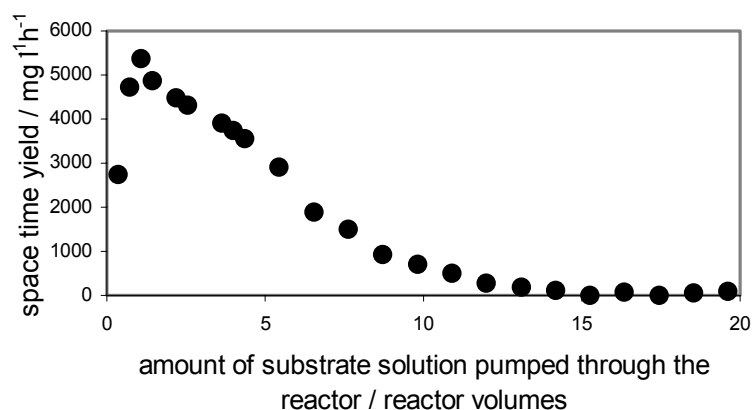


**Figure 12:** Continuous allylic alkylation.

The decrease in activity caused by wash out was calculated to be only 25% (retention of ligand 98.1%). The drop in activity was therefore ascribed to the decomposition of the palladium catalyst. Addition of membrane material to batch catalysis experiments did not change the conversion showing that this was not the cause of decomposition. Further investigations using model compounds showed, that neither the formation of  $PdCl_2$  by a reaction with the solvent, as suggested by Brinkmann *et al.*<sup>29</sup>, caused the observed rapid deactivation. Palladium leaching after formation of  $Pd(0)$  was also excluded by experiments.

The authors concluded therefore that the presence of allyl acetate facilitated the decomposition.

More dendritic ligand systems were synthesized with an ethylene spacer between the terminal silicon atom and the phosphorus atom.<sup>31</sup> This enlarged system showed a higher stability in the continuous allylic amination. During the exchange of 15 reactor volumes, a more or less constant conversion was observed, slowly decreasing from its maximum (~70%) after 5 h, to ~50% after 15 reactor volumes. When the P / Pd ratio was increased from 2 to 4, the activity increased significantly giving almost quantitative conversion after about 7 exchanged reactor volumes which slightly decreased to ca. 80% after 15 reactor volumes (Figure 13). This finding showed that a relative small change in the backbone of dendritic catalysts could increase the stability significantly.

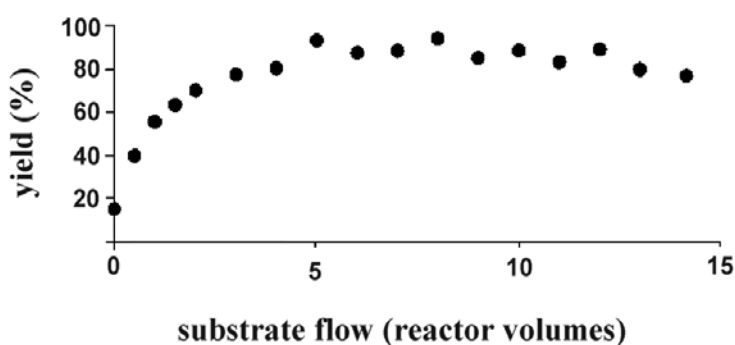


**Figure 13:** Continuous allylic amination with a modified catalyst.

A noncovalently functionalized dendrimer was also applied in a continuous allylic amination reaction.<sup>32</sup> PPI dendrimers functionalized with urea adamantyl groups can act as host molecules for phosphorus ligands equipped with urea acetic groups (Figure 14). The so formed supramolecular complex was reacted with a palladium precursor and used as catalyst in the allylic amination reaction.

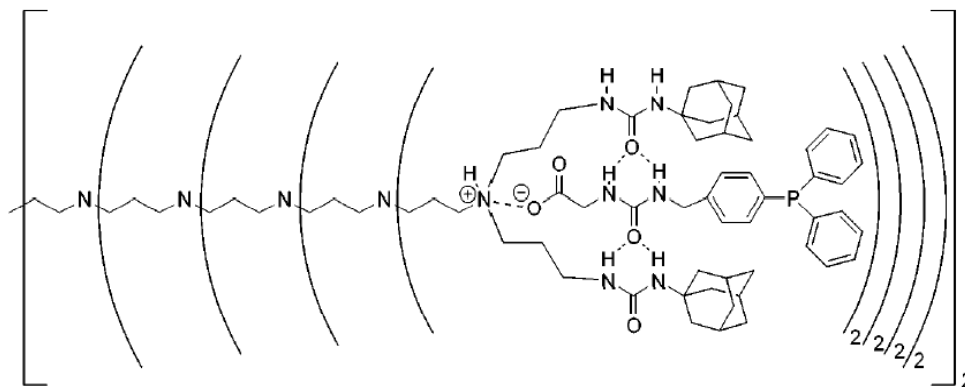


**Figure 14:** G<sub>5</sub> PPI dendrimer with 32 host-guest complexes.

Both the acid and ester were applied in continuous allylic amination. The maximum conversion (ca. 80%) was reached after 1h in both experiments. Using the acid derivative of the guest, a slight drop in activity was observed ((a) in Figure 15), which is probably caused by a slow deactivation of the catalyst and has also been observed for covalently functionalized dendrimers (described above). When using the ester-functionalized guest, the activity dropped more dramatically ((b) in Figure 15). This decrease in activity is caused by lack of retention (99.4% for the acid vs. 97% for the ester) as well as by deactivation.

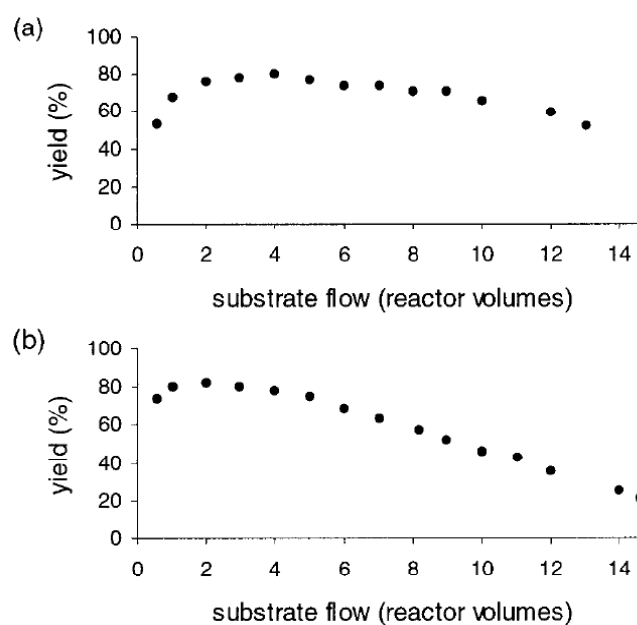


**Figure 15:** Continuous catalysis with non-covalently functionalized dendrimers a) acid-, b) ester-functionalized guest.

### 1.4.3 Hydrovinylation Reaction

In the group of Vogt, zeroth and first generation carbosilane dendrimers were functionalized on the periphery with 4, respectively 12 hemilabile P,O-ligands (Figure 16).<sup>7,8</sup> The allyl palladium complexes of these systems were used as catalysts in the hydrovinylation reaction. At higher conversion, isomerization of the product to internal achiral alkenes occurs. Performing this reaction continuously is therefore interesting since it can combine a high productivity with incomplete conversion suppressing the isomerization reaction.

The retention of the free [G<sub>0</sub>]-ligand system (without palladium) was 85%, the molecular weight of the actual catalyst is much larger (M<sub>w</sub> = 2868 Da versus 1314 Da for the G<sub>0</sub>-system) which should be sufficient for initial experiments. The result of this continuous hydrovinylation is shown in Figure 17.

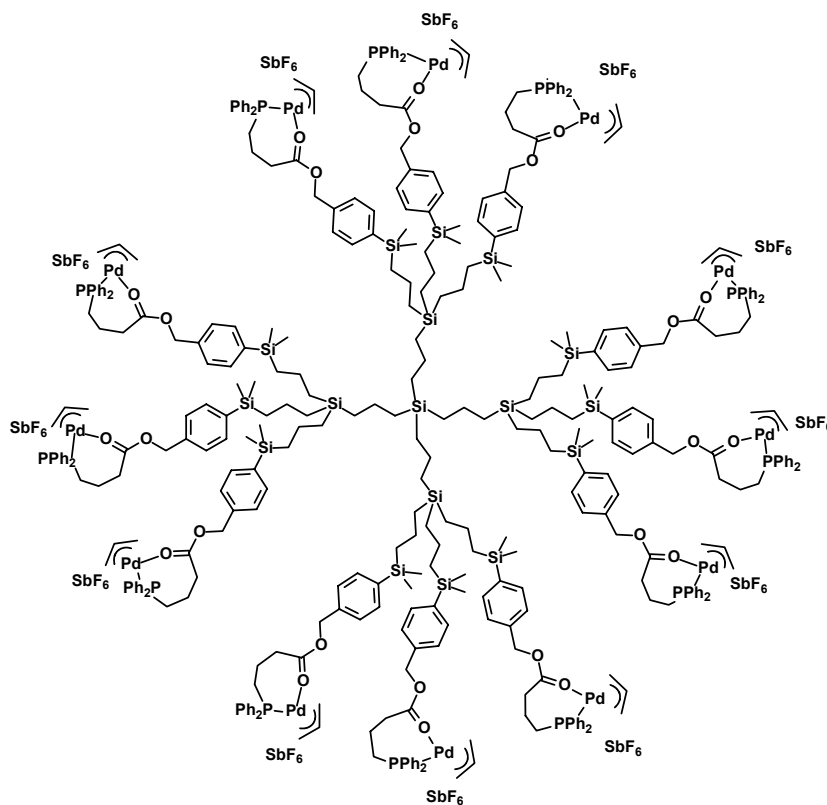


Figure 16: G<sub>1</sub> carbosilane dendrimer with 12 Pd-complexes.

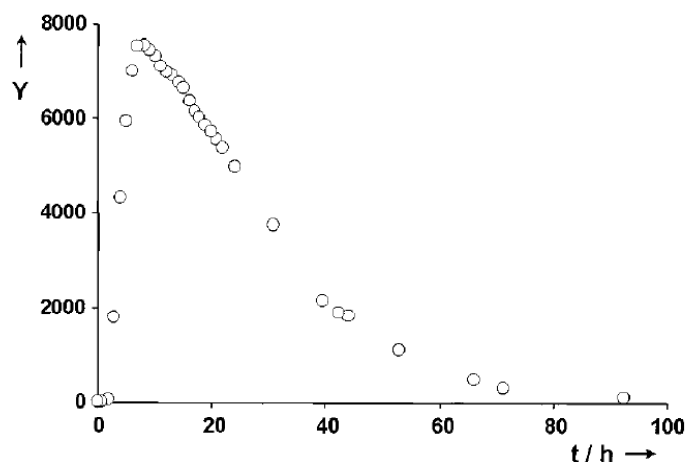


Figure 17: Continuous hydrovinylation experiment.

After an induction period of ca. 9 hours, the maximum productivity was reached. This was followed by a decrease in activity, which cannot solely be explained by the lack of retention. Calculations showed that at least 20% of the catalyst should still remain in the reactor after 80 h. Additionally to this wash-out effect, a deactivation process took place, visible by precipitation of palladium black on the surface of the membrane. Although the catalytic system suffered from deactivation, its selectivity towards 3-phenylbut-1-ene was excellent, which was 98% and 85% for the  $G_0$ - and  $G_1$ -catalyst, respectively.

#### 1.4.4 Hydrogenation Reaction

A set of core-functionalized dendrimers was synthesized by Van Leeuwen *et al.* and one compound was applied in continuous catalysis<sup>42</sup>. The dendritic dppf, Nixantphos and triphenylphosphine derivatives (Figures 18, 26 and 27) were highly active in rhodium-catalyzed hydroformylation and hydrogenation reactions (performed batch-wise). Dendritic effects were observed which are discussed in paragraph 1.5. The dendritic rhodium-dppf complex was applied in a continuous hydrogenation reaction of dimethyl itaconate.



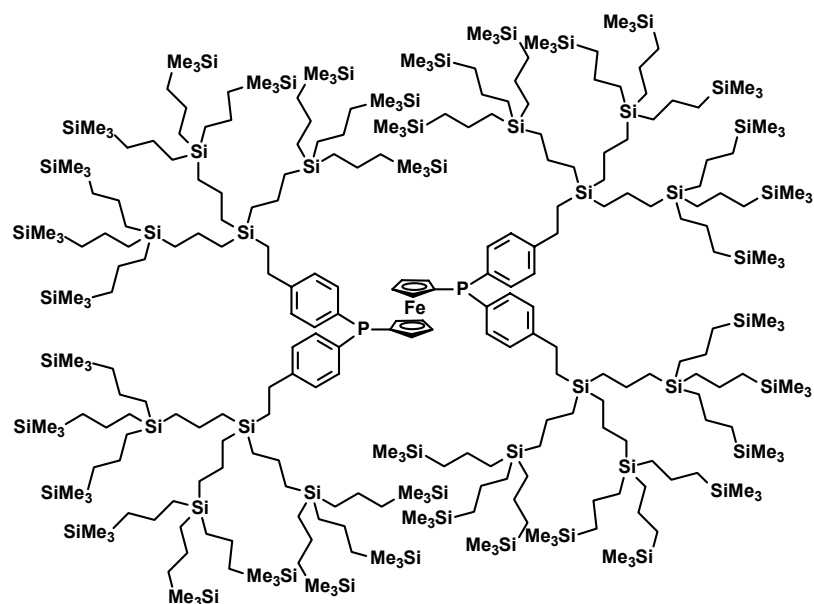


**Figure 18:** Core functionalized dppf-carbosilane dendrimers.

In their experiments, an unsubstituted dppf-complex was compared with analogous dendritic complex (Figure 19). After 35 exchanged reactor volumes the dendritic catalyst still showed a conversion of 77% (maximum: 85% after 10 reactor volumes) while the unsubstituted catalyst deactivated from 70% to 15% at the end of the catalytic run. The drop in activity for both systems can be completely explained by their retention (97% and 99.8% for the unsubstituted and the dendritic complex, respectively). This means, no deactivation of the catalyst occurred during catalysis, which is often the case for palladium catalyzed continuous catalysis.

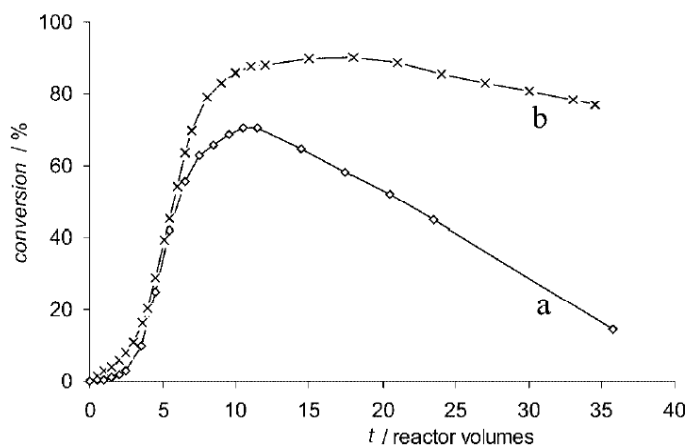


**Figure 19:** Continuous hydrogenation using dppf (a) and dendritic ligand system (b).

The same ligand system was used in the allylic alkylation of allyl trifluoroacetate with sodium diethyl-2-methylmalonate showing a more or less constant conversion over 8 h (20 exchanged reactor volumes). This is in contrast to peripheral functionalized dendrimers (discussed in paragraph 1.4.2), which deactivated at longer reaction times.

## 1.5 Dendritic Effects

Dendrimers are not only unreactive support molecules for homogeneous catalysts, as discussed in the previous paragraph, but they can also have an important influence on the performance in catalysis. The dendrons of a dendrimer can form a microenvironment in which catalysis shows different results compared to classical homogeneous catalysis while peripheral functionalized dendrimers can enforce cooperative interactions between catalytic sites because of their relative proximity. These effects are called “dendritic effects”. Dendritic effects can alter the stability, activity and (enantio)selectivity of the catalyst. In this paragraph, different dendritic effects will be discussed.

Cole-Hamilton *et al.* reported one of the first dendritic effects. Dendrimers based on polyhedral oligomeric silsesquioxane (POSS) cores were synthesized (Figure 20); the dendrons of this dendrimer were functionalized on the periphery with 8, 24 and 72  $\text{PR}_2$  arms, respectively ( $\text{R} = \text{Me}, \text{Et}, \text{hexyl}, \text{Cy}, \text{or Ph}$ ).<sup>33</sup>

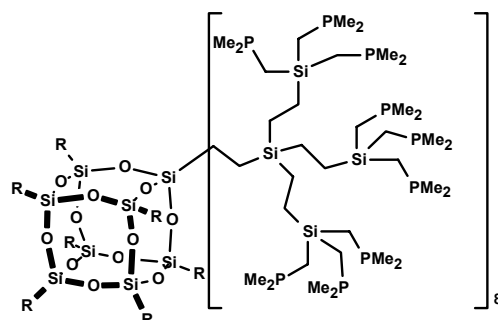


**Figure 20:** POSS core with 72  $\text{PMe}_2$  groups.

The dendritic ligands were tested in the rhodium-catalyzed hydroformylation of alkenes toward alcohols in ethanol as solvent. A remarkable increase in selectivity was observed using

the dendritic ligand systems with  $\text{PEt}_2$  bound to 24 arms. A linear to branched ratio (l:b) of 3.1 was observed in the product distribution while unsubstituted  $\text{PEt}_3$  has a l:b of 2.4 suggesting that perhaps large dendrimer-based ligands exert some control over the reaction. For the  $\text{PMe}_2$  and  $\text{PPh}_2$  derivatized dendrimers, the l:b is similar to that obtained using related monodentate phosphines.

In a later publication<sup>34</sup> a more in-depth study was performed on this dendritic effect using the POSS dendrimers with 16  $\text{PPh}_2$  arms. In the hydroformylation of 1-octene, an l:b of 14:1 was observed while unsubstituted analogues give a l:b of 3-4:1. From this study was concluded that the dendrimers have sufficient steric crowding to make eight-membered ring bidentate coordination favorable and that these rings enhance the selectivity towards the linear aldehydes in hydroformylation reactions.

Jacobsen *et al.* reported enhanced catalytic activity by cooperative effects in the asymmetric ring opening (ARO) of epoxides.<sup>35</sup> Chiral Co-salen complexes (Figure 21) were used which were bound to different generations of commercial PAMAM dendrimers. As a direct consequence of the second-order kinetic dependence on the concentration of the  $[\text{Co}(\text{salen})]$  complex of the hydrolytic kinetic resolution (HKR), reduction of the catalyst loading using unsubstituted catalyst leads to a sharp decrease in overall reaction rate. In order to assess whether intramolecular cooperativity could occur, catalysis was performed with very low (dendritic) catalyst loading (0.027 mol% against 0.5 mol% for the unsubstituted catalyst). Complete kinetic resolution was effected by the dendritic Co complex (98% ee, 50% conversion), while the unsubstituted analogue showed no measurable conversion.

To investigate this dendritic effect, a dimeric model compound was synthesized which mimics the tethered relationship of two catalytic units within a branch of the PAMAM dendrimer. All dendritic catalysts were more active in the HKR than the parent complex. Furthermore, the dendritic catalysts also displayed significant higher activities than the dimeric model compound. The authors proposed that this positive dendritic effect arises from restricted conformation imposed by the dendritic dendrimer structure, thereby creating a bigger effective molarity of  $[\text{Co}(\text{salen})]$  units. Alternatively, the multimeric nature of the dendrimer, may lead to higher order in productive cooperative interactions between the catalytic units.

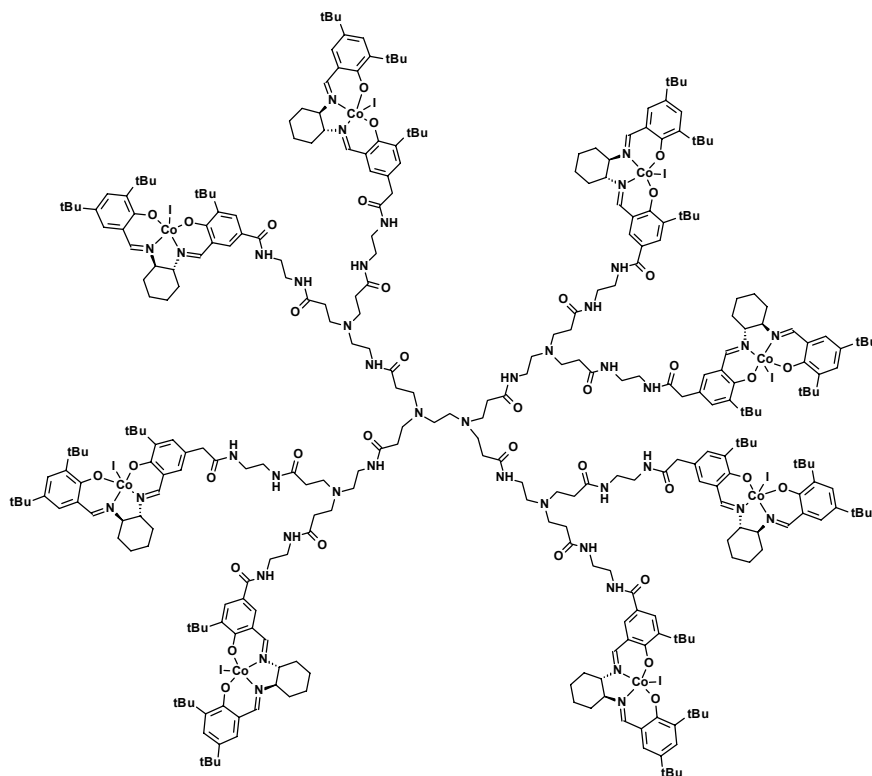


**Figure 21:** G<sub>1</sub> PAMAM dendrimer with 8 [(salen)Co] units.

Van Koten *et al.* reported on a negative dendritic effect in the Kharasch addition reaction.<sup>36,37</sup> A fast deactivation for the carbosilane dendrimer supported NCN pincer catalyst (Figure 23) was observed by comparison with a mononuclear analogue. This deactivation is expected to be caused by irreversible formation of catalytic inactive Ni(III) sites on the periphery of these dendrimers (Figure 22). This hypothesis was supported by results of model studies as well as ESR spectroscopic investigations.

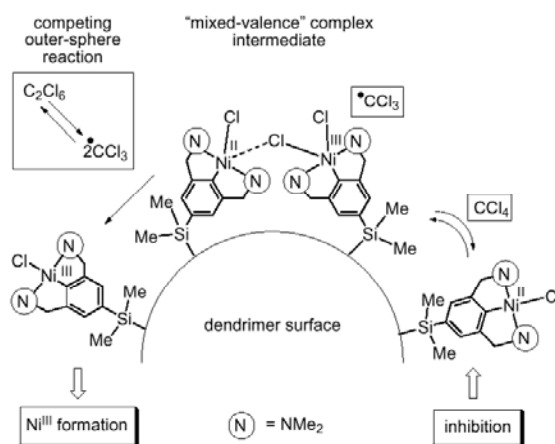


**Figure 22:** Formation of inactive Ni(III) species.

The use of alternative Ni-containing dendrimers in which the distance between the Ni sites was increased, led to significantly improved catalytic efficiencies (Figure 24).

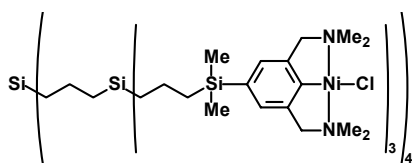


**Figure 23:** Carbosilane dendrimer with 12 Ni-NCN groups.

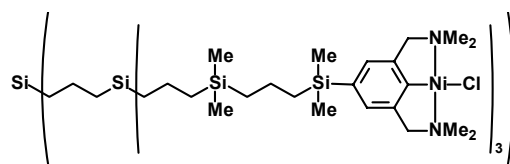


**Figure 24:** G<sub>1</sub> Carbosilane dendrimer with an ethylene bridge.

Zeroth to fourth generation poly(propyleneimine) (PPI) dendrimers functionalized with Pyrphos ligands were synthesized by Gade *et al.*<sup>38</sup> In the asymmetric hydrogenation reaction of acetamidocinnamate the activity of the catalysts decreased when going to higher generations. Also the enantioselectivity decreased from 93 to 88% on going from G<sub>2</sub> to G<sub>4</sub>. Back folding of the attached rhodium complexes is expected to be the cause of the drop in activity for higher generations of dendrimers. It reduces the accessibility of the catalytic centers and at the same time renders their immediate environment less uniform than originally envisaged. It was stated that the use of more rigid dendrimers might partially suppress this negative effect.

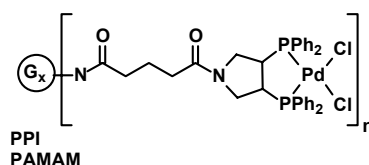


**Figure 25:** PPI and PAMAM dendrimers functionalized with Pyrphos.

In 2003 Gade *et al.* reported on poly(amidoamine) (PAMAM) dendrimers functionalized with Pyrphos ligands (Figure 25).<sup>39</sup> In the palladium catalyzed allylic amination reaction, an increase in enantioselectivity was observed on going from the mononuclear BOC-Pyrphos to the fifth generation PAMAM dendrimers bearing 64 Pyrphos ligands. The results of the PAMAM supported catalysts were compared to PPI supported catalysts. The latter dendrimers had a smaller, but still positive effect on the enantioselectivity when going to higher generations. In contrast to the highly charged cationic Pyrphos-rhodium dendrimers used in the aforementioned asymmetric hydrogenation, the neutral dichloropalladium derivatives showed no significant tendency to aggregate in solution or upon precipitation. This was

concluded from TEM studies and from the determination of the hydrodynamic radii in solution. The aggregation of the cationic dendrimers can contribute to the lower activity and selectivity discussed above.

A slight increase in reactivity and enantioselectivity in Diels-Alder reactions was reported by Chow and Wan.<sup>40</sup> Rigid catalysts bearing three and six (chiral) [1,1'-binaphthalene]-2,2'-diol (Binol) groups were compared to their unsubstituted analogues. The turn-over-frequency (TOF) increased from 2.0 h<sup>-1</sup> for the unsubstituted Binol to 15.0 h<sup>-1</sup> for the catalyst with six Binol groups. The ee increased from 10 to 16%, respectively. The increase in ee was not further investigated.

Simanek *et al.* investigated the structure dependence of the kinetics of thiol-disulfide exchange reactions.<sup>41</sup> In general, the rate of exchange decreased as the size of the dendrimers increased. Dendrimers with disulfides attached near the core undergo exchange more slowly than dendrimers with disulfides at the periphery. No evidence was found for intramolecular macrocyclization (cooperative) exchange.

The last example of a dendritic effect discussed in this chapter is the use of core-functionalized dendritic mono- and diphosphine rhodium complexes by Van Leeuwen *et al.*<sup>42</sup> Carbosilane dendrimers were functionalized in the core with Xantphos, bis(diphenylphosphino)ferrocene (dppf) and triphenylphosphine (Figures 18, 26 and 27). Rhodium complexes of these mono- and bidentate ligands were tested in the hydroformylation of 1-octene. Depending on the ligand, a small effect of the dendritic encapsulation was observed. When bulky substrates were used in the hydroformylation reaction with the dppf-based ligand, a decrease in reactivity was observed on going to higher generations. This is in agreement with the first order dependency in substrate concentration observed for these types of reactions because of the lower diffusion rate of bulky substrates to the active center. The authors suggest to use this decreased activity for larger substrates as a possibility for substrate selective catalysis.

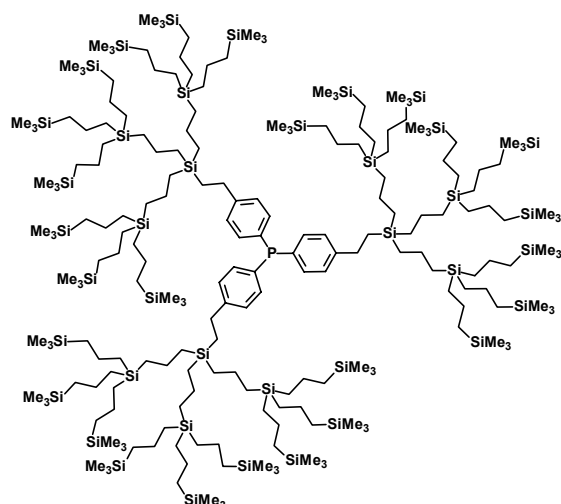


Figure 26: Triphenylphosphine derived dendrimer.

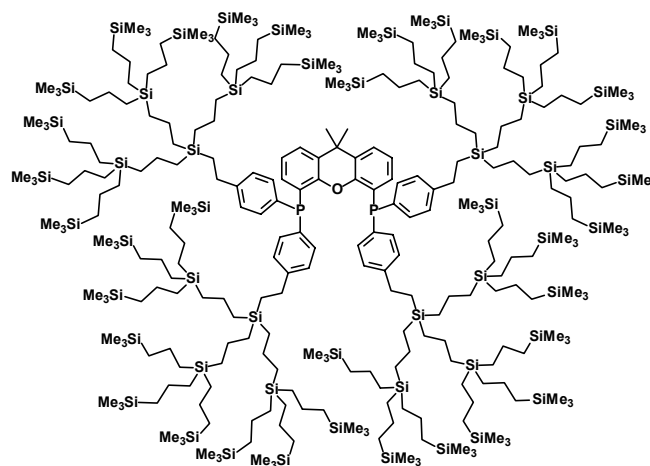


Figure 27: Nixantphos derived dendrimer.

## 1.6 Unmodified or Non-Dendritic Catalysts

Under carefully adjusted experimental conditions unmodified catalyst can be used in nanofiltration coupled homogeneous catalysis. Also non-dendritic but nanosized rigid catalytic systems can be retained by nanofiltration membranes. In this part, unmodified catalysts and rigid nondendritic systems applied in continuous catalysis will be discussed.

### 1.6.1 Hydrogenation Reaction

Using unmodified Ru-BINAP and Rh-Et-DUPHOS catalysts (Figures 28 and 29) Jacobs *et al.* performed hydrogenation reactions of dimethylitaconate (DMI) and methyl-2-acetamidoacrylate (MAA), respectively.<sup>43</sup>

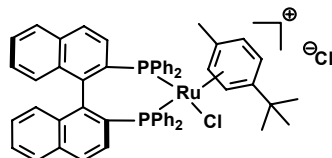


Figure 28: Ru-BINAP.

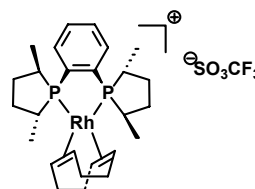
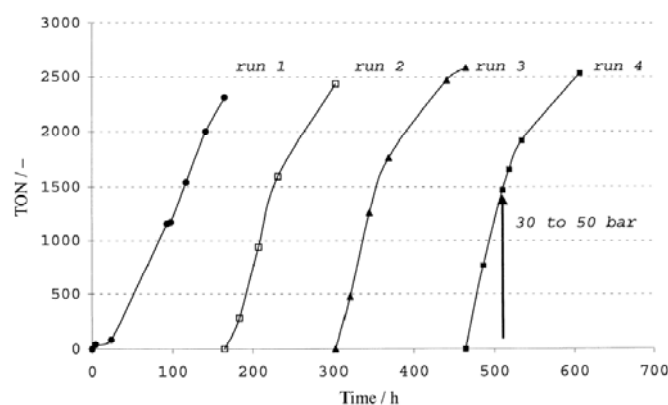


Figure 29: Rh-Et-DUPHOS.

The continuous hydrogenation reactions were performed in a stirred 100 mL autoclave containing a Koch MPF-60 membrane at the bottom. The hydrogenation of DMI was

performed for more than 40 h (10 exchanged reactor volumes) without a significant loss in enantiomeric excess. However a slight decrease in activity was observed caused by the incomplete retention (>98%) of the catalyst. In the hydrogenation of MAA with Rh-Et-DUPHOS, a significant drop in activity and selectivity was observed. The retention of 97% alone, cannot account for this effect. A slow deactivation of the catalyst, possibly due to oxidation of the phosphine ligand, is assumed but needs further investigation. The total TON for the hydrogenation with Ru-BINAP and Rh-Et-DUPHOS are 1950 and 930, respectively.

Another setup used for the hydrogenation of DMI with Ru-BINAP was equipped with dense PDMS elastomer membranes (Jacobs *et al.*<sup>44</sup>). The catalyst solution was present in a submerged membrane system, prepared as a sealed “PDMS capsule”. The catalytically active complex was retained by the membrane while substrate and products, dissolved in the bulk phase, can cross the membrane under influence of the concentration difference without the need of mechanical pressure.



**Figure 30:** Catalysis using a catalyst in a PDMS capsule.

The catalysis was performed batch-wise (Figure 30). After reaching ca. 90% conversion, the bulk phase was replaced and similar turnover frequencies (TOF) of around  $25 \text{ h}^{-1}$  were obtained in the following three runs 2, 3 and 4. When the catalyst capsule was removed, no further activity was detected. Furthermore, the Ru content in the bulk phase was always below the detection limit of AAS, which shows the high catalyst retention by the used membranes.



Keurentjes *et al.* performed a continuous hydrogenation of 1-butene in supercritical carbon dioxide<sup>10, 11</sup>. A fluoros derivative of Wilkinson's catalyst was prepared *in situ* by mixing the ligand with  $[(\text{COD})\text{RhCl}]_2$  under hydrogen / carbon dioxide pressure (Figure 31).

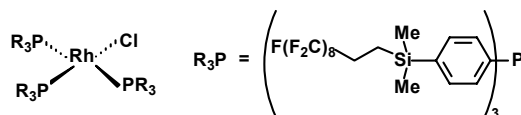


**Figure 31:** Fluoros derivative of Wilkinson's catalyst.

After preformation, the substrates and carbon dioxide were supplied continuously. The membrane reactor was pressurized at the feed side up to 20 MPa with the reaction mixture. A trans-membrane pressure was created by opening a needle valve on the permeate side after which the continuous process started.

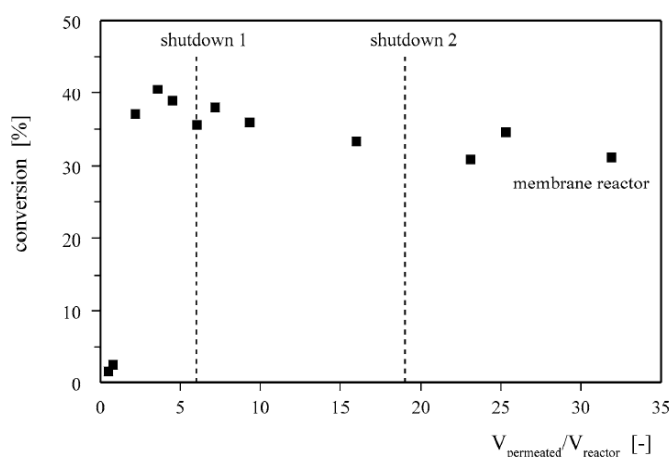


**Figure 32:** Continuous hydrogenation of 1-butene in supercritical  $\text{CO}_2$ .

After an activation period of 4 h, the conversion showed a maximum of 40% followed by a steady decrease in conversion (Figure 32). Overnight, the pressure was decreased to 6 MPa and the needle valve on the permeate side was closed. This shutdown procedure caused the catalyst to precipitate and no reaction occurred anymore. The precipitated catalyst can be used for a new cycle by pressurization of the membrane reactor, redissolving the catalyst. At the end of the third run the conversion had dropped to ~33%. A TON of  $1.2 \times 10^5$  in 32 h ( $\tau \sim 62$  min) was obtained. ICP-AAS analysis of the permeate stream indicated that complete

retention of the catalyst occurred. The authors propose possible traces of oxygen as source for the decrease in activity of the catalyst.

### 1.6.2 Michael Addition Reaction

A dodecakis(NCN-Pd<sup>II</sup>) catalyst synthesized in the group of Van Koten (Figure 33), was applied in the a continuous double Michael addition reaction between methyl vinyl ketone (MVK) and ethyl  $\alpha$ -cyanoacetate.<sup>45</sup> The reaction was performed in the dead-end reactor discussed in paragraph 1.2.1. Two catalytic runs were performed differing in the amount of catalyst and in the applied flow (both increased by a factor 2.5). Both runs showed high productivity for more than 24 h (Figure 34).

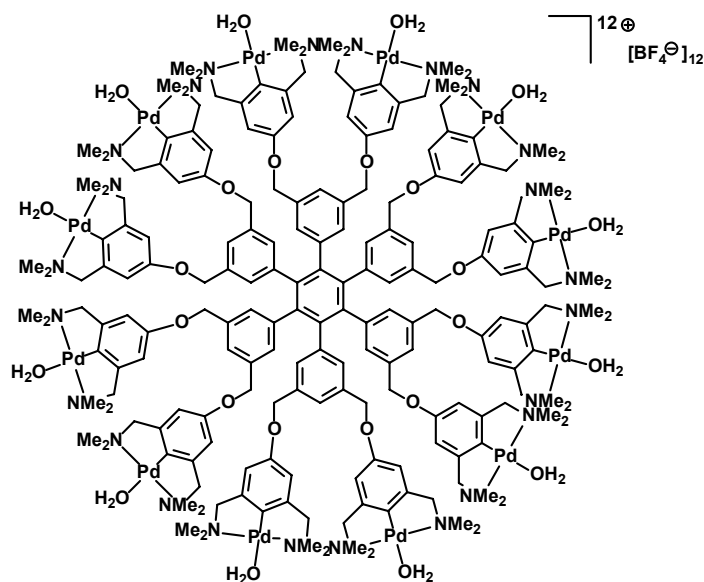


Figure 33: Dodecakis(NCN-Pd<sup>II</sup>).

For run II, the Pd-concentration in both the retentate and the permeate was determined by ICP-AAS analysis. A catalyst retention of 99.5% was determined, this is almost identical to the value determined earlier for an isostructural platinum analogue ( $R = 99,9\%$ ).<sup>46</sup> This low leaching of the catalyst completely accounts for the slow decrease in activity after reaching stable conversion.

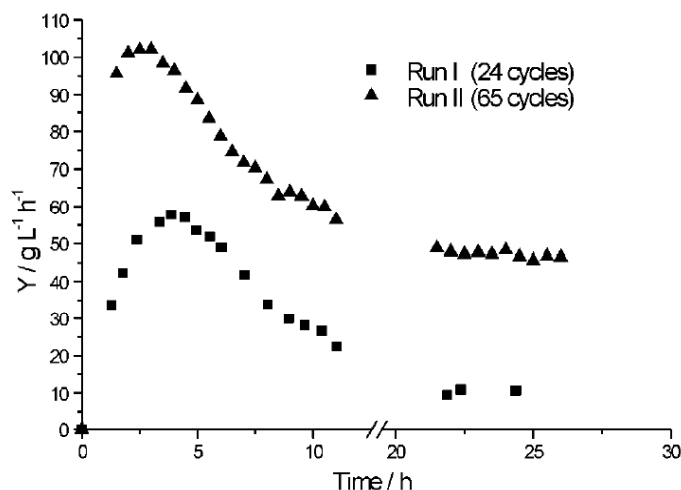


Figure 34: Continuous double Michael addition.

### 1.6.3 Phase Transfer Catalysis

Livingston *et al.* performed phase transfer catalysis (PTC) using membrane technology to separate the catalyst from the products in the post-reaction mixture.<sup>47,48</sup> The PT catalyst (tetroctylammonium bromide) was re-used after separation in subsequent reactions. The conversion of bromoheptane into iodoheptane was performed in a 100 mL glass vessel with 40 mL aqueous phase (2 M KI) and 40 mL organic phase (0.5 M bromoheptane and 0.05 M catalyst). After complete reaction, the organic phase was transferred into a separation cell equipped (SEPA ST, Osmonics, CA, USA) with a STARMEM<sup>TM</sup> 122 membrane. The cell was pressurized to 30 bars at room temperature starting the filtration of the post reaction mixture. After filtering 35 mL of the original 40 mL of organic liquid, the catalyst was washed out using toluene or fresh bromoheptane to form a new organic phase for the next catalytic run. Both procedures were applied for the recycling of the catalyst in three consecutive runs. Similar conversions were obtained in all three runs while the catalyst was retained in more than 99%.

In a later publication,<sup>49</sup> Heck reactions (between iodobenzene and styrene) were performed in the same way. In contrast to the PTC, the catalyst for the Heck reaction had a retention lower than 90% (for the first cycle). This catalyst was nevertheless recycled for 5 times but in the last run only 20% of the initial activity was obtained.

The retentions of the catalysts were also measured on a synthetic reaction mixture. The Heck-catalyst showed a retention of 96% while under experimental conditions retentions lower than 90% were obtained. For the PTC the values are both higher than 99%. The authors assume that this big difference for the Heck-catalyst is caused by the formation of smaller Pd species in the catalytic cycle. However, no precipitation or Pd-black formation was observed.

### **1.7 Aim and Scope of this Thesis**

For the development of supported or immobilized homogeneous catalysts, one feature is of utmost importance. The stability of the catalyst is a key factor determining the success of an approach. In the work described in this thesis, a stable tridentate ligand system is used, leading to very stable coordination to transition metals. The supports used, consisted of polyphenylene molecules, resulting in rigid, shape persistent catalyst systems. This rigidity favors high retention in membrane filtration and minimizes possible cooperative (most of the time negative) dendritic effects. The aim of this thesis is to synthesize rigid molecular enlarged catalyst systems able to perform continuous catalysis with high TON. Dendritic catalysts as well as smaller, non-dendritic systems will be compared in order to obtain information about the required size and shape for these catalysts.

The synthesis of these rigid supported PCP-pincer ligand systems is described in **Chapter 2**. The ligands were coupled to three different support molecules using nucleophilic substitution reactions. With this series of ligands retention tests were performed in a nanofiltration membrane reactor in CH<sub>2</sub>Cl<sub>2</sub> and THF to investigate the influence of solvent on the ligand systems and on the nanofiltration membrane. Furthermore, catalytic tests were performed in allylic substitution reactions.

The kinetics of the allylic amination reaction catalyzed by pincer-Pd systems is investigated in **Chapter 3**. The reaction orders were determined and the rate constant was measured. These values were used to predict conversions when the pincer ligand systems are applied in a continuous stirred tank reactor.

**Chapter 4** describes the application of the largest pincer system in continuous homogeneous catalysis. Both the allylic alkylation and amination were performed in a continuously operated nanofiltration membrane reactor. Reactions were performed for more than 10 h.

In **Chapter 5**, a side project is performed in which diphosphine ligands, bearing secondary amine groups, are coupled to different supports. The actual coupling reaction was a palladium catalyzed amine coupling to support molecules functionalized with aryl bromide groups. Also the nucleophilic substitution reaction explored in Chapter two was used for the coupling of these ligands to rigid supports.

Alternative coupling methods are tested in **Chapter 6**. Here the Suzuki coupling was tested in the reaction of boronic acid derivatives of the pincer ligand to aryl halide groups on the support and vice versa. Furthermore a coupling reaction was investigated between phenolic pincer ligand derivatives and support molecules containing aryl halide groups, a so-called Ullmann diaryl ether synthesis.

## 1.8 References and Notes

- <sup>1</sup> B. Cornils, W. A. Herrmann, *Applied Homogeneous Catalysis with Organometallic Compounds*, VCH, Weinheim, Germany, **1996**.
- <sup>2</sup> U. Kragl, T. Dwars, *Trends Biotechnol.* **2001**, *19*, 442.
- <sup>3</sup> C. C. Tzschucke, C. Markert, W. Bannwarth, S. Roller, A. Hebel, R. Haag, *Angew. Chem. Int. Ed.* **2002**, *41*, 3964.
- <sup>4</sup> U. Kragl, D. Gyax, O. Ghisalba, C. Wandrey, *Angew. Chem., Int. Ed.* **1991**, *30*, 827.
- <sup>5</sup> J. Wöltinger, A. S. Bommarius, K. Drauz, C. Wandrey, *Org. Process Res. Dev.* **2001**, *5*, 241
- <sup>6</sup> U. Kragl, C. Dreisbach, *Angew. Chem., Int. Ed.* **1996**, *35*, 642.
- <sup>7</sup> N. J. Hovestad, E. B. Eggeling, H. J. Heidebüchel, J. T. B. H. Jastrzebski, U. Kragl, W. Keim, D. Vogt, G. van Koten, *Angew. Chem. Int. Ed.* **1999**, *38*, 1655.
- <sup>8</sup> E. B. Eggeling, N. J. Hovestad, J. T. B. H. Jastrzebski, D. Vogt, G. van Koten, *J. Org. Chem.* **2000**, *65*, 8857.
- <sup>9</sup> R. Sablong, U. Schlotterbeck, S. Mecking, D. Vogt, *Adv. Synth. Catal.* **2003**, *345*, 333.
- <sup>10</sup> L. J. P. van den Broeke, E. L. V. Goetheer, A. W. Verkerk, E. de Wolf, B.-J. Deelman, G. van Koten, J. T. F. Keurentjes, *Angew. Chem. Int. Ed.* **2001**, *40*, 4473.
- <sup>11</sup> E. L. V. Goetheer, A. W. Verkerk, L. J. P. van den Broeke, E. de Wolf, B.-J. Deelman, G. van Koten, J. T. F. Keurentjes, *J. Catal.* **2003**, *219*, 126.
- <sup>12</sup> D. E. de Vos, I. F. J. Vankelecom, P. A. Jacobs (Editors), *Chiral Catalyst Immobilization and Recycling*, Wiley-VCH ISBN 3-527-29952-1, **2000**.
- <sup>13</sup> Millipore, Billerica, USA, <http://www.millipore.com>
- <sup>14</sup> Schleicher & Schuell MicroScience GmbH, Dassel, Germany, <http://www.schleicher-schuell.com>.
- <sup>15</sup> D. Nair, J. T. Scarpello, I. F. J. Vankelecom, L. M. Freitas Dos Santos, L. S. White, R. J. Kloetzing, T. Welton, A. G. Livingston, *Green Chemistry* **2002**, *4*, 319.
- <sup>16</sup> D. Nair, J. T. Scarpello, L. S. White, L. M. Freitas, Dos Santos, I. F. J. Vankelecom, T. Welton, A. G. Livingston, *Tetrahedron Lett.* **2001**, *42*, 8219.
- <sup>17</sup> I. F. J. Vankelecom, *Chem. Rev.* **2002**, *102*, 3779.
- <sup>18</sup> K. K. Sirkar, P. V. Shanbhag, A. S. Kovvali, *Ind. Eng. Chem. Res.* **1999**, *38*, 3715.

- <sup>19</sup> Koch Membrane Systems, Wilmington, USA, <http://www.kochmembrane.com>.
- <sup>20</sup> C. Linder, M. Nemas, M. Perry, R. Katrarro, U.S. patent no. 5.265.734.
- <sup>21</sup> E. Gibbins, M. D'Antonio, D. Nair, L. S. White, L. M. S. dos Santos, I. F. J. Vankelecom, A. G. Livingston, *Desalination* **2002**, *147*, 307.
- <sup>22</sup> Membrane Extraction Technology, London, U.K., <http://www.membrane-extraction-technology.com>.
- <sup>23</sup> <http://www.gewater.com>
- <sup>24</sup> M. K. Koukou, N. Papayannakos, N. C. Markatos, M. Bracht, H. M. Van Veen, A. Roskam, *J. Membr. Sci.* **1999**, *155*, 241.
- <sup>25</sup> Hermsdorfer Institut für Technische Keramik, Hermsdorf, Germany, <http://www.hitk.de>.
- <sup>26</sup> Corning, New York, U.S.A., <http://www.corning.com>.
- <sup>27</sup> E. Buhleier, W. Wehner, F. Vögtle, *Synthesis* **1978**, 155.
- <sup>28</sup> J. W. J. Knapen, A. W. van der Made, J. C. de Wilde, P. W. N. M., P. Wijkens, D. M. Grove, G. van Koten, *Nature*, **1994**, *372*, 659.
- <sup>29</sup> N. Brinkmann, D. Giebel, G. Lohmer, M. T. Reetz, U. Kragl, *J. Catal.*, **1999**, *183*, 163.
- <sup>30</sup> D. de Groot, E. B. Eggeling, J. C. de Wilde, H. Kooijmans, R. J. van Haaren, A. W. van der Made, A. L. Spek, J. N. H. Reek, D. Vogt, P. C. J. Kamer, P. W. N. M. van Leeuwen, *Chem. Commun.*, **1999**, *17*, 1623.
- <sup>31</sup> D. de Groot, J. N. H. Reek, P. C. J. Kamer, P. W. N. M. van Leeuwen, *Eur. J. Org. Chem.* **2002**, 1085.
- <sup>32</sup> D. de Groot, B. F. M. de Waal, J. N. H. Reek, A. P. H. J. Schenning, P. C. J. Kamer, E.W. Meijer, P. W. N. M. van Leeuwen, *J. Am. Chem. Soc.* **2001**, *123*, 8453.
- <sup>33</sup> L. Ropartz, R. E. Morris, G. P. Schwarz, D. F. Foster, D. J. Cole-Hamilton, *Inorg. Chem. Commun.* **2000**, *3*, 714.
- <sup>34</sup> L. Ropartz, R. E. Morris, D. F. Foster, D. J. Cole-Hamilton, *Chem. Commun.* **2001**, 361.
- <sup>35</sup> R. Breinbauer, E.J. Jacobsen, *Angew. Chem. Int. Ed.* **2000**, *39*, 3604.
- <sup>36</sup> A. W. Kleij, R. A. Gossage, J. T. B. H., J. Boersma, G. van Koten, *Angew. Chem. Int. Ed.* **2000**, *39*, 176.
- <sup>37</sup> A. W. Kleij, R. A. Gossage, R. J. M. Klein Gebbink, N. Brinkmann, E. J. Reijerse, U. Kragl, M. Lutz, A.L. Spek, J. Boersma, G. van Koten, *J. Am. Chem. Soc.* **2000**, *122*, 12112.
- <sup>38</sup> G. D. Engel, L. H. Gade, *Chem. Eur. J.* **2002**, *8*, 4319.
- <sup>39</sup> Y. Ribourdouille, G. D. Engel, M. Richard-Plouet, L. H. Gade, *Chem. Commun.* **2003**, 1228.
- <sup>40</sup> H.-F. Chow, C.-W. Wan, *Helv. Chim. Acta*, **2002**, *85*, 3444.
- <sup>41</sup> W. Zhang, S. E. Tichy, L. M. Pérez, G. C. Maria, P. A. Lindahl, E.E. Simanek, *J. Am. Chem. Soc.* **2003**, *125*, 5086.
- <sup>42</sup> G. E. Oosterom, S. Steffens, J. N. H. Reek, P. C. J. Kamer, P. W. N. M. van Leeuwen, *Topics in Catal.* **2002**, *19*, 61.
- <sup>43</sup> K. de Smet, S. Aerts, E. Ceulemans, I. F. J. Vankelecom, P. A. Jacobs, *Chem. Commun.* **2001**, 597.
- <sup>44</sup> K. de Smet, A. Pleysier, I. F. J. Vankelecom, P. A. Jacobs, *Chem. Eur. J.* **2003**, *9*, 334.
- <sup>45</sup> H. P. Dijkstra, N. J. Ronde, G. P. M. van Klink, D. Vogt, G. van Koten, *Adv. Synth. Catal.* **2003**, *345*, 364.
- <sup>46</sup> H. P. Dijkstra, C. A. Kruithof, N. J. Ronde, R. van de Coevering, D. J. Ramón, D. Vogt, G. P. M. van Klink, G. van Koten, *J. Org. Chem.* **2003**, *68*, 675.
- <sup>47</sup> S. S. Luthra, X. Yang, L. M. Freitas dos Santos, L. S. White, A. G. Livingston, *Chem. Commun.* **2001**, 1468.
- <sup>48</sup> S. S. Luthra, X. Yang, L. M. Freitas dos Santos, L. S. White, A. G. Livingston, *J. Membr. Sci.* **2002**, *201*, 65.
- <sup>49</sup> D. Nair, S. S. Luthra, J. T. Scarpello, L. S. White, L. M. Freitas dos Santos, A. G. Livingston, *Desalination* **2002**, *147*, 301.



# 2

## Pincer Ligand Coupling via Nucleophilic Substitution

### Abstract

---

Three different pincer ligand systems were synthesized via nucleophilic substitution reactions of phenolic ligand precursors and support molecules functionalized with benzylic bromide groups. Retention tests in a nanofiltration membrane reactor showed moderate to good retentions in THF and CH<sub>2</sub>Cl<sub>2</sub>. The difference in retention for both solvents was negligible. Concentration dependent NMR spectroscopy showed no indication for the formation of aggregates in solution. The three ligand systems were active in both the allylic alkylation and allylic amination reaction and showed high selectivity towards the linear *trans*-product.

---



## 2.1 Introduction

In spite of the superior performance of homogeneous catalysts regarding mild reaction conditions, high activity and selectivity as well as the detailed mechanistic insights, industrial catalysis is in the greater part relying on heterogeneous catalysis (~75% vs. ~25%).<sup>1,2,3</sup> To become of greater interest for large scale industrial applications, specific points of attention for homogeneous catalysts are:

- lowering of the costs of the ligands and metal by increasing the productivity of the catalyst (total turn over number)
- improving the productivity of the catalytic system (space time yield)
- preventing precious metal loss by leaching
- enabling the recycling of the catalyst

When these or at least parts of these problems are solved, homogeneous catalysis can become of broader interest for applications in industrial processes. The methods used nowadays for the separation of products from the catalyst often involve destructive methods, e.g. distillation or the application of expensive procedures such as precipitation followed by filtration.<sup>4</sup> An example of a non-destructive method is biphasic catalysis in which the catalyst and substrates/products are dissolved in different phases, making their separation possible.<sup>5</sup> Another method to improve cost efficiency is the heterogenization of the homogeneous catalyst. However, these methods often suffer from decreased selectivity and activity compared to their homogeneous counterparts.<sup>4,6</sup>

Recently membrane filtration has gained considerable attention in the application of homogeneous catalysts.<sup>7</sup> The use of membrane filtration coupled to a continuous catalytic process can be the answer to some of the aforementioned problems. For the application of homogeneous catalysts in nanofiltration-coupled catalysis, these catalysts should have a sufficient size to be retained by membranes. In our group carbosilane dendrimers have been used successfully for this purpose.<sup>8</sup> A second-generation carbosilane dendrimer was functionalized with phosphino-carboxylic acid ester groups. The resulting catalyst could be retained in the reactor by nanofiltration membranes, without the need to be heterogenized and thus does not suffer from the above-mentioned problems due to e.g. mass transfer limitations. Application of the catalyst in a continuous hydrovinylation of styrene, using nanofiltration

membranes showed the potentiality of such a catalytic system. Because of the tedious synthesis of these dendrimers and their high costs, the research presented in this thesis focuses on the use of smaller but more rigid molecules as supports for homogeneous catalysts.<sup>9</sup>

Instead of using flexible carbosilane supports we set out to use rigid support molecules consisting of multiple phenyl rings. Due to their aromatic character they form stable and rigid core molecules, which can easily be functionalized. Polyphenyl molecules were synthesized with different sizes and shapes. This makes it possible to investigate the influence of these parameters on the retention in a reactor equipped with a nanofiltration membrane.

The ligand of choice for immobilization on a support is the widely used PCP-pincer ligand.<sup>10,11</sup> This ligand is known to form metal complexes via the donating phosphorus atoms as well as a covalent C-metal  $\sigma$ -bond (Figure 1). Their stability is demonstrated in C-C coupling reactions like the Heck and Suzuki coupling in which PCP-metal catalysts show very high turnover numbers (>100 000) at a reaction temperature above 140°C. The high stability will prevent catalyst degradation under continuous catalytic conditions, as this was one of the problems in the studies mentioned earlier. The ligand can easily be functionalized in the *para* position (R group in Figure 1) and together with the aforementioned stability, which makes it an ideal ligand for immobilization purposes.

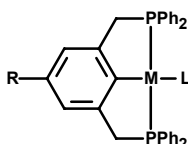
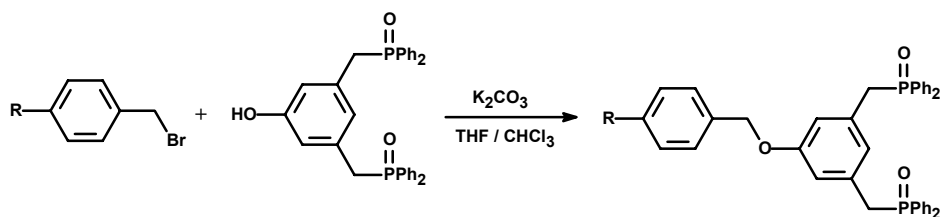


**Figure 1:** General PCP-metal complex.

PCP-metal complexes have shown activities in the palladium-catalyzed Heck and Suzuki coupling, hydroamination, ruthenium-catalyzed transfer hydrogenation and iridium-catalyzed dehydrogenation. We tested the activity of this ligand in a palladium catalyzed allylic alkylation and amination reaction.

For the coupling of the ligand to a support, a reaction is needed which can easily be performed and gives the coupled product in high yields without any side reactions. We chose

the nucleophilic substitution of a benzylic bromide with the hydroxy-group of a phenol because it fulfills the aforementioned needs (Scheme 1).



**Scheme 1:** Nucleophilic substitution reaction (R = support molecule depicted in **Figure 2**).

The resulting P-protected phosphine ligands will be tested for retention by a nanofiltration membrane using a commercially available membrane (Koch). Dichloromethane and THF were used as solvents in order to investigate their influence on the compounds and membranes. The catalytic performance in the palladium-catalyzed allylic alkylation and amination will be investigated.

## 2.2 Results and Discussion

Support core molecules **1** and **2** were synthesized by radical bromination of their corresponding methyl-substituted precursors, using N-bromosuccinimide in the presence of AIBN.<sup>12</sup> In case of support **1**, commercially available mesitylene was used. The precursor of **2** was synthesized via a threefold condensation of 4-methylacetophenone under the influence of SiCl<sub>4</sub> in ethanol (Scheme 2).<sup>13</sup>

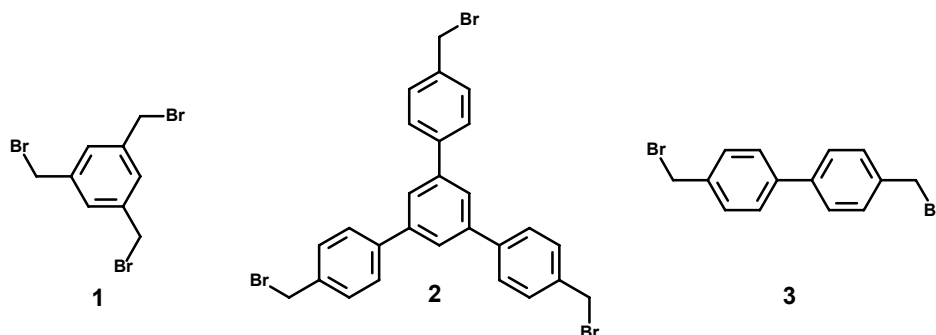
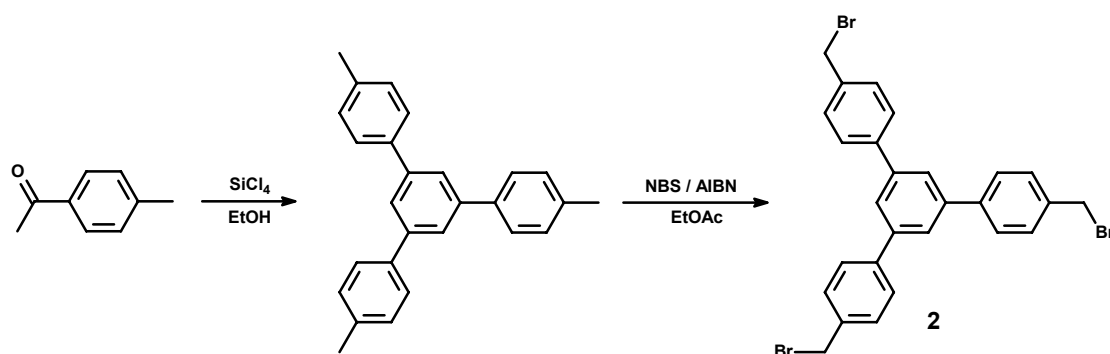
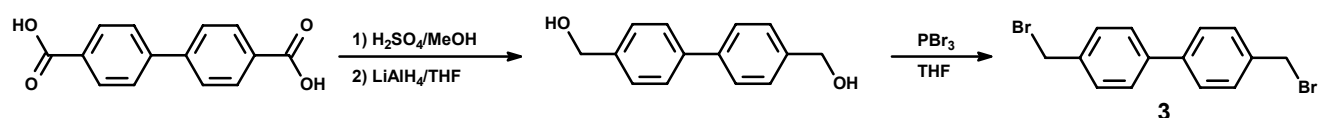


Figure 2: Used support molecules.



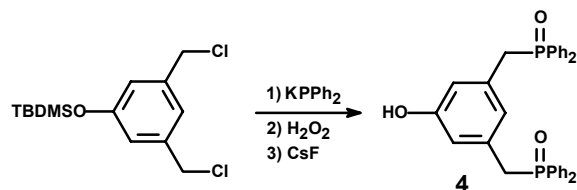
Scheme 2: Synthesis of support 2.

Support molecule **3** was synthesized starting from 4,4'-biphenyldicarboxylic acid, which was esterified and subsequently reduced with  $\text{LiAlH}_4$  in THF.<sup>14</sup> The obtained dihydroxy compound was converted to the bromo-derivative by a reaction with  $\text{PBr}_3$  (Scheme 3).<sup>15</sup>



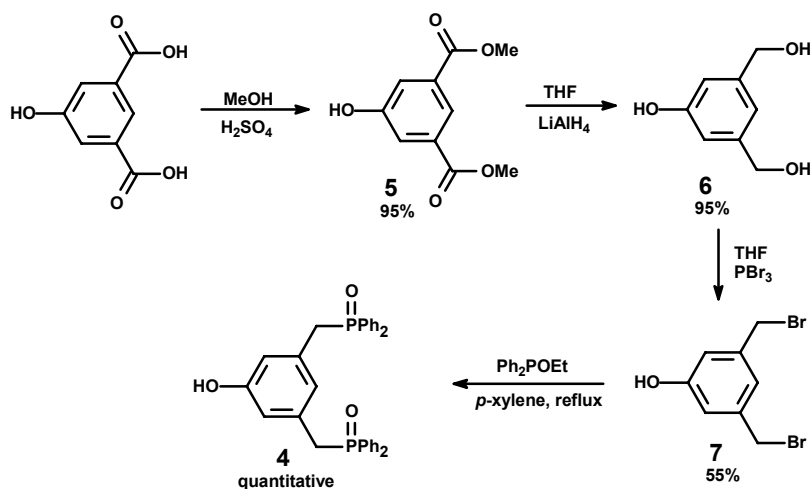
Scheme 3: Synthesis of support 3.

In 1997, Reinhoudt *et al.* published the synthesis of building block **4**.<sup>16</sup> Potassium diphenylphosphide was coupled to a protected di(chloromethyl)phenol (Scheme 4). The resulting diphosphine was oxidized and deprotected with cesium fluoride giving the compound in 31% yield.



**Scheme 4:** Synthesis of building block **4** according to a literature procedure.<sup>16</sup>

We decided to synthesize this building block in a different way, in order to obtain the compound in a higher yield. A 4-step synthesis was chosen, starting with the esterification of commercially available 4-hydroxyisophthalic acid. The ester groups were subsequently reduced to hydroxy groups **6** followed by bromination using  $\text{PBr}_3$  deriving 3,5-bis(hydroxymethyl)phenol **7**. The last step in this synthesis involves an Arbusov type of reaction,<sup>17</sup> coupling the diphenylphosphineoxide groups to the benzylic position to give the building block **4** in a total yield of 50%. This yield is significantly higher than reported for the above-mentioned method. However, the bromination steps give low yields, while the previous steps are high in yield. Further optimization of this step can possibly lead to a high overall yield.



**Scheme 5:** Synthesis of phenolic building block **4**.

All ligand systems were synthesized using nucleophilic substitution of the benzyl bromide groups on the support molecules by a deprotonated phenolic ligand precursor **4** (Scheme 1).<sup>16</sup> The excess of building block **4**, used to ensure full conversion of the benzyl bromide groups, was removed by size exclusion chromatography (SEC) using Biobeads S-X1 and  $\text{CH}_2\text{Cl}_2$  as eluent. SEC is preferred over classical column chromatography because the products slowly

decompose during chromatography (Reinhoudt *et al.*<sup>16</sup>). Using this synthetic approach, all three P-protected pincer ligand systems **8**, **9**, and **10** were synthesized (Figure 3). However, yields were low due to not optimal SEC.

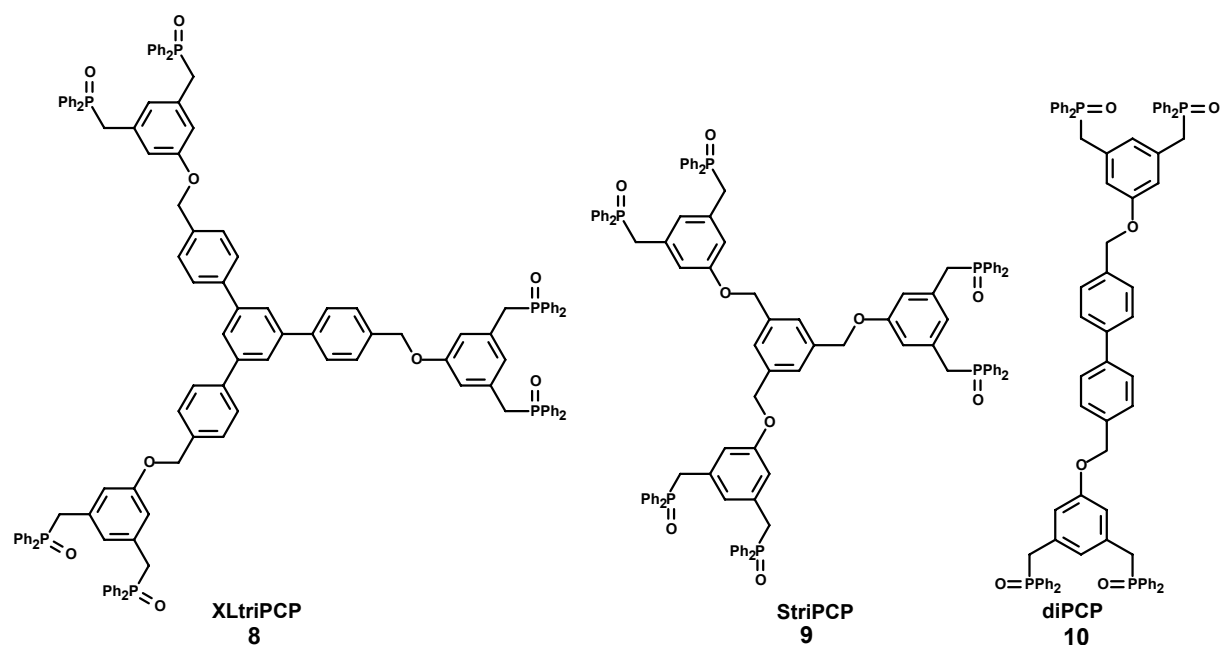
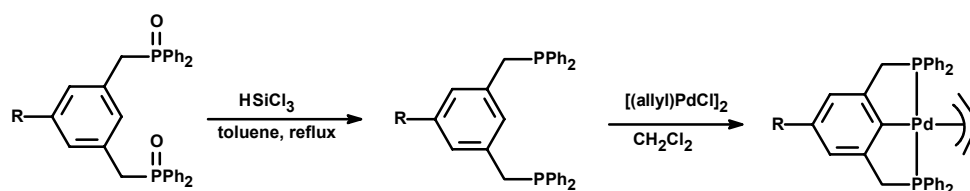


**Figure 3:** Three synthesized protected pincer ligand systems.

The corresponding unprotected phosphine ligands were obtained by reduction of the phosphineoxides using HSiCl<sub>3</sub> in toluene to give the products in almost quantitative yields. Palladium complexes were synthesized by reacting the freshly prepared phosphines with [(allyl)PdCl]<sub>2</sub> in dichloromethane (Scheme 6). The so formed complexes were used in the catalytic experiments (*vide infra*).



**Scheme 6:** Reduction and complexation of pincer ligand.

### 2.2.1 Retention Measurements

In order to investigate the retention behavior of the three P-protected ligands systems (**8**, **9** and **10**), with respect to the nanofiltration (NF) membrane (Koch MPF 50), the retention of the three compounds was measured in CH<sub>2</sub>Cl<sub>2</sub> and THF. Retention can be defined as the chance that a particle will cross the membrane with one exchanged reactor volume of solvent (equation 1.1 and 1.2).

$$R = 1 + \frac{V_r}{V_p} \ln \left( \frac{m_r}{m_r + m_f} \right) \quad \text{equation 1.1}$$

$$= 1 + \frac{V_r}{V_p} \ln \left( \frac{c_r}{c_r + c_f} \right) \quad \text{equation 1.2}$$

From earlier studies it was known that the retention of flexible polymeric and dendritic compounds dramatically decreased by using THF instead of CH<sub>2</sub>Cl<sub>2</sub>.<sup>18</sup> We believe that this is caused by the swelling of the polymeric membrane and structural changes in the dendritic structure itself due to solvation. Since the supports we used have a quite rigid structure, structural changes will play a less significant role. This will especially be the case for **XLtriPCP 8**, which has a large rigid core with ligands connected to it. As can be seen in Table 1, the dimensions of all compounds are in the same range. The difference in these values however, is that the structure of **diPCP 10** is that of a stick-like compound, where the smallest diameter will be important for the retention, while **XLtriPCP 8**, and to minor extend also **StriPCP 9**, has a disc-like structure where the biggest diameter determines the retention.

**Table 1:** Retention values measured using CH<sub>2</sub>Cl<sub>2</sub> and THF as solvent.

| Compound          | MW<br>(g/mol) | biggest<br>dimension (Å) <sup>a</sup> | smallest<br>dimension (Å) <sup>a</sup> | R in CH <sub>2</sub> Cl <sub>2</sub><br>(%) <sup>b</sup> | R in THF<br>(%) <sup>b</sup> |
|-------------------|---------------|---------------------------------------|--|--|------------------------------|
| diPCP <b>10</b>   | 1223          | 27.6                                  | 9.7                                    | 71.0   | 70.4                         |
| StriPCP <b>9</b>  | 1682          | 21.6                                  | 9.6                                    | 93.4   | 97.5                         |
| XLtriPCP <b>8</b> | 1910          | 27.8                                  | 8.0                                    | 98.1   | 99.4                         |

<sup>a</sup>Determined using Syble 6.8 molecular modeling software with a Tripos force field.

<sup>b</sup>Average values of two measurements, stirring 200 r.p.m., 20 bar, 50 mL filtrate collected.

From the molecular weight it was expected that **XLtriPCP 8** would have the highest retention and the **diPCP 10** would have a low retention. Also based on the molecular structure, this order in retention is expected. In Table 1 it is shown that indeed **XLtriPCP 8** has the highest, retention while **diPCP 10** has a very low retention. Changing the solvent from dichloromethane to THF did not have such a big influence on the retention as could be expected from earlier studies. The retention of **StriPCP 9** and **XLtriPCP 8** increased a little bit while the retention of **diPCP 10** decreased less than one percent. This small influence is in contrast to the described dramatic decrease in retention<sup>18</sup>. From this it can be concluded that the decrease in retention found in earlier studies was caused by structural changes of the tested compound, rather than influencing the pore size of the membranes.

As shown in Table 1, these rather small molecules already have retentions, which can be compared to second-generation carbosilane dendrimers. Furthermore, the retention of the compound is less influenced by the solvent. The retentions are sufficient for lab scale tests, but have to be increased for practical applications.

### **2.2.2 Investigation of Aggregation**

The retentions of **StriPCP 9** and **XLtriPCP 8** are quite high for these small molecules. To be sure that the retentions were determined for monomeric compounds and are not due to the formation of aggregates, potential staggering ( $\pi$ -stacking) of the molecules was investigated by measuring the chemical shift of some selected protons at different concentrations via NMR spectroscopy. Moore *et al.* used this method to show the aggregation behavior of phenylacetylene macrocycles.<sup>19</sup> In this work, a clear shift was observed for various endo- and exo-annular functional groups. This NMR-determined aggregation was additionally verified by vapor pressure osmometry measurements.



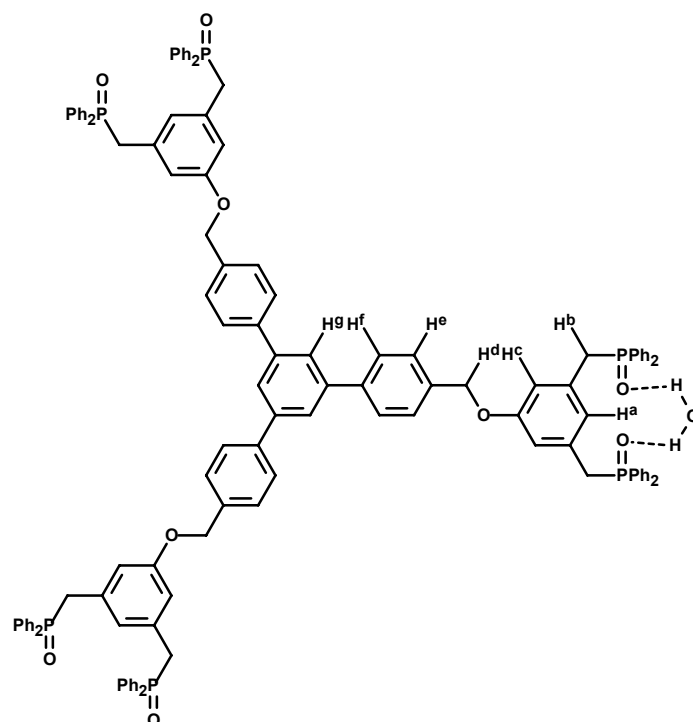
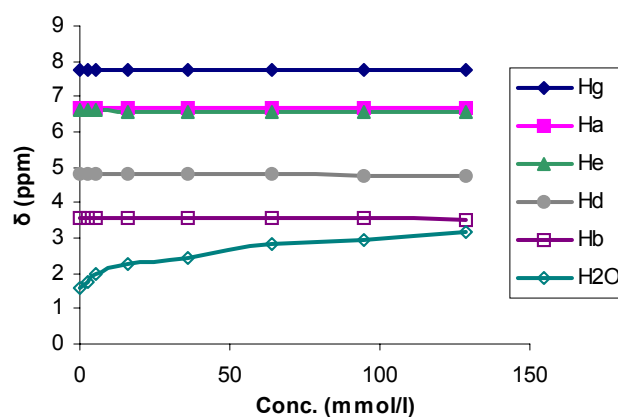


Figure 4: Protons in XltriPCP 8.

Graph 1: Concentration dependent  $^1\text{H}$  NMR.

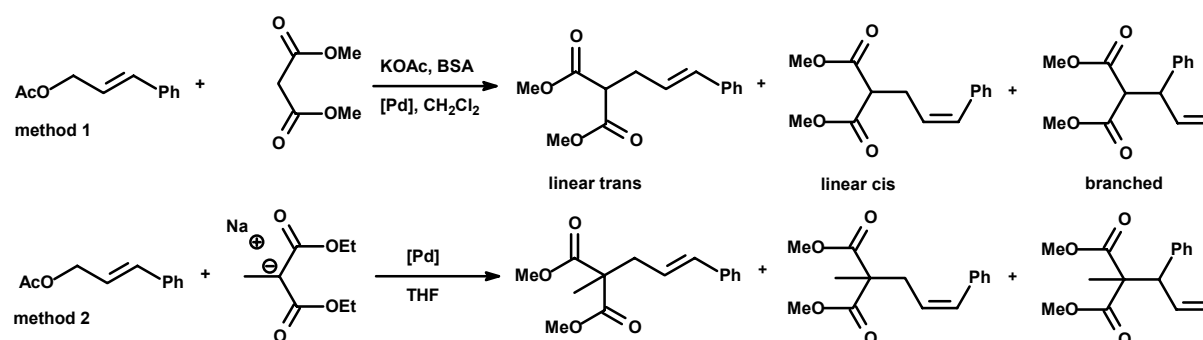
Graph 1 shows the chemical shift of the selected protons (see Figure 4) depending on the concentration. As can be seen, the chemical shifts remain unchanged upon varying the concentration of the compound, except for the protons belonging to coordinated water. This can be caused by concentration influences of the compound on the coordinated water. At higher concentrations one water molecule can possibly coordinate intramolecularly to two  $\text{P}(\text{O})\text{Ph}_2$  substituents of different XltriPCP molecules. These non-changing NMR spectra's give an indication that indeed no aggregates are formed in  $\text{CDCl}_3$  at concentrations between

0.3 mmol/l – 130 mmol/l. The high retention for the compound is thus solely attributed to their rigid structure.

### 2.2.3 Allylic Alkylation Reaction

Zhang *et al.* published in 1997 results on asymmetric allylic alkylation using PCP-metal complexes as catalyst.<sup>20</sup> The palladium complexes used were prepared *in situ* by addition of one of the various palladium precursors, such as  $[\text{Pd}(\text{OAc})_2]$ ,  $\text{Pd}_2(\text{dba})_3$  and  $[(\text{allyl})\text{PdCl}]_2$ , to the PCP ligands. This work inspired us to use this system with our multiple pincer ligands. The precursor used in our work was  $[(\text{allyl})\text{PdCl}]_2$ . Using this precursor, soluble catalysts were obtained without having a catalytic reaction of the precursor itself which was observed for  $\text{Pd}_2(\text{dba})_3$ . First the phosphineoxide ligand systems were reduced by the reaction with  $\text{HSiCl}_3$  in toluene, after which the palladium complexes were formed by stirring the free diphosphine with  $[(\text{allyl})\text{PdCl}]_2$  in dichloromethane for 0.5 h (Scheme 6).

In literature, different procedures are described to perform allylic alkylation reactions. The most common method is the coupling of a nucleophile, e.g. dimethyl malonate (Scheme 7, method 1) or sodium diethyl 2-methylmalonate (method 2) to an allyl acetate, e.g. cinnamyl acetate. In case of dimethyl malonate, a base should be added together with a cocatalyst (N,O-bis(trimethylsilyl) acetamide (BSA)) to form the active nucleophile.



Scheme 7: Allylic alkylation method 1 and 2.

Usually method 2 gives higher activities, which can be explained by a higher concentration of the active carbon nucleophile. In case of method 1 the nucleophile must be formed first by reaction of dimethyl malonate (DM) with BSA and potassium acetate. As can be seen in Table 2 (entry 8), the reaction rate is indeed higher using sodium diethyl methyl malonate

(NaDEM) as nucleophile. However, a drawback of this method is the pronounced background reaction, i.e. reaction in absence of any catalyst (entry 1 and 2). This makes it almost impossible to accurately determine the kinetic parameters, such as rate constant and reaction orders.

**Table 2:** Results in allylic alkylation using PCP ligands<sup>a</sup>.

| Entry          | Ligand                           | Nucleophile | Conversion (%) <sup>b</sup> | Selectivity linear trans (%) | Selectivity branched (%) |
|----------------|----------------------------------|-------------|-----------------------------|------------------------------|--------------------------|
| 1              | none, no [Pd]                    | DM          | 0.0 <sup>c</sup>            |                              |                          |
| 2              | none, [(allyl)PdCl] <sub>2</sub> | DM          | 0.0                         |                              |                          |
| 3              | monoPCP                          | DM          | 51.4                        | 91.9                         | 8.1                      |
| 4              | diPCP                            | DM          | 22.0                        | 99.0                         | 1.0                      |
| 5              | StriPCP                          | DM          | 60.4                        | 88.6                         | 11.4                     |
| 6              | XLtriPCP                         | DM          | 93.0                        | 89.7                         | 10.3                     |
| 7 <sup>d</sup> | none, no [Pd]                    | NaDEM       | 11.0 <sup>e</sup>           | 100.0                        | not observed             |
| 8 <sup>d</sup> | monoPCP                          | NaDEM       | 97.6                        | 95.8                         | 4.2                      |

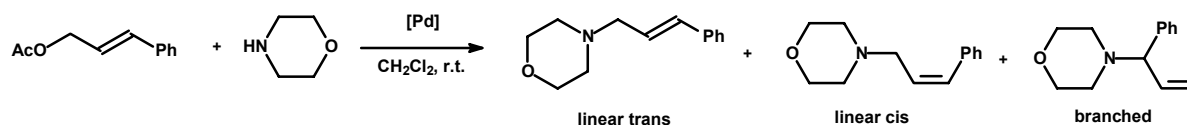
<sup>a</sup>Room temperature, solvent: CH<sub>2</sub>Cl<sub>2</sub>; volume: 10 mL; S/cat=500; <sup>b</sup>Conversion after 1 h; <sup>c</sup>After 6 h still no conversion; <sup>d</sup>Solvent: THF; <sup>e</sup>59.1% conversion overnight

As can be seen in table 2, the most active catalyst is the **XLtriPCP**-Pd system while the **diPCP**-Pd has moderate activity. Electronic influences of the aryl groups can cause this higher activity of the **XLtriPCP**-Pd system.<sup>21</sup> The selectivity of all ligand-Pd systems was comparable; all gave higher than 89% of the linear *trans*-product. Catalyst **diPCP**-Pd gave a very high selectivity of 99% towards the *trans*-product.

#### 2.2.4 Allylic Amination Reaction

The allylic amination is an important route towards allylic amines. These allylic amines can be converted to amino acids, alkaloids or carbohydrate derivatives.<sup>22,23,24</sup> The reaction is also used in many total synthesis reactions.<sup>25</sup> For these reasons it is often used as a test reaction for mono and bidentate phosphine-metal complexes. In the allylic amination an amine is coupled to an allylic acetate by substituting the acetate group (Scheme 8). Together with the

investigation of kinetic parameters, the proposed mechanism will be discussed in Chapter 3. To our knowledge, PCP pincer ligands have never been used for this reaction before.



**Scheme 8:** Allylic amination reaction.

The catalyst is prepared as described earlier for the allylic alkylation, i.e. in situ formation by mixing solutions of [(allyl)PdCl]<sub>2</sub> and the ligand. Because of the solubility, complexation of **XLtriPCP** was performed in dichlorobenzene instead of dichloromethane. Cinnamyl acetate was used as substrate and morpholine as the nucleophile.

**Table 3:** Results of the allylic amination with PCP pincer ligand systems<sup>a</sup>.

| Entry | Ligand                           | Conversion (%) <sup>b</sup> | Selectivity linear trans (%) | Selectivity branched (%) |
|-------|----------------------------------|-----------------------------|------------------------------|--------------------------|
| 1     | none, no [Pd]                    | 0.0 <sup>c</sup>            |                              |                          |
| 2     | none, [(allyl)PdCl] <sub>2</sub> | 0.0 <sup>c</sup>            |                              |                          |
| 3     | mono PCP                         | 26.9                        | 94.3                         | 5.7                      |
| 4     | diPCP                            | 53.7                        | 94.3                         | 5.7                      |
| 5     | StriPCP                          | 75.9                        | 95.1                         | 4.9                      |
| 6     | XLtriPCP                         | 52.2                        | 93.0                         | 7.0                      |

<sup>a</sup>Room temperature, solvent: CH<sub>2</sub>Cl<sub>2</sub>; volume: 10 mL; S/cat=500; <sup>b</sup>Conversion after 1 h;

<sup>c</sup>Overnight still no conversion.

In contrast to the results obtained in the allylic alkylation reaction, the **StriPCP**-Pd system gave the most active catalyst in the allylic amination reaction, followed by the **diPCP**-Pd and **XLtriPCP**-Pd systems. The lower activity of the latter compound could be caused by the use of dichlorobenzene as solvent to solve the solubility problems. The selectivity towards the *trans*-product is quite similar (~94%) and is thus not influenced by the nature of the substituents on the ligands.

## 2.3 Conclusions

Three ligand systems bearing two and three pincer ligands, respectively were synthesized by nucleophilic substitution of benzylic bromide groups on support molecules by a phenolic pincer ligand precursor. In all cases complete conversion of the benzylic bromides was achieved, but removing the excess of phenolic ligand precursor by size exclusion chromatography caused significant loss of product.

The molecular enlarged ligands are retained by an organic nanofiltration membrane (Koch MPF-50) ranging from 70% for the **diPCP 10** to 99% for the **XLtriPCP 8**. Retention tests performed in THF and CH<sub>2</sub>Cl<sub>2</sub> showed that the solvent has little effect on the retention of these ligands whereas in literature the opposite was shown for flexible dendritic molecules. A <sup>1</sup>H NMR study of the **XLtriPCP 8** compound in solution at different concentrations showed no evidence for the formation of aggregates, indicating that the compound is monomeric in solution.

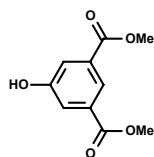
All three ligand systems were reacted with [(allyl)PdCl]<sub>2</sub> and showed activity in the allylic alkylation and amination reactions. The **XLtriPCP**-Pd system will be used for continuous allylic substitution reactions as described in Chapter 4.

## 2.4 Experimental

### General

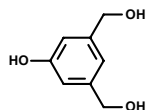
All reactions were performed under an inert atmosphere of argon using standard Schlenk techniques. Chemicals were purchased from Aldrich Chemical Co., Acros or VWR. Solvents were purified using basic alumina columns after degassing. NMR spectra were recorded on a Varian Mercury 400 or 300 spectrometer. GC analyses were performed on a Shimadzu GC-17A (HP Ultra 2 25 m\*0.25 mm column, FID detector).

### Dimethyl 5-hydroxyisophthalate **5**



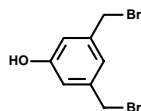
To a solution of 24.0 g 5-hydroxyisophthalic acid (65.9 mmol) in 100 mL MeOH, 6 mL concentrated H<sub>2</sub>SO<sub>4</sub> were added at room temperature. After refluxing the mixture for 20 h, 100 mL of water were added at room temperature giving a solid that was filtered off and washed with cold water. Water was removed by azeotropic drying using toluene. Yield: 13.1 g (95%) as a white solid. <sup>1</sup>H NMR (CD<sub>3</sub>COCD<sub>3</sub>, 300 MHz, δ ppm): 8.12 (s, 1H, ArH), 7.71 (s, 2H, ArH), 3.94 (s, 6H, -OCH<sub>3</sub>).

### 3,5-Bis(hydroxymethyl)phenol **6**



Dimethyl 5-hydroxyisophthalate **5** (10.0 g, 47.6 mmol) was added to a suspension of 4.6 g LiAlH<sub>4</sub> (120 mmol) in 100 mL dry THF. The mixture was stirred for 1 h at room temperature. Afterwards 60 mL 10% H<sub>2</sub>SO<sub>4</sub> were added carefully to hydrolyse the excess LiAlH<sub>4</sub>. After evaporating the solvent, water was added and the product was extracted with ethyl acetate. After drying with MgSO<sub>4</sub>, and evaporation of the solvent, 6.8 g (95%) of product were obtained as a yellow, viscous liquid. <sup>1</sup>H NMR (CD<sub>3</sub>COCD<sub>3</sub>, 300 MHz, δ ppm): 8.29 (s, 1H, ArOH) 6.87 (s, 1H, ArH), 6.80 (s, 2H, ArH), 4.60 (s, 4H, -CH<sub>2</sub>-).

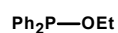
### 3,5-Bis(bromomethyl)phenol **7**



Neat PBr<sub>3</sub> (6.3 mL, 67.0 mmol) was added dropwise using a syringe to a solution of 5.2 g (34.7 mmol) 3,5-bis(hydroxymethyl)phenol **6** in 60 mL dry THF. The so formed clear solution was stirred at room temperature for 4 days. After evaporation of solvent, the product was purified by column chromatography using a mixture of hexane and ethyl acetate (4:1) as eluent, yielding 5.9 g (61%) of the product were a white solid that could be crystallized from ether/hexane. Mp: 80-83 °C. <sup>1</sup>H NMR (CDCl<sub>3</sub>, 300 MHz, δ ppm): 6.99 (s, 1H, ArH) 6.81 (s,

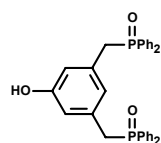
2H, ArH), 4.40 (s, 2H,  $-\text{CH}_2\text{Br}$ ).  $^{13}\text{C}$  NMR ( $\text{CDCl}_3$ , 100 MHz,  $\delta$  ppm): 156.02, 140.10, 122.25, 116.38, 32.98.

### Ethyl diphenylphosphinite



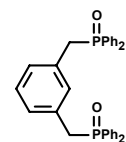
Chlorodiphenylphosphine (20.0 mL, 111 mmol) was added dropwise to a solution of 9.8 mL (120 mmol) pyridine and 7.0 mL (120 mmol) ethanol in 100 mL dry ether. After evaporation of the solvent, the product was purified by vacuum distillation yielding 26.8 g (58 %) of a colorless oil.  $^1\text{H}$  NMR ( $\text{CDCl}_3$ , 400 MHz,  $\delta$  ppm): 7.56-7.33 (m, 10H, ArH), 3.94 (m, 2H), 1.36 (t,  $^3J_{\text{H-H}} = 6.8$  Hz, 3H).  $^{31}\text{P}$  NMR ( $\text{CDCl}_3$ , 162 MHz,  $\delta$  ppm): 110.98.  $^{13}\text{C}$  NMR ( $\text{CDCl}_3$ , 100 MHz,  $\delta$  ppm): 142.54 (d,  $^1J_{\text{P-C}} = 17.4$  Hz), 130.65 (d,  $^2J_{\text{P-C}} = 21.3$  Hz), 129.53, 128.62 (d,  $^2J_{\text{P-C}} = 6.8$  Hz), 66.21 (d,  $^2J_{\text{P-C}} = 19.8$  Hz), 17.50 (d,  $^3J_{\text{P-C}} = 7.5$  Hz).

### 3,5-Bis[(diphenylphosphinoyl)methyl]phenol 4



3,5-Bis(bromomethyl)phenol **7** (6.7 g, 24.0 mmol) was dissolved in *p*-xylene and 11.5 g (50.0 mmol) ethyl diphenylphosphinite were added. After refluxing for 1 h, the mixture was cooled to room temperature and a white solid was formed. The solid was filtered off and washed with cold hexane yielding 12.5 g (98%) of product. Mp: 121-123 °C.  $^1\text{H}$  NMR ( $\text{CDCl}_3$ , 400 MHz,  $\delta$  ppm): 10.09 (s, 1H, ArOH), 7.65-7.35 (m, 20H), 6.78 (s, 2H), 6.45 (s, 1H), 3.46 (d,  $^2J_{\text{P-H}} = 14$  Hz, 4H,  $-\text{CH}_2$ ).  $^{31}\text{P}$  NMR ( $\text{CDCl}_3$ , 162 MHz,  $\delta$  ppm): 30.77.  $^{13}\text{C}$  NMR ( $\text{CDCl}_3$ , 100 MHz,  $\delta$  ppm): 158.32, 132.92, 132.27, 132.08, 131.93, 131.45, 131.36, 128.91, 128.79, 123.30, 116.54, 37.96 (d,  $^1J_{\text{P-C}} = 67.5$  Hz).

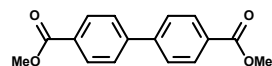
### 3,5-Bis[(diphenylphosphinoyl)methyl]benzene



The experimental conditions are similar to those described for 3,5-bis[(diphenylphosphinoyl)methyl]phenol **4**. Yield: 10.2 g (70.3%). Mp: 144-149 °C.  $^1\text{H}$  NMR ( $\text{CDCl}_3$ , 300 MHz,  $\delta$  ppm): 7.67-7.60 (m, 8H), 7.49-7.36 (m, 12H), 7.00-6.93 (m, 4H), 3.53

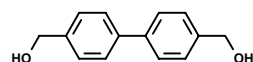
(d,  $^2J_{H-P} = 15$  Hz, 4H,  $-\text{CH}_2$ ).  $^{31}\text{P}$  NMR ( $\text{CDCl}_3$ , 162 MHz,  $\delta$  ppm): 29.6.  $^{13}\text{C}$  NMR ( $\text{CDCl}_3$ , 100 MHz,  $\delta$  ppm): 134.90, 133.23, 132.44, 132.38, 132.30, 132.00, 131.92, 131.66, 131.53, 131.42, 131.36, 131.30, 129.15, 128.82, 128.67, 38.15 (d,  $^1J_{C-P} = 66.0$  Hz).

### Dimethyl-4,4'-biphenylcarboxylate



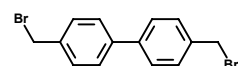
4,4'-Biphenyldicarboxylic acid (0.5 g, 12.3 mmol) was suspended in dry MeOH. 1.6 mL  $\text{H}_2\text{SO}_4$  were added and the mixture was refluxed overnight. The mixture was cooled to room temperature and  $\text{H}_2\text{O}$  was added. The product was filtered off, washed with water and azeotropically dried using toluene. Yield: 3.0 g (90%) of a white solid.  $^1\text{H}$  NMR ( $\text{CDCl}_3$ , 400 MHz,  $\delta$  ppm): 8.14-8.12 (m, 4H, ArH), 3.97 (s, 6H,  $-\text{OMe}$ ).  $^{13}\text{C}$  NMR ( $\text{CDCl}_3$ , 100 MHz,  $\delta$  ppm): 158.15, 144.85, 139.50, 130.63, 127.66, 52.88.

### 4,4'-Dihydroxymethyl biphenyl



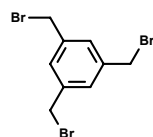
Dimethyl 4,4'-biphenylcarboxylate (3.0 g, 11.1 mmol) were added in portions to a suspension of 1.7 g (44.0 mmol)  $\text{LiAlH}_4$  in dry THF. The resulting mixture was stirred for 1 h at room temperature. Subsequently  $\text{H}_2\text{O}$  was added to hydrolyze the excess of  $\text{LiAlH}_4$ . After evaporating the THF *in vacuo*, the product was isolated by extracting the aqueous solution with ethyl acetate, giving 1.1 g (48%) of the product as a white solid.  $^1\text{H}$  NMR ( $\text{CD}_3\text{COCD}_3$ , 400 MHz,  $\delta$  ppm): 7.69-7.66 (m, 4H, ArH), 7.52-7.49 (m, 4H, ArH), 4.74 (s, 4H,  $\text{CH}_2$ ), 4.37 (br, 2H,  $-\text{OH}$ ).  $^{13}\text{C}$  NMR ( $\text{CD}_3\text{COCD}_3$ , 100 MHz,  $\delta$  ppm): 141.60, 139.41, 127.07, 126.54, 63.51.

### 4,4'-Bis(bromomethyl)biphenyl 3

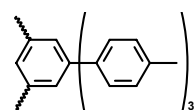


The experimental conditions are similar to those described for 3,5-bis(bromomethyl)phenol. The product was purified by column chromatography using a mixture of EtOAc and hexane as eluent. Yield: 2.0 g (56%).  $^1\text{H}$  NMR ( $\text{CDCl}_3$ , 400 MHz,  $\delta$  ppm): 7.56 (d,  $^3J_{H-H} = 11.6$  Hz, 2H), 7.47 (d,  $^3J_{H-H} = 11.2$  Hz, 2H), 4.55 (s, 2H).  $^{13}\text{C}$  NMR ( $\text{CDCl}_3$ , 100 MHz,  $\delta$  ppm): 140.91, 137.45, 129.91, 127.85, 33.58.

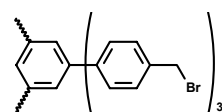


**1,3,5-Tris(bromomethyl)benzene 1**

Mesitylene (10.0 g, 84.0 mmol), NBS (50.0 g, 280 mmol) and AIBN (1.4 g, 8.0 mmol) were suspended in 150 mL EtOAc. This suspension was heated under reflux using an IR bulb. After 18 h, the mixture was cooled to room temperature and concentrated *in vacuo*. Next the product was extracted with boiling hexane. Upon cooling a yellow oil was formed on the bottom of the combined hexane extracts. By removing the hexane and drying *in vacuo*, 26.5 g (88%) product were obtained which were further purified by recrystallizing from hexanes. Yield: 6.8 g (23%).  $^1\text{H}$  NMR ( $\text{CDCl}_3$ , 400 MHz,  $\delta$  ppm): 7.35 (s, 3H), 4.45 (s, 6H).  $^{13}\text{C}$  NMR ( $\text{CDCl}_3$ , 100 MHz,  $\delta$  ppm): 139.22, 129.77, 32.44.

**1,3,5-Tris(*p*-methylphenyl)benzene**

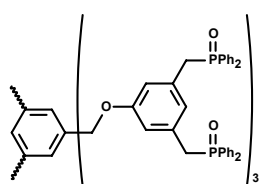
To a solution of 5.0 g (37.3 mmol) 4-methylacetophenone in 200 mL dry ethanol, 47 mL (0.41 mol)  $\text{SiCl}_4$  were added carefully at  $-20\text{ }^\circ\text{C}$ . This yellow solution was heated under reflux for 3 h. After cooling to room temperature,  $\text{H}_2\text{O}$  was added resulting in the formation of a gel-like solid. The excess ethanol was removed under vacuum and the resulting gel was extracted with toluene. The combined organic fractions were washed with 4 M HCl, 4 M NaOH and brine. After drying and removal of the solvent *in vacuo*, 4.3 g (quantitative) product were obtained as a light yellow solid that could be crystallized from toluene.  $^1\text{H}$  NMR ( $\text{CDCl}_3$ , 300 MHz,  $\delta$  ppm): 7.82 (s, 3H, ArH), 7.67 (d,  $^3J_{\text{H-H}} = 7.8\text{ Hz}$ , 6H), 7.37 (d,  $^3J_{\text{H-H}} = 7.8\text{ Hz}$ , 6H).  $^{13}\text{C}$  NMR ( $\text{CDCl}_3$ , 100 MHz,  $\delta$  ppm): 142.51, 138.74, 137.60, 129.87, 127.52, 124.91, 21.48 (ArCH<sub>3</sub>).

**1,3,5-Tris[*p*-bromomethylphenyl]benzene 2**

1,3,5-Tris(*p*-methylphenyl)benzene (1.2 g, 3.4 mmol) was dissolved in 50 mL ethyl acetate, after which 2.1 g (12 mmol) NBS and a few mg of AIBN were added. This mixture was

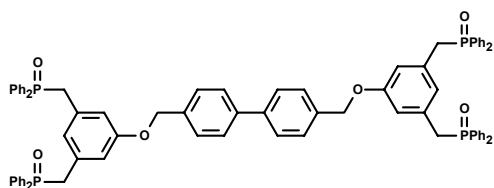
heated to reflux overnight using an IR-bulb. After cooling to room temperature, the solvent was removed *in vacuo*, products were redissolved in chloroform and filtered. Subsequently, the solution was washed with NaHCO<sub>3</sub> and brine. After filtration, the product was precipitated with hexane yielding 1.1 g (50%) product as a light yellow solid. Mp: 170-173 °C. <sup>1</sup>H NMR (CDCl<sub>3</sub>, 300 MHz, δ ppm): 7.75 (s, 3H, ArH), 7.68-7.50 (m, 12H, ArH), 4.58 (s, 6H, -CH<sub>2</sub>Br). <sup>13</sup>C NMR (CDCl<sub>3</sub>, 100 MHz, δ ppm): 142.09, 141.35, 137.59, 129.97, 128.07, 125.62, 33.56(-CH<sub>2</sub>Br).

### $\alpha, \alpha', \alpha''$ -Tris[[3,5-bis[(diphenylphosphinoyl)methyl]phenyl]oxy]mesitylene (StriPCP) **9**



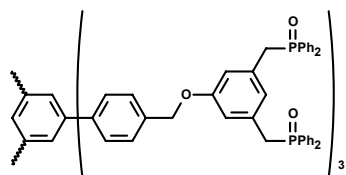
1,3,5-Tris(bromomethyl)benzene **2** (0.61 g, 1.7 mmol) and 3.0 g (5.7 mmol) 3,5-bis[(diphenylphosphinoyl)methyl]phenol **4** were dissolved in CH<sub>3</sub>Cl. Subsequently, 1.4 g (10 mmol) K<sub>2</sub>CO<sub>3</sub> and some 18-crown-6 were added. After stirring for 1 week, water was added and the organic phase was separated and washed with a 4 M NaOH solution. After drying with MgSO<sub>4</sub>, 2.4 g (84%) product were obtained. The product was further purified using SEC with CH<sub>2</sub>Cl<sub>2</sub> as eluent, giving 0.84 g (29%) of pure product. Mp: 139-148 °C. <sup>1</sup>H NMR (CDCl<sub>3</sub>, 400 MHz, δ ppm): 7.67-7.59 (m, 27H), 7.49-7.37 (m, 36H), 7.18 (s, 3H), 6.58 (s, 6H), 6.58 (s, 6H), 4.69 (s, 6H, -CH<sub>2</sub>O), 3.53 (d, <sup>2</sup>J<sub>P-H</sub> = 4.0 Hz, 12H, -CH<sub>2</sub>P). <sup>31</sup>P NMR (CDCl<sub>3</sub>, 162 MHz, δ ppm): 29.37. <sup>13</sup>C NMR (CDCl<sub>3</sub>, 100 MHz, δ ppm): 158.51, 137.44, 132.86, 131.81, 131.15 (d, <sup>2</sup>J<sub>P-C</sub> = 9.1 Hz), 128.57 (d, <sup>2</sup>J<sub>P-C</sub> = 11.4 Hz), 125.82, 125.10, 115.21, 69.44, 38.06 (d, <sup>1</sup>J<sub>P-C</sub> = 65.2 Hz). MALDI-TOF-MS: m/z 1682.4 ([M+H]<sup>+</sup>, calcd 1682.71), 1704.4 ([M+Na]<sup>+</sup>, calcd 1704.7), 1720.4 ([M+K]<sup>+</sup>, calcd 1720.8). Anal. calcd for C<sub>105</sub>H<sub>96</sub>O<sub>12</sub>P<sub>6</sub>·3H<sub>2</sub>O: C, 72.66; H, 5.57; P, 10.71. Found: C, 72.76; H, 5.53; P, 10.71.

### 4,4'-Bis[[3,5-bis[(diphenylphosphinoyl)methyl]phenyl]oxy]dimethylbiphenyl (diPCP) **10**



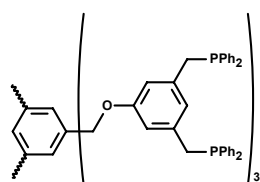
The experimental conditions are similar to those described for **StriPCP 9**. Yield: 1.4 g of a light brown solid which was further purified by SEC yielding 0.34 g (28 %) product. Mp: 110-112 °C.  $^1\text{H}$  NMR ( $\text{CDCl}_3$ , 400 MHz,  $\delta$  ppm): 7.66-7.33 (m, 48H), 6.65 (s, 2H), 6.58 (s, 4H), 4.76 (s, 4H,  $\text{CH}_2\text{O}$ ), 3.52 (d,  $^2J_{P-H} = 13.6$  Hz, 8H,  $\text{CH}_2\text{-P}$ ).  $^{31}\text{P}$  NMR ( $\text{CDCl}_3$ , 162 MHz,  $\delta$  ppm): 29.56.  $^{13}\text{C}$  NMR ( $\text{CDCl}_3$ , 100 MHz,  $\delta$  ppm): 158.67, 140.53, 136.22, 133.02, 132.93, 132.83, 132.04, 131.97, 131.32 (d,  $^2J_{P-C} = 9.1$  Hz), 128.73 (d,  $^2J_{P-C} = 12.2$ ), 128.17, 127.34, 125.22, 115.48, 69.60, 38.15 (d,  $^1J_{P-H} = 66.0$  Hz). MALDI-TOF-MS:  $m/z$  1223.4 ( $[\text{M}]^+$ , calcd 1223.3), 1245.4 ( $[\text{M}+\text{Na}]^+$ , calcd 1245.4), 1261.3 ( $[\text{M}+\text{K}]^+$ , calcd 1261.3). Anal. calcd for  $\text{C}_{78}\text{H}_{66}\text{O}_6\text{P}_4 \cdot \text{CH}_2\text{Cl}_2$ : C, 72.53; H, 5.24. Found: C, 72.65; H, 5.37.

**$\alpha, \alpha', \alpha''$ -Tris[[3,5-bis[(diphenylphosphino)ethyl]phenyl]oxy]-1,3,5-tris(*p*-methylphenyl)benzene (XLtriPCP) 8**



The experimental conditions are similar to those described for **StriPCP 9**. Yield: 2.2 g (61%) which was further purified by SEC yielding 1.0 g (27%) product.  $^1\text{H}$  NMR ( $\text{CDCl}_3$ , 400 MHz,  $\delta$  ppm): 7.78 (s, 3H), 7.68-7.63 (m, 24H), 7.51-7.42 (m, 48H), 6.67 (s, 3H), 6.60 (s, 6H), 4.81 (s, 6H,  $\text{CH}_2\text{-O}$ ), 3.53 (d,  $^2J_{P-H} = 13.6$  Hz 12H).  $^{31}\text{P}$  NMR ( $\text{CDCl}_3$ , 162 MHz,  $\delta$  ppm): 29.55.  $^{13}\text{C}$  NMR ( $\text{CDCl}_3$ , 100 MHz,  $\delta$  ppm): 158.78, 142.35, 140.90, 136.63, 133.13, 132.11, 131.45 (d,  $^2J_{P-C} = 9.1$  Hz), 128.85 (d,  $^2J_{P-C} = 12.1$ ), 128.35, 127.73, 125.43, 115.61, 69.72, 38.29 (d,  $^1J_{P-C} = 66.8$  Hz). MALDI-TOF-MS:  $m/z$  1910.7 ( $[\text{M}+\text{H}]^+$ , calcd 1911.0), 1932.7 ( $[\text{M}+\text{Na}]^+$ , calcd 1933.0). Anal. calcd for  $\text{C}_{123}\text{H}_{102}\text{O}_9\text{P}_6 \cdot 1.5\text{CH}_2\text{Cl}_2$ : C, 73.40; H, 5.19. Found: C, 73.91; H, 5.33.

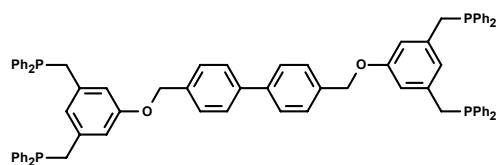
**$\alpha, \alpha', \alpha''$ -Tris[[3,5-bis[(diphenylphosphino)ethyl]phenyl]oxy]mesitylene**



Phosphinoyl **9** (0.8 g, 0.5 mmol) was suspended in toluene and 1.4 mL (15 mmol)  $\text{HSiCl}_3$  were added by syringe. Subsequently this mixture was refluxed for 2 h, cooled to room

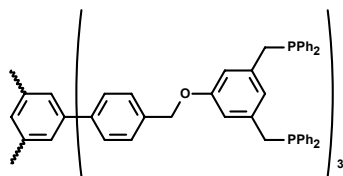
temperature and concentrated *in vacuo*. The resulting oil was dissolved in  $\text{CH}_2\text{Cl}_2$  and hydrolysed with degassed 4 M NaOH. The aqueous phase was separated and extracted 3 times with  $\text{CH}_2\text{Cl}_2$ . The combined organic fractions were dried using  $\text{MgSO}_4$  and concentrated *in vacuo* giving the product in quantitative yield as an off white solid.  $^1\text{H}$  NMR ( $\text{CDCl}_3$ , 300 MHz,  $\delta$  ppm): 7.70-7.29 (m, 63H), 6.58 (s, 3H), 6.44 (s, 6H), 4.73 (s, 6H,  $\text{ArCH}_2\text{O}$ ), 3.31 (s, 12H,  $\text{ArCH}_2\text{P}$ ).  $^{31}\text{P}$  NMR ( $\text{CDCl}_3$ , 162 MHz,  $\delta$  ppm): -9.33.  $^{13}\text{C}$  NMR ( $\text{CDCl}_3$ , 75 MHz,  $\delta$  ppm): 139.14, 138.76, 138.56, 138.05, 133.25 (d,  $^2J_{\text{P-C}} = 18.8$  Hz), 132.16, 131.53, 128.86 (d,  $^2J_{\text{P-C}} = 20.0$ ), 128.64, 126.18, 123.71, 113.88, 100.50, 69.75, 36.32 (d,  $^1J_{\text{P-C}} = 15.9$  Hz).

#### 4,4'-Bis[[3,5-bis((diphenylphosphino)methyl)phenyl]oxy]dimethylbiphenyl



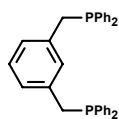
The experimental conditions are similar to those described for **StriPCP**. Yield: quantitative as white solid.  $^1\text{H}$  NMR ( $\text{CDCl}_3$ , 300 MHz,  $\delta$  ppm): 7.60-7.30 (m, 48H), 6.56 (s, 2H), 6.43 (s, 4H), 4.77 (s, 4H,  $\text{ArCH}_2\text{O}$ ), 3.29 (s, 8H,  $\text{ArCH}_2\text{P}$ ).  $^{31}\text{P}$  NMR ( $\text{CDCl}_3$ , 162 MHz,  $\delta$  ppm): -15.93.  $^{13}\text{C}$  NMR ( $\text{CDCl}_3$ , 75 MHz,  $\delta$  ppm): 194.81, 158.87, 139.15, 138.79, 138.58, 133.26 (d,  $^2J_{\text{P-C}} = 18.2$  Hz), 128.85 (d,  $^2J_{\text{P-C}} = 19.4$  Hz), 128.64, 128.31, 127.55, 113.99, 69.75, 36.35 (d,  $^1J_{\text{P-C}} = 15.9$  Hz).

#### $\alpha, \alpha', \alpha''$ -Tris[3,5-bis-(diphenylphosphino)methyl)phenyl]oxy]-1,3,5-tri(p-methylphenyl) benzene



The experimental conditions are similar to those described for **StriPCP**. Yield: quantitative as light yellow solid.  $^1\text{H}$  NMR ( $\text{CDCl}_3$ , 400 MHz,  $\delta$  ppm): 7.77 (s, 3H, ArH), 7.69 (d,  $^3J_{\text{H-H}} = 8.0$  Hz, 6H), 7.43 (d,  $^3J_{\text{H-H}} = 8.4$  Hz, 6H), 7.45-7.30 (m, 60H), 6.55 (s, 3H), 6.43 (s, 6H), 4.79 (s, 6H,  $\text{ArCH}_2\text{O}$ ), 3.30 (s, 12H,  $\text{ArCH}_2\text{P}$ ).  $^{31}\text{P}$  NMR ( $\text{CDCl}_3$ , 162 MHz,  $\delta$  ppm): -9.88.

### 3,5-Bis[diphenylphosphino)methyl]benzene



The experimental conditions are similar to those described for **StriPCP**. Yield: quantitative as colorless oil.  $^1\text{H}$  NMR ( $\text{CDCl}_3$ , 400 MHz,  $\delta$  ppm): 7.64-7.41 (m, 20H, ArH), 7.19 (m, 2H, ArH), 7.06 (m, 2H, ArH), 3.57 (s, 4H,  $-\text{CH}_2$ ).  $^{31}\text{P}$  NMR ( $\text{CDCl}_3$ , 162 MHz,  $\delta$  ppm): -9.94.  $^{13}\text{C}$  NMR ( $\text{CDCl}_3$ , 100 MHz,  $\delta$  ppm): 138.63 (d,  $^1J_{\text{P-C}} = 15.1$  Hz), 137.64 (d,  $^3J_{\text{P-C}} = 8.4$  Hz), 133.21 (d,  $^1J_{\text{P-C}} = 18.2$  Hz), 130.76 (t,  $^3J_{\text{P-C}} = 6.8$  Hz), 128.95, 128.64 (d,  $^3J_{\text{P-C}} = 6.8$  Hz), 128.41, 127.30 (d,  $^3J_{\text{P-C}} = 6.8$  Hz), 36.18 (d,  $^1J_{\text{P-C}} = 15.2$  Hz).

#### Allylic alkylation reaction

In an oven-dried Schlenk flask were successively added, under protective atmosphere, 0.5 mmol decane (internal standard), 1.0 mmol cinnamyl acetate, 2.0 mmol dimethyl malonate, 2.0 mmol BSA ((N,O-bis(trimethylsilyl) acetamide) and a small amount of KOAc.  $\text{CH}_2\text{Cl}_2$  was added to a total volume of 10 mL. The catalyst was prepared *in situ* by mixing the respective ligand with  $[(\text{allyl})\text{PdCl}]_2$  in  $\text{CH}_2\text{Cl}_2$  (ratio 2:1) and stirring this solution a room temperature for 0.5 h. In the case of **XLtriPCP** the catalyst preformation was performed in dichlorobenzene for solubility reasons. The catalysis was started by adding the catalyst to the premixed substrate solution. Samples were taken, filtered over a small pad of silica with diethyl ether as eluent, and analysed by GC.

#### Allylic amination reaction

In an oven-dried Schlenk flask were successively added, under protective atmosphere, 0.5 mmol decane (internal standard), 1.0 mmol cinnamyl acetate, 2.0 mmol morpholine.  $\text{CH}_2\text{Cl}_2$  was added to a total volume of 10 mL. The catalyst was prepared similar to the catalyst used for the allylic alkylation. The catalysis was started by adding the catalyst to the premixed substrate solution. Samples were taken, filtered over a small pad of basic column with MeOH as eluent, and analyzed by GC.

## Retention measurement

### Retention measurement in CH<sub>2</sub>Cl<sub>2</sub>

The nanofiltration membrane, stored in water/ethanol mixture, was immersed overnight in methanol and put into a CH<sub>2</sub>Cl<sub>2</sub> bath for 1 h prior to use. Subsequently, the membrane was cut and installed into the membrane reactor and flushed with 25 mL of CH<sub>2</sub>Cl<sub>2</sub>. The test compound was dissolved in 3 mL of CH<sub>2</sub>Cl<sub>2</sub> of which 2 mL were injected into the reactor. Next 50 mL of solvent were flushed through the reactor, with a flow rate of 20 mL/h at 20 bar, and collected in a measuring flask. The retention was determined by UV/vis spectroscopy.

### Retention measurement in THF

The retention was measured similar to the measurement in CH<sub>2</sub>Cl<sub>2</sub>, but the membrane was immersed only for 1 h in THF before use. Since the compounds are absorbing light in the same wavelength region as THF, the solvent was replaced by CH<sub>2</sub>Cl<sub>2</sub>, by evaporating the THF *in vacuo* followed by stripping the solvent using 5 mL of CH<sub>2</sub>Cl<sub>2</sub>, for 3 times. Subsequently, the compound was redissolved in CH<sub>2</sub>Cl<sub>2</sub>, and the UV/Vis spectrum was measured.

## 2.5 References and Notes

- <sup>1</sup> B. Cornils, W. A. Herrmann, *J. Catal.* **2003**, *216*, 23.
- <sup>2</sup> A. Zapf, M. Beller, *Topics in Catal.* **2002**, *19*, 101.
- <sup>3</sup> W. A. Herrmann, B. Cornils, *Angew. Chem.* **1997**, *109*, 1074.
- <sup>4</sup> U. Kragl, C. Dreisbach, C. Wandrey, in B. Cornils, W. A. Herrmann (Eds.): *Applied Homogeneous Catalysis with Organometallic Compounds*, vol. 2, VCH, Weinheim, **1996**, p 832.
- <sup>5</sup> A. Behr, *Chemie Ing. Tech.*, **1998**, *70*, 685.
- <sup>6</sup> I. F. J. Vankelecom, P. A. Jacobs, in *Immobilization of Chiral Catalysts*, ed. D. de Vos, I.F.J. Vankelecom and P. A. Jacobs, VCH, Weinheim, 2000, ch. 2, p 19.
- <sup>7</sup> H. P. Dijkstra, G. P. M. van Klink, G. van Koten, *Acc. Chem. Res.* **2002**, *35*, 798.
- <sup>8</sup> E. B. Eggeling, N. J. Hovestad, J. T. B. H. Jastrzebski, D. Vogt, G. van Koten, *J. Org. Chem.* **2000**, *65*, 8857.
- <sup>9</sup> H. P. Dijkstra, N. J. Ronde, G. P. M. van Klink, D. Vogt, G. van Koten, *Adv. Synth. Catal.* **2003**, *345*, 364.
- <sup>10</sup> J. T. Singleton, *Tetrahedron*, **2003**, *59*, 1837.
- <sup>11</sup> M. E. van der Boom, D. Milstein, *Chem. Rev.* **2003**, *103*, 1759.
- <sup>12</sup> R. E. Pearson, J. C. Martin, *J. Am. Chem. Soc.* **1963**, *85*, 3142.
- <sup>13</sup> S. S. Elmorsy, A. Pelter, K. Smith, *Tetrahedron Lett.* **1991**, *32*, 4175.

- <sup>14</sup> P. R. Ashton, D. W. Anderson, C. L. Brown, A. N. Shipway, J. F. Stoddart, M. S. Tolley, *Chem. Eur. J.* **1998**, *4*, 781.
- <sup>15</sup> V. Boekelheide, R. W. Griffin, *J. Org. Chem.* **1969**, *34*, 1960.
- <sup>16</sup> W. T. S. Huck, B. Snellink-Ruël, F. C. J. M. van Veggel, D. N. Reinhoudt, *Organometallics* **1997**, *16*, 4287.
- <sup>17</sup> P. Steenwinkel, S. Kolmschot, R. A. Gossage, P. Dani, N. Veldman, A. L. Spek, G. van Koten, *Eur. J. Inorg. Chem.* **1998**, 477.
- <sup>18</sup> D. de Groot, *Dendrimers as Homogeneous Transition Metal Catalysts*, Thesis, Universiteit van Amsterdam, **2001**.
- <sup>19</sup> A. S. Shetty, J. Zhang, J. S. Moore, *J. Am. Chem. Soc.* **1996**, *118*, 1019.
- <sup>20</sup> J. M. Longmire, X. Zhang, *Tetrahedron Lett.* **1997**, *38*, 1725.
- <sup>21</sup> H. P. Dijkstra, M. Q. Slagt, A. McDonald, C. A. Kruithof, R. Kreiter, A. M. Mills, M. Lutz, A. L. Spek, W. Klopper, G. P. M. van Klink, G. van Koten, *Eur. J. Inorg. Chem.* **2003**, 830.
- <sup>22</sup> K. Burgess, L. T. Liu, B. Pal, *J. Org. Chem.* **1993**, *58*, 4758.
- <sup>23</sup> P. Magnus, J. Lacour, I. Coldham, B. Mugrage, W.B. Bauta, *Tetrahedron*, **1995**, *51*, 11078.
- <sup>24</sup> B. M. Trost, D. L. Van Vranken, *J. Am. Chem. Soc.* **1993**, *115*, 444.
- <sup>25</sup> B. M. Trost, M. L. Crawley, *Chem. Rev.* **2003**, *103*, 2921.

# 3

## The Kinetics of the Allylic Amination Reaction

### Abstract

---

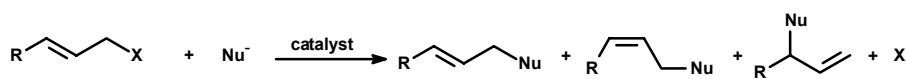
In this chapter a study on the kinetic parameters of the allylic amination reaction is presented. The catalyst used for this reaction is the PCP-Pd system discussed in Chapter 2. It was found that the reaction of cinnamyl acetate (CA) with morpholine (Mor) is zeroth order in cinnamyl acetate and first order in morpholine. The order in catalyst was found to be one. Furthermore, the rate constant  $k'$  was determined for a reaction under standard conditions, to have a value of  $6.68 \cdot 10^{-2} \text{ h}^{-1}$ . This led to the rate equation:  $r = k[CA]^0[Mor]^{1.0}[Cat]^{1.2} = k'[Mor]$ .

---



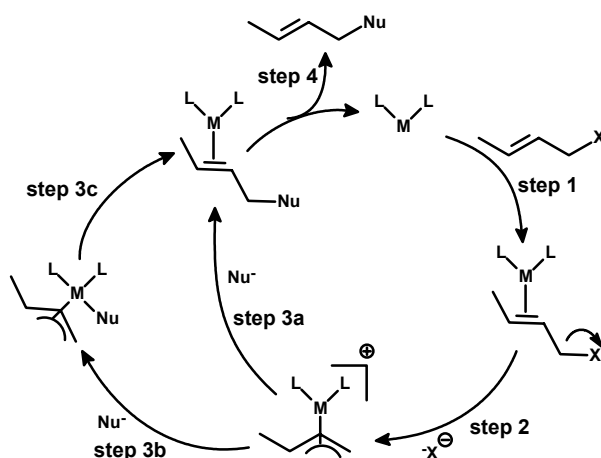
### 3.1 Introduction

Since the discovery of the palladium-catalyzed allylic alkylation reaction by Tsuij *et al.* in 1965,<sup>1</sup> intensive research has been carried out in the field of allylic substitution reactions. The general reaction is shown in Scheme 1. A leaving group, e.g. an acetate group, is displaced by a nucleophile. This nucleophile can be for example dimethyl malonate in case of the allylic alkylation reaction or by morpholine in case of the allylic amination reaction. The allylic alkylation and amination reaction can be catalyzed by nickel,<sup>2</sup> platinum,<sup>3</sup> rhodium,<sup>4</sup> iron,<sup>5,6</sup> iridium,<sup>7</sup> ruthenium,<sup>8</sup> molybdenum,<sup>9</sup> copper,<sup>10</sup> cobalt<sup>11</sup> and tungsten<sup>12</sup> complexes. However, palladium complexes have mostly been investigated.<sup>13,14</sup>



**Scheme 1:** General allylic substitution reaction.

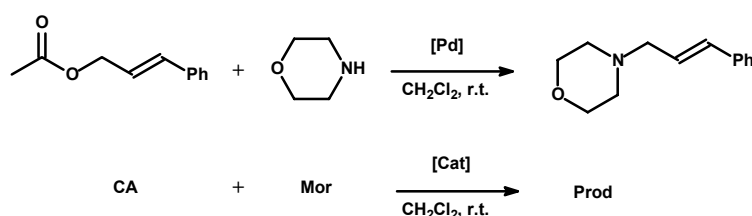
The mechanism of the palladium-catalyzed allylic amination is generally accepted to proceed via either a neutral or a cationic  $\pi$ -allyl palladium complex, which is formed by oxidative addition of the substrate to the palladium (step 1 and 2, Scheme 2). The so formed allyl-palladium complexes have been thoroughly investigated<sup>15</sup> and are often relatively easy to crystallize.<sup>16, 17</sup> In the case of hard nucleophiles, the next step is the attack of the nucleophile on the palladium followed by insertion of the nucleophile into the allyl-metal bond. When soft nucleophiles are used, the attack takes place directly on the allyl fragment<sup>13</sup> (step 3).



**Scheme 2:** Mechanism of allylic substitution reaction.

The allylic alkylation and amination reactions are applied in total synthesis reactions<sup>18</sup> as well as in the synthesis of amino acids, alkaloids or carbohydrate derivatives by transformation of the allyl amines produced by allylic amination.<sup>19,20,21</sup> The substitution reactions have also become a method for testing and comparing novel mono- and bidentate phosphorus ligands, whether or not chiral. The experimental conditions are very mild, the reaction is carried out at room temperature and at ambient pressure in common organic solvents such as dichloromethane, THF or in more polar solvents like methanol, DMF or DMSO. The products can easily be analyzed by gas chromatography making this an ideal test reaction.

These reasons lead us to use this reaction to test our catalytic systems in continuous reactions using nanofiltration membranes for the separation of the catalyst from the products.<sup>22,23</sup> For this purpose we used pincer ligand systems, coordinated to palladium. From literature it is known that these systems are active in the allylic substitution reactions.<sup>24</sup> To gain complete understanding of the processes going on in the reactor and to calculate the expected conversions at a given residence time,<sup>25</sup> the kinetics should be known. To our knowledge these data have not been determined for the system we are using. The reagents used in our reactions are cinnamyl acetate (CA) as the allyl source and morpholine (Mor) acting as nucleophile (Scheme 3).



**Scheme 3:** Allylic amination reaction examined in this work.

Equation 1.1 gives the rate of the reaction, which can be expressed in terms of concentrations, where m, n and o are the orders in reactants, respectively, as shown in equation 1.2.<sup>26</sup>

$$r = -\frac{d[\text{CA}]}{dt} = -\frac{d[\text{Mor}]}{dt} = \frac{d[\text{prod}]}{dt} \quad \text{equation 1.1}$$

$$= k[\text{CA}]^m [\text{Mor}]^n [\text{Cat}]^o \quad \text{equation 1.2}$$

The concentration of the catalyst can be taken as a constant since it is neither consumed nor produced (one of the definitions of a catalyst) leading to *equation 1.3*.

$$r = k'[CA]^m[Mor]^n \quad \text{equation 1.3}$$

When the concentration of morpholine is high (> 5 times higher than [CA]) compared to the concentration of cinnamyl acetate, it can be taken as a constant and can be put into the rate constant (*equation 1.4*).<sup>27</sup>

$$r = k''[CA]^m \quad \text{equation 1.4}$$

This gives a rate expression of a pseudo first order reaction. The same can be done with the concentration of cinnamyl acetate giving *equation 1.5*.

$$r = k'''[Mor]^n \quad \text{equation 1.5}$$

Performing a series of catalytic runs, varying one concentration while keeping the others constant, information can be obtained about the order in the different compounds. When the logarithm of the rate of the reaction is plotted versus the logarithm of the starting concentrations, a straight line is obtained with a slope equal to the order of the reagent (*equations 2.1 – 2.3*).

$$\ln r = \ln k'''+m \ln[CA] \quad \text{equation 2.1}$$

$$\ln r = \ln k'''+n \ln[Mor] \quad \text{equation 2.2}$$

$$\ln r = \ln k'''+o \ln[Cat] \quad \text{equation 2.3}$$

In this way, the order in the three “reactants” can be determined. The final parameter to determine is the rate constant, which can be determined by following a catalytic run in time and plotting the concentrations versus time. The tangent of the line at lower conversions gives

the reaction speed (equation 3.1) and dividing this rate by the concentrations gives the rate constant (equation 3.2).

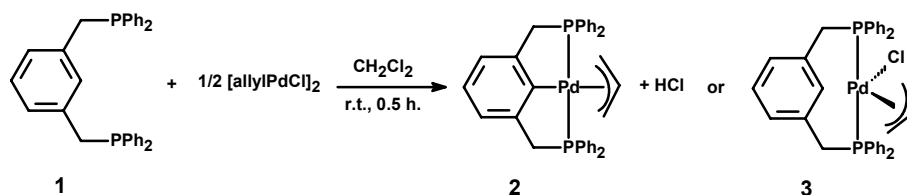
$$r = -\frac{d[CA]}{dt} = -\frac{d[Mor]}{dt} = \frac{d[prod]}{dt} = k[CA]^m[Mor]^n[Cat]^o \quad \text{equation 3.1}$$

$$k = -\frac{\Delta[CA]/\Delta t}{[CA]^m[Mor]^n[Cat]^o} \quad \text{equation 3.2}$$

In this chapter the kinetic parameters, the orders in reactants, as well as the rate constant of the allylic amination reaction of cinnamyl acetate and morpholine are investigated.

### 3.2 Results and Discussion

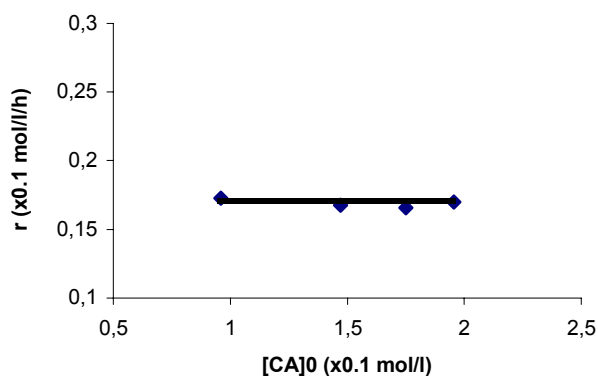
As discussed above, in this study, cinnamyl acetate and morpholine are used as reagents in the allylic amination. These reagents are often used in allylic aminations, which facilitates the comparison of different catalytic systems. The catalyst used in this study was synthesized by reaction of [(allyl)PdCl]<sub>2</sub> with PCP-pincer ligand<sup>28</sup> **1** in a ratio of 1:2 (Scheme 4) at room temperature within 0.5 h. Normally, PCP-metal complexes are synthesized by refluxing the precursor with a ligand in e.g. toluene<sup>29</sup> or acetonitrile.<sup>30</sup> In this study we do not heat the ligand/metal mixture during preformation according to the procedure used by Zhang *et al.*<sup>24</sup> This makes it debatable whether a PCP complex **2** (with a carbon metal bond) or a PP complex **3** (coordinated as a diphosphine) is formed. NMR studies of this in situ complex show multiple species including a fluxional species, with a broad peak in the <sup>31</sup>P NMR (Scheme 4). The exact nature of this palladium complex is currently under investigation.



Scheme 4: Complexation of Pd ligand **1**.

### 3.2.1 Variation in Cinnamyl Acetate

To determine the order in cinnamyl acetate, a series of four catalytic experiments is carried out using an excess of morpholine (5 mol/l), 2  $\mu\text{mol}$  catalyst and a varied concentration of cinnamyl acetate (1.0 – 2.0 mol/l). By keeping the concentration of morpholine and the catalyst constant, the reaction becomes pseudo first order in cinnamyl acetate. When  $d[\text{prod}]/dt$  is plotted versus the starting concentration  $[\text{CA}]_0$  no change in reaction speed is observed, which indicates a zeroth order in cinnamyl acetate (Graph 1).



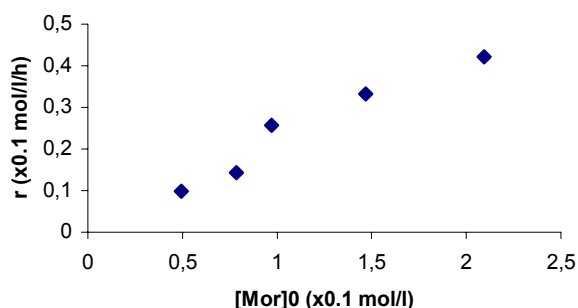
**Graph 1:** Influence of  $[\text{CA}]$  on the reaction rate.

This zeroth order in cinnamyl acetate can be explained by the rapid formation of the allyl-palladium species, while one of the next steps determines the rate of the reaction. This rate-determining step could be the insertion of the amine on palladium or directly on the allyl species, substrate deprotonation or product dissociation (*vide infra*).

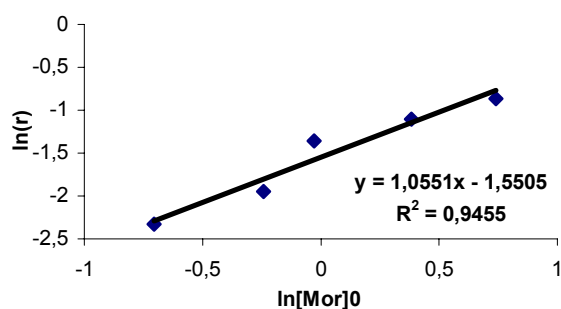
### 3.2.2 Determination of the Order in Morpholine

The order in morpholine is determined in the same way as described for cinnamyl acetate. The concentration was varied in 5 steps between 0.5 – 2.0 mol/l. Samples were taken after 0.5 h and analyzed by GC. When the reaction rate is plotted versus the varied starting concentrations of morpholine  $[\text{Mor}]_0$ , a linear relation is observed pointing towards a first

order in morpholine. The exact order can be obtained by plotting the logarithm of  $r$  versus the logarithm of the starting concentrations of morpholine as given by *equation 2.2*.



**Graph 2:** Influence of [Mor] on the reaction rate.

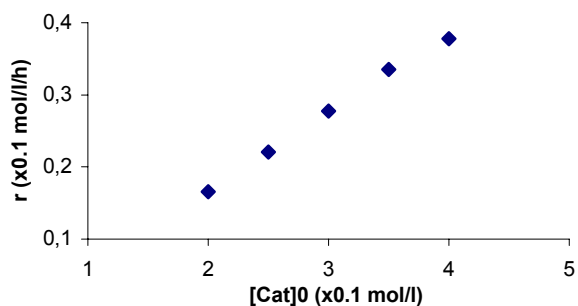


**Graph 3:** Determination of the order in morpholine.

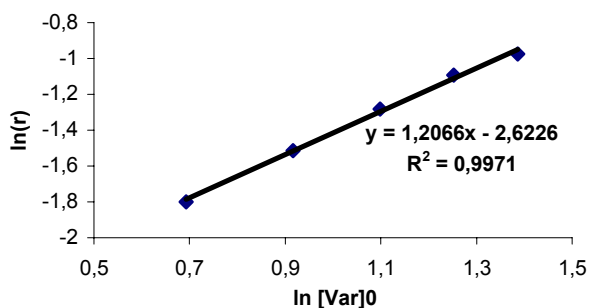
From Graph 3 the order can be determined from the slope of the obtained line. The intercept of the line gives the pseudo rate constant. As can be seen in the graph, the order in morpholine is 1 and the obtained pseudo rate constant has a value of  $0.4 \text{ h}^{-1}$ . A first order in morpholine means that morpholine plays a role in the rate-determining step. This can be explained, for example, by the addition of morpholine to the palladium center or direct attack on the allyl fragment, or the deprotonation of the Zwitterions formed in a previous step (step 3 or 4, Scheme 5).

### 3.2.3 Order in Catalyst

The order in catalyst was determined by varying the concentration of catalyst between  $2 \cdot 10^{-4}$  and  $4 \cdot 10^{-4}$  mmol/mL. By plotting the logarithm of the reaction rate against the logarithm of the starting concentrations a straight line is obtained with a slope of 1.2 (Graph 5).



**Graph 4:** Influence of [cat] on the reaction rate.



**Graph 5:** Determination of the order in catalyst.

The meaning of this nearly first order in catalyst is the involvement of a mononuclear species in the catalytic cycle.

### 3.2.4 Determination of the Rate Constant

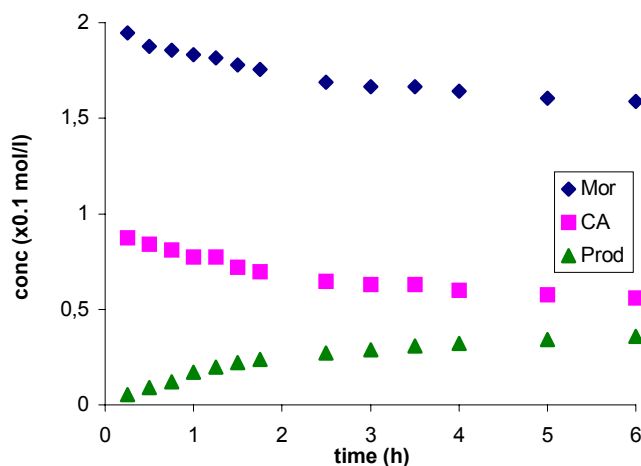
As shown previously, the order in cinnamyl acetate is zero and the concentration of the catalyst will stay constant during the reaction. These terms of the rate equation can be put into the rate constant to give rate *equation 4.1*.

$$r = -\frac{d[Mor]}{dt} = k'[Mor] \quad \text{equation 4.1}$$

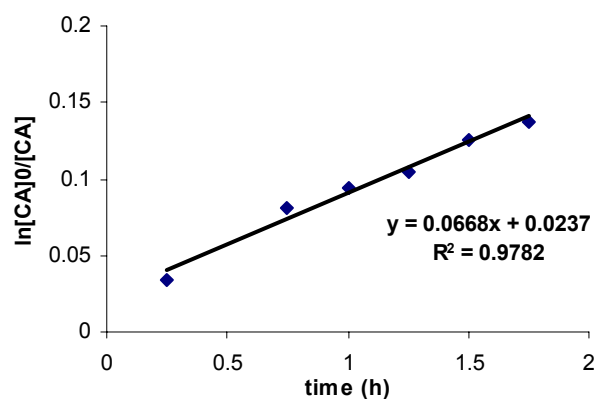
This is the rate equation for an irreversible first order reaction. Integrating of this equation gives equation 4.2.

$$k't = \ln\left(\frac{[Mor]_0}{[Mor]}\right) \quad \text{equation 4.2}$$

This permits one to find the  $k'$  from the slope of a plot of  $\ln[Mor]/[Mor]_0$  versus time, as is shown in Graph 7.



Graph 6: Concentration gradients in time.



Graph 7: Determination of  $k'$ .



From Graph 7 it can be seen that the rate constant  $k'$  is  $6.68 \cdot 10^{-2} \text{ h}^{-1}$  when using  $[\text{CA}]_0 = 0.1 \text{ mol/l}$ ,  $[\text{Mor}]_0 = 0.2 \text{ mol/l}$ , and  $[\text{Cat}]_0 = 0.2 \cdot 10^{-3} \text{ mol/l}$ .

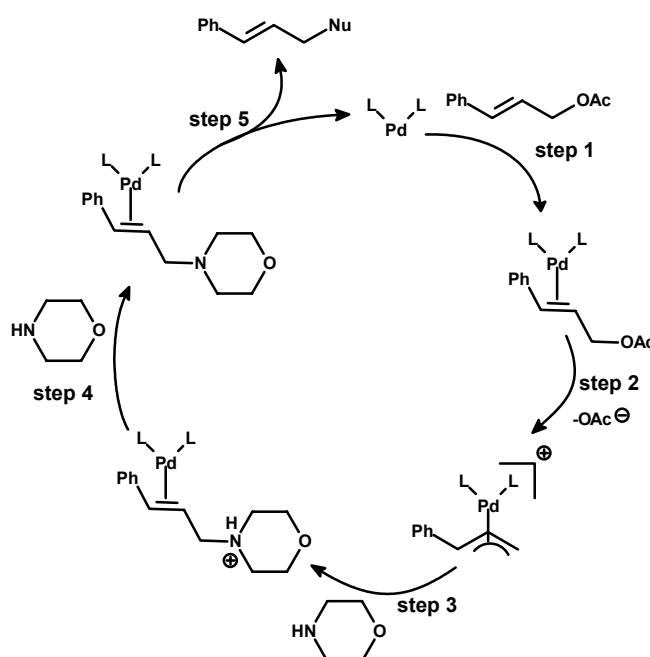
### 3.3 Conclusions

In summary, we have investigated the kinetics of the allylic amination of cinnamyl acetate with morpholine. We have found that this reaction is zeroth order in cinnamyl acetate, first order in morpholine and almost first order in catalyst giving the rate *equation 5.1*.

$$r = k[\text{CA}]^0[\text{Mor}]^{1.0}[\text{Cat}]^{1.2} = k'[\text{Mor}] \quad \text{equation 5.1}$$

The rate constant  $k'$  found for the reaction under standard conditions is  $6.68 \cdot 10^{-2} \text{ h}^{-1}$ .

The zero order in cinnamyl acetate can be explained by a fast oxidative addition of cinnamyl acetate to the palladium center (step 1 and 2, Scheme 5), followed by a slow step involving morpholine causing a first order in morpholine. This slow step can be the attack of the amine on the allyl fragment (step 3) or the deprotonation of the Zwitterions formed (step 4) as discussed by Åkermark *et al.*<sup>31</sup> and Jutand *et al.*<sup>32</sup>



**Scheme 5:** Mechanism of allylic amination of cinnamyl acetate.

### 3.4 Experimental

#### General

All reactions were performed under an inert atmosphere of argon using standard Schlenk techniques. Chemicals were purchased from Aldrich Chemical Co., Acros or VWR. Solvents were purified using basic alumina columns after degassing. 1,3-Bis[(diphenylphosphino)methyl]benzene<sup>33</sup> and [(allyl)PdCl]<sub>2</sub><sup>34</sup> were synthesized according to literature procedures. Morpholine and decane were distilled from CaH<sub>2</sub>, cinnamyl acetate was degassed and stored over molecular sieves. Gas chromatographic analyses were performed on a Shimadzu GC-17A equipped with a 25 m ULTRA-2 column.

#### Typical allylic amination experiment

In an oven-dried Schlenk flask were added under inert atmosphere 100 µl (0.51 mmol) decane (internal standard), 167 µl (1.0 mmol) cinnamyl acetate and 174 µl (2.0 mmol) morpholine. Dichloromethane was added to a total volume of 10 mL. Subsequently the catalyst solution was added to start the catalysis. Samples were taken using a pipette, which were filtered over basic alumina using MeOH as eluent. Conversions were determined using GC analysis.

### 3.5 References and Notes

- <sup>1</sup> M. Morikawa, J. Takahashi, J. Tsuji, *Tetrahedron Lett.* **1965**, *6*, 4387.
- <sup>2</sup> H. Bricout, J.-F. Carpentier, A. Mortreux, *Tetrahedron* **1998**, *54*, 1073.
- <sup>3</sup> J. M. Brown, J. E. Macintyre, *J. Chem. Soc. Perkin Trans. 2* **1985**, 961.
- <sup>4</sup> P. A. Evans, L.J. Kennedy, *Tetrahedron Lett.* **2001**, *42*, 7015.
- <sup>5</sup> R. S. Srivastava, K. M. Nicholas, *J. Am. Chem. Soc.* **1997**, *119*, 3302.
- <sup>6</sup> M. Johannsen, K. A. Jørgensen, *J. Org. Chem.* **1994**, *59*, 214.
- <sup>7</sup> C. A. Kiener, C. Shu, C. Incarvito, J. F. Hartwig, *J. Am. Chem. Soc.* **2003**, *125*, 14272.
- <sup>8</sup> M. D. Mbaye, B. Demerseman, J.-L. Renaud, L. Toupet, C. Bruneau, *Angew. Chem. Int. Ed.* **2003**, *42*, 5066.
- <sup>9</sup> O. Belda, C. Moberg, *Synthesis* **2002**, *11*, 1601.
- <sup>10</sup> R. S. Srivastava, *Tetrahedron Lett.* **2003**, *44*, 3271.
- <sup>11</sup> I. Minami, I. Shimizu, J. Tsuji, *J. Organometallic Chem.* **1985**, *296*, 269.
- <sup>12</sup> A. V. Malkov, I. R. Baxendale, D. Dvorak, D. J. Mansfield, P. Kocovsky, *J. Org. Chem.* **1999**, *64*, 2737.
- <sup>13</sup> B. M. Trost, D. L. Van Vranken, *Chem. Rev.* **1996**, *96*, 395.
- <sup>14</sup> M. Johannsen, K. A. Jørgensen, *Chem. Rev.* **1998**, *98*, 1689.
- <sup>15</sup> P. E. Blöchl, A. Togni, *Organometallics* **1996**, *15*, 4125.
- <sup>16</sup> A. Togni, U. Burckhardt, V. Gramlich, P. S. Oregosin, R. Salzmänn, *J. Am. Chem. Soc.* **1996**, *118*, 1031.
- <sup>17</sup> U. Burckhardt, M. Baumann, G. Trabesinger, V. Gramlich, A. Togni, *Organometallics* **1997**, *16*, 5252.

- <sup>18</sup> B. Trost, M. L. Crawley, *Chem. Rev.* **2003**, *103*, 2921.
- <sup>19</sup> K. Burgess, L. T. Liu, B. Pal, *J. Org. Chem.* **1993**, *58*, 4758.
- <sup>20</sup> P. Magnus, J. Lacour, I. Coldham, B. Mugrage, W. B. Bauta, *Tetrahedron* **1995**, *51*, 11078.
- <sup>21</sup> B. M. Trost, D. L. Van Vranken, *J. Am. Chem. Soc.* **1993**, *115*, 444.
- <sup>22</sup> D. de Groot, E. B. Eggeling, J. C. de Wilde, H. Kooijmans, R. J. van Haaren, A. W. van der Made, A. L. Spek, J. N. H. Reek, D. Vogt, P. C. J. Kamer, P. W. N. M. van Leeuwen, *Chem. Commun.* **1999**, *17*, 1623.
- <sup>23</sup> H. P. Dijkstra, N. Ronde, G. P. M. Klink, D. Vogt, G. van Koten, *Adv. Synth. Catal.* **2002**, *3*, 364.
- <sup>24</sup> J. M. Longmire, X. Zhang, *Tetrahedron Lett.* **1997**, *38*, 1725.
- <sup>25</sup> R. A. van Santen, P. W. M. N. van Leeuwen, J. A. Moulijn, B. A. Averill (Editors), *Catalysis: An Integrated Approach, Second, Revised and Enlarged Edition*, Elsevier, Amsterdam, **1999**, p 392.
- <sup>26</sup> R. A. van Santen, J. W. Niemantverdriet, *Chemical Kinetics and Catalysis*, Plenum Press, New York, **1995**, p 21.
- <sup>27</sup> H. C. M. Ricken, *Reactiekinetiek, Fysische chemie deel 2*, 4th ed., Oss, **1995**, p V.4 .  
G. F. Froment, K. B. Bischoff, *Chemical Reactor Analysis and Design*, 2<sup>nd</sup> ed., Wiley, New York, **1990**, p 7, 42.
- <sup>28</sup> M. E. van der Boom, D. Milstein, *Chem. Rev.* **2003**, *103*, 1759.
- <sup>29</sup> M. R. Eberhard, S. Matsukawa, Y. Yamamoto, C. M. Jensen, *J. Organom. Chem.* **2003**, *687*, 185.
- <sup>30</sup> A. P. Beletskaya, A. V. Chuchurjukin, H. P. Dijkstra, G. P. M. van Klink, G. van Koten, *Tetrahedron Lett.* **2000**, *41*, 1081.
- <sup>31</sup> A. Vitagliano, B. Åkermark, *J. Organometallic. Chem.* **1988**, *349*, C22.
- <sup>32</sup> T. Cantat, E. Génin, C. Giroud, G. Meyer, A. Jutand, *J. Organometallic Chem.* **2003**, 365.
- <sup>33</sup> R. P. Hughes, A. Williamson, C. D. Incarvito, A. L. Rheingold, *Organometallics* **2001**, *20*, 4741.
- <sup>34</sup> Y. Tatsuno, T. Yoshida, Seiotsuka, *Inorg. Synthesis*, **XIX**, 220.

# 4

## Continuous Allylic Substitution Reactions

### Abstract

---

The **XLtriPCP**-Pd complex, for which the synthesis and catalytic performance is described in Chapter 2, was used in continuous allylic alkylation and amination reactions. The continuous allylic alkylation reaction was performed using the double concentrations of all reagents compared to the batch reactions discussed in Chapter 2, in order to speed up the reaction and to limit the residence time needed. A maximum conversion of almost 30% was obtained after which a deactivation of the catalyst was observed. A second attempt, with a modified (by reaction with trimethyl orthoformate) nanofiltration membrane, showed similar behavior.

In the allylic amination reactions, a maximum conversion of 80% was reached after two exchanged reactor volumes, which was maintained for a while. But also in this process deactivation occurred after about eight exchanged reactor volumes. However, no palladium black, that would indicate the formation of palladium(0) clusters, was found subsequently. Batch catalysis showed that neither water nor membrane material influenced the performance of the catalyst. A test reaction in the presence of air showed no activity, indicating that the system is very sensitive to oxygen causing immediate deactivation of the catalyst.

---

## 4.1 Introduction

Increasing the total turnover number (TON) of a catalyst is one of the possibilities to limit the contributions of the costs of transition metal catalysts to the cost of (industrial) products.<sup>1</sup> Furthermore, preventing by-product formation by limiting the conversion while still having high activities as described by Vogt *et al.*<sup>2</sup> and removal of the catalyst from the product stream<sup>3,4</sup> are of key interest for future industrial processes. Continuous homogeneous catalysis can provide solutions for these points of interest. It was pioneered by Kragl *et al.* who build on experience with enzyme catalysis in membrane reactors.<sup>5,6</sup> They applied dendrimer supported homogeneous catalysts in continuous catalysis. The first processes performed by Kragl *et al.* were the allylic amination<sup>7</sup> reaction and the Kharasch addition in cooperation with Van Koten.<sup>8</sup> From these first continuous catalysis experiments it is evident that it is of extreme importance to have stable catalyst systems. However, catalysts which are stable in batch catalysis and reach high total turnover numbers, do not necessarily have to be good catalyst for continuous processes.

An ideal catalyst for continuous catalysis should have sufficient size to be retained by a membrane, must be stable and should be active in suitable catalytic reactions. Molecular enlarged catalysts were prepared as described in Chapter 2. Retention tests showed relatively high retentions, sufficient for test applications. The system bears pincer ligands able to form stable complexes by tridentate coordination with transition metals. Their stability was demonstrated in Heck coupling reactions performed at 180 °C in N-methylpyrrolidone by Milstein *et al.*<sup>9</sup> Total TON's of more than 500.000 were reached.

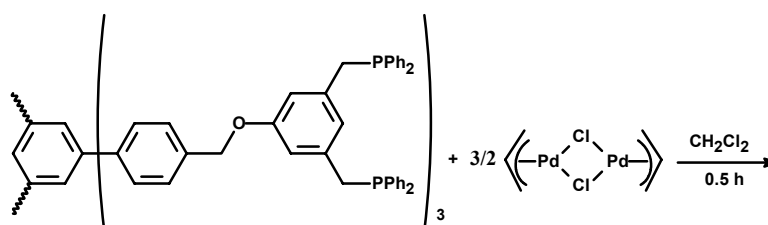
Unfortunately not all catalytic reactions can be performed in membrane reactors. Nanofiltration membranes nowadays have limited temperature and solvent stability. Furthermore, it is difficult to perform reactions involving gasses as reagents since only solutions of reagents can be handled in common set-ups (see Chapter 1 for details). Only if the gas used has sufficient solubility in the solvent it is possible to perform gas liquid reactions as demonstrated by Vogt *et al.* in the hydrovinylation of styrene in the same reactor which has been used for this work.<sup>10</sup> Reactions that can be carried out without difficulties are reactions performed at relatively low temperature (preferentially at room temperature),

involving only liquids or solutions of the reagents. Furthermore, fast reactions are preferable because these facilitate small residence times (thus high flow) enabling high productivity.

As described in Chapter 2, allylic substitution reactions can be performed at room temperature showing sufficient activity. These reactions were chosen as test experiments for continuous catalytic processes. The kinetics of the allylic amination reaction were investigated in Chapter 3, providing the possibility to calculate expected conversions when batch catalysis is compared to a continuous process. In this chapter first the continuous allylic alkylation will be discussed followed by the allylic amination reaction.

## 4.2 Results and Discussion

The **XLtriPCP**-Pd was found to be active and selective in allylic substitution reactions (amination and alkylation) as discussed in Chapter 2. The catalyst was prepared reacting the ligand system with  $[(\text{allyl})\text{PdCl}]_2$  as palladium precursor (Scheme 1) in analogy to the procedure reported by Zhang *et al.*<sup>11</sup>

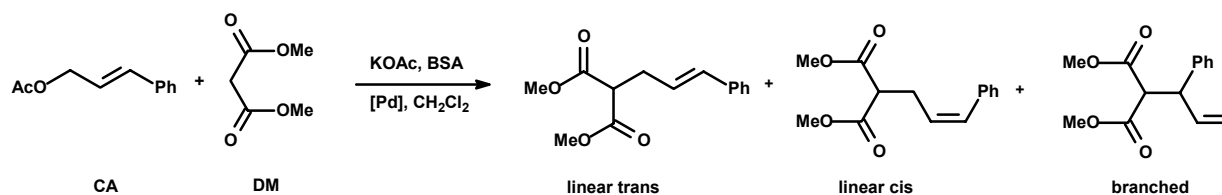


**Scheme 1:** Catalyst preformation.

Using this catalytic system, the allylic alkylation and the amination reactions were performed in a continuous way, using a nanofiltration membrane reactor (discussed in Chapter 1).

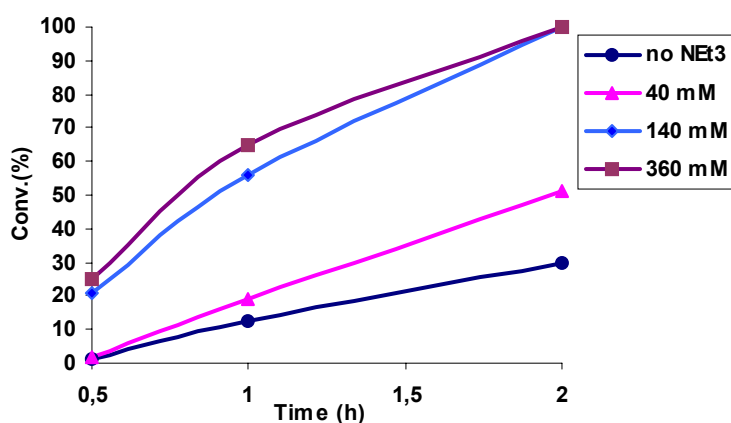
### 4.2.1 Continuous Allylic Alkylation Reactions

Potassium acetate is a standard base for the allylic alkylation reaction (Scheme 2).<sup>11, 12</sup> Since all reactants must be dissolved for the continuous catalysis, an alternative base had to be found.



**Scheme 2:** The allylic alkylation reaction.

A saturated  $\text{CH}_2\text{Cl}_2$  solution of KOAc showed little activity, probably caused by the very low solubility of KOAc in  $\text{CH}_2\text{Cl}_2$  (20.6 % conversion using a saturated KOAc solution versus 90.9% conversion when solid KOAc was used; standard conditions, 2 h). In literature other bases are reported such as: NaOAc, LiOAc, CsOAc<sup>13</sup>,  $\text{Cs}_2\text{CO}_3$ ,  $\text{Et}_2\text{Zn}$ <sup>14</sup>, KOH, LDA<sup>15</sup> but most of the salts have a low solubility in the used solvents. Also the use of sodium salts of various nucleophiles, e.g. diethyl 2-methylmalonate reacted with  $\text{NaH}$ ,<sup>16,17,18</sup> is a method often applied but it suffers from a fast background reaction as discussed in Chapter 2. A non-nucleophilic base, which is often used, is triethylamine. It is soluble in  $\text{CH}_2\text{Cl}_2$  and it is easy to handle because it is a liquid. Batch allylic alkylation reaction showed that triethylamine is a suitable base for this reaction but gives a slightly lower activity compared to catalysis using solid KOAc as base (69.5% conversion versus 90.9% conversion using solid KOAc as base; standard conditions, 2 h). The amount of  $\text{NEt}_3$  added, proved to be important for the activity of the catalyst (Graph 1).

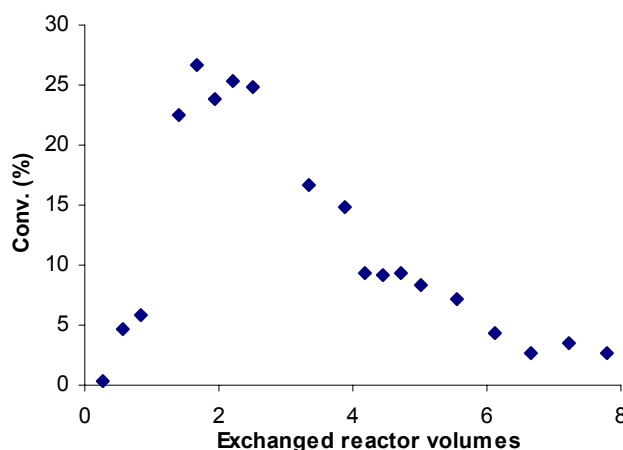


**Graph 1:** Influence of  $[\text{NEt}_3]$  on the activity.

As can be seen in Graph 1, there is an optimum activity close to 360 mM in  $\text{NEt}_3$ . When less  $\text{NEt}_3$  is used, the deprotonation is probably the rate-determining step in this reaction. When

stoichiometric amounts of base are used relative to the nucleophile (DM), this deprotonation is no longer rate determining. Exact stoichiometric conditions were used during continuous catalysis.

Without knowing the exact kinetic parameters (determination of the values failed for the allylic alkylation) a continuous allylic alkylation was performed using the concentrations and amounts used in standard batch catalysis, i.e. total volume in batch is 10 mL, [CA] = 0.1 mol/l, [DM] = 0.3 mol/l, [BSA] = 0.3 mol/l, [NEt<sub>3</sub>] = 0.3 mol/l and 2 μmol of catalyst. A flow rate of 20 mL/h was used which resulted in a residence time (time to exchange 1 reactor volume of 18 mL) of 1.1 h. Batch catalysis under these conditions showed 45.9% conversion after 1 h. In Graph 2 it can be seen that after an initiation period of approximately 1.5 h, a maximum activity of the catalyst is reached. After this maximum, a fast deactivation of the catalyst is observed. The retention of the ligand system was 98.5% as determined in Chapter 2. The lack of complete retention cannot cause such a loss of activity, since after eight reactor volumes only 11.4% of the starting amount of catalyst should be washed out of the reactor. The formation of an inactive species is expected because no formation of palladium black is observed, which is often the case in palladium-catalyzed reactions.<sup>19</sup>



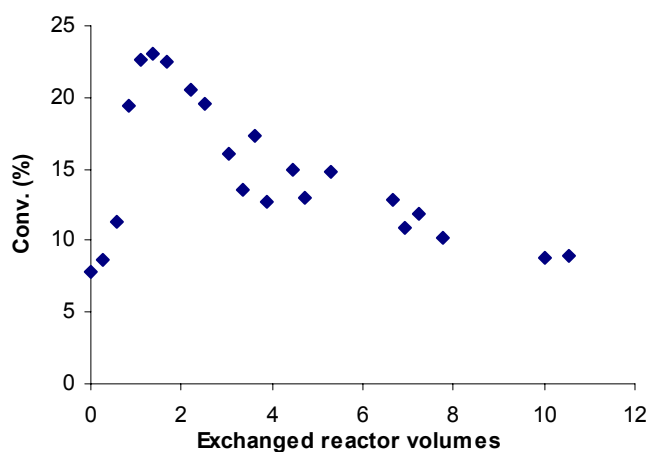
**Graph 2:** Continuous allylic alkylation 1.

A second continuous catalysis experiment was performed using the same conditions to exclude possible errors in the first catalytic run. This time the membrane was first treated with trimethyl orthoformate, to remove traces of water and alter the surface of the membrane.



Eggeling *et al.* reported earlier on the treatment of membranes with trimethyl orthoformate to remove traces of water and possibly altering the surface of the membrane.<sup>20</sup> A significant increase in total turnover number was observed in the hydrovinylation reaction compared to non-treated membranes. Furthermore, extensive washing of the reactor and membrane were performed to remove possible traces of oxygen.

Unfortunately the same behavior was observed: Increased activity during the first two reactor volumes followed by a rapid deactivation process resulting in very low conversion after eight exchanged reactor volumes.



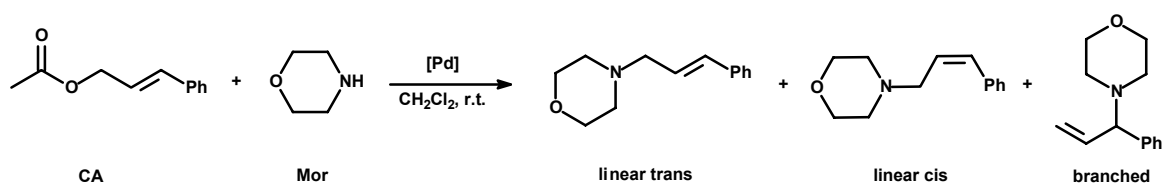
**Graph 3:** Continuous allylic alkylation 2.

Since the lack of complete retention does not cause this rapid loss of activity, a different deactivation process must be present. In batch catalysis, total turn over numbers higher than 1300 were obtained showing this catalyst to be stable over longer times under these reaction conditions. Experimental evidence for some sort of deactivation pathway was not found. In literature, the presence of allyl acetate is expected to facilitate deactivation.<sup>21</sup> The concentration of this substrate in continuous catalysis is higher than in batch catalysis because of the constant feed of fresh substrate solution in contrary to batch catalysis where the substrate is consumed going to higher conversions. Another deactivation pathway was found by Kragl *et al.* using NMR spectroscopy. The formation of inactive “PdCl<sub>2</sub>” species was observed<sup>7</sup> possibly by reaction with CH<sub>2</sub>Cl<sub>2</sub>. A more plausible explanation for this deactivation can be the contamination with oxygen. Either present in the used solutions or

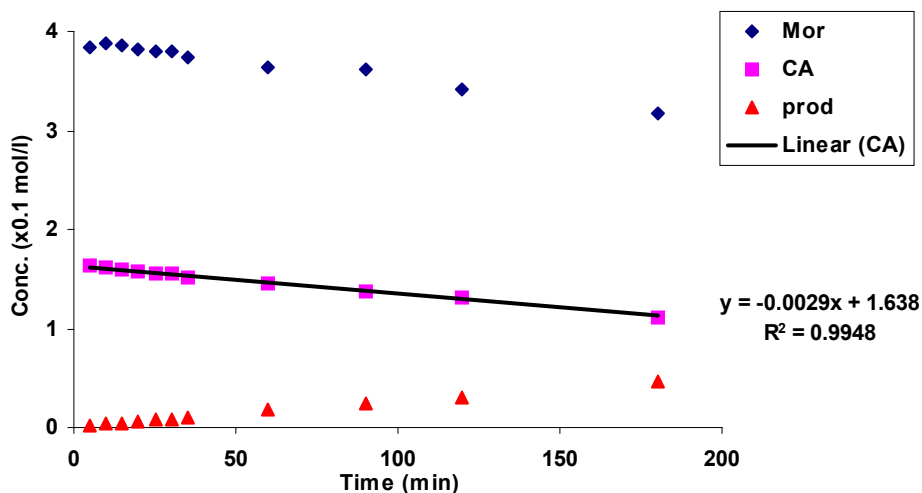
introduced by a leak in the system since such a rapid deactivation is not observed in batch catalysis.

#### 4.2.2 Continuous Allylic Amination Reactions

The first continuous allylic amination (Scheme 3) was performed using concentrations twice as high as those used in the batch experiment of Chapter 2. With these solutions, a batch test run was performed to determine the rate constant at higher concentrations.



Scheme 3: Allylic Amination reaction.



Graph 4: Determination of the rate constant.

From Graph 4, the reaction rate can be obtained taking the slope of the concentration curve in its linear area. Doing this, a reaction rate of  $1.7 \cdot 10^{-2} \text{ mol} \cdot \text{l}^{-1} \cdot \text{h}^{-1}$  ( $2.9 \cdot 10^{-4} \text{ mol} \cdot \text{l}^{-1} \cdot \text{min}^{-1}$ ) is determined. With *equation 1* the rate constant can be calculated for a first order reaction<sup>22</sup> (the order was determined to be one in morpholine, see also Chapter 3).

$$r = k_w[Mor]$$

equation 1

The calculated rate constant  $k_w$  for this reaction becomes  $4.7 \cdot 10^{-2} \text{ h}^{-1}$ . The expected conversion can be calculated using *equation 2*, where  $\tau_0$  is the residence time, ( $V_{\text{reactor}}/\text{flow}$ ). In this first run, a flow rate of  $4.1 \text{ mL}\cdot\text{h}^{-1}$  for each pump, leading to a total flow of  $8.2 \text{ mL}\cdot\text{h}^{-1}$ , was used.

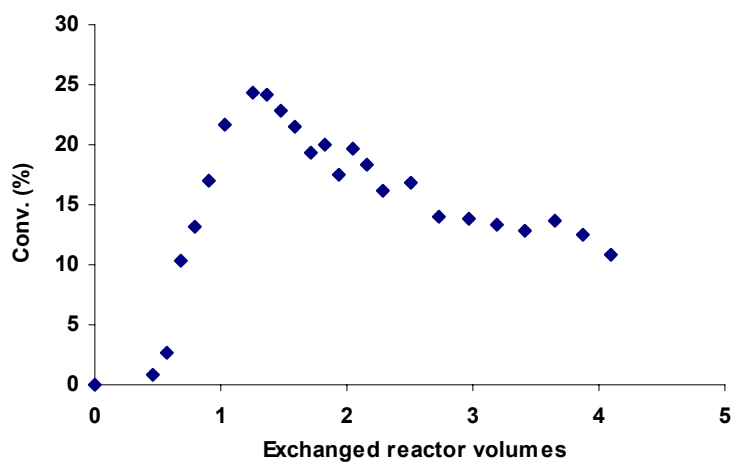
$$X_{CA} = \frac{k_w \tau_0}{1 + k_w \tau_0} = 9.4\%$$

$$\tau_0 = 2.2 \text{ h}$$

$$k_w = 4.7 \cdot 10^{-2} \text{ h}^{-1}$$

equation 2

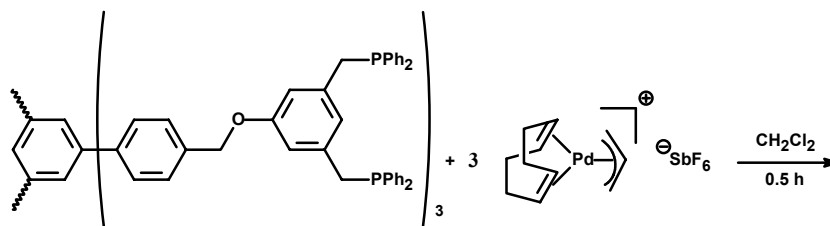
The expected conversion using  $[CA] = 0.2 \text{ mol/l}$ ,  $[Mor] = 0.4 \text{ mol/l}$ , with  $[Cat] = 0.4 \cdot 10^{-3} \text{ mol/l}$  is thus 9.4%.



**Graph 5:** Continuous allylic amination 1.

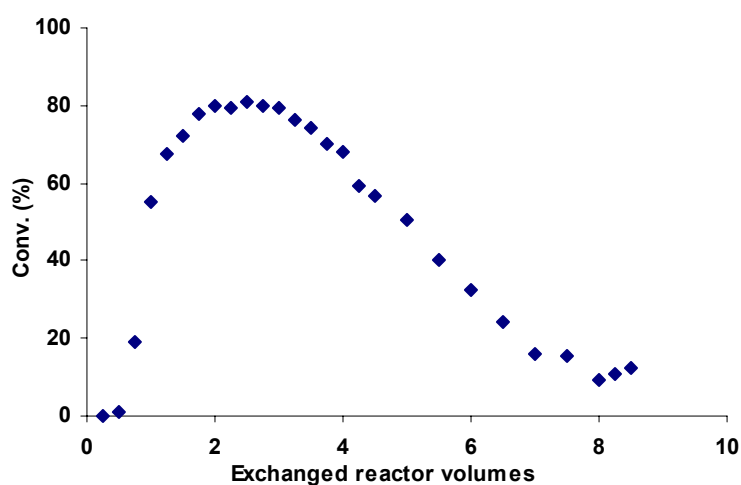
As can be seen in Graph 5, after an induction period in which the catalyst is pumped into the reactor, the conversion reaches its maximum after 3 h (1.3 exchanged reactor volumes) followed by a drop in conversion. The maximum conversion of ~25% is significantly higher than calculated on beforehand. Inaccuracy in the flow or in the added amount of catalyst can cause this difference. Since the retention of the catalyst is ~98.5% (*vide infra*) a deactivation process takes place. In batch catalysis, it was observed that after about 500 turnovers the

catalyst lost its activity. To find a more stable catalytic system, different palladium precursors were tested. It is known that cationic precursors can sometimes increase solubility and activity of catalyst.<sup>20</sup> This was also found for our system.



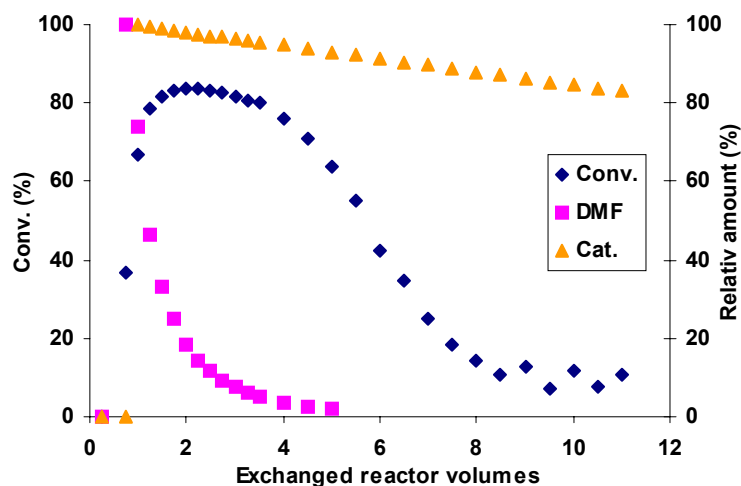
**Scheme 4:** Alternative preformation.

When  $[(allyl)Pd(cod)]SbF_6$  (Scheme 4) was used, an enormous increase in activity was observed. In a batch reaction full conversion was reached within 0.5 h, compared to 62.6% conversion in 2 h for the catalyst derived from  $[(allyl)PdCl]_2$ . Also the stability of the system increased, total TONs of 5000 were reached in batch catalysis. The resulting catalyst however has a low solubility in  $CH_2Cl_2$ . Therefore DMF was used to preform the catalyst. During batch-wise catalytic runs, the catalyst proved to stay in solution. Using this system, continuous catalysis was performed. This time, the same concentrations were used as in previous experiments but the amount of catalyst was increased by a factor of 4 and the total flow rate was 15 mL/h. The  $k_w$  was determined in a separated batch catalysis (with the appropriate concentrations) and proved to be  $1.7\text{ h}^{-1}$ . Using these values, the calculated expected conversion becomes 67%.



**Graph 6:** Continuous allylic amination 2.

The conversion increased during the first 2 h to a maximum of ~80% which is slightly higher than calculated from the kinetics determined in batch catalysis (Graph 6). This higher conversion can be caused by a small error in the amount of catalyst or by an inaccuracy of the pumps. Furthermore, a decrease in conversion is again observed after reaching the maximum conversion. Since the total TON in batch catalysis reached over 5000, it was expected that a leakage in the system caused the drop in activity. Another experiment was performed using the same concentrations and the same amount of catalyst but only one pump was used to pump the substrates into the reactor, in contrast to the first continuous experiment where a morpholine solution and a solution containing the internal standard (decane) and cinnamyl acetate were pumped independently into the reactor by 2 pumps. The excluded pump (Latek P-400<sup>23</sup>) was expected to contaminate the feed solution with oxygen. The remaining pump was a newer type (Bischoff HPLC pump<sup>24</sup>), without possible contact between air and substrate solution. As can be seen in Graph 7 (diamond markers), the use of only one substrate pump did not alter the course of the reaction. In Graph 7, the additional curve (square markers) represents the solvent of the catalyst (DMF). It can be concluded that the maximum conversion is reached just after the maximum of DMF has left the reactor. This is the moment at which all catalyst has been flushed inside the reactor from the injection point. After this maximum, the catalyst deactivates rapidly. After about 8 exchanged reactor volumes almost no catalytic activity could be observed. The top line (triangular markers) represents the relative amount of catalyst starting at the maximum of DMF and taking into account the retention of the catalytic system. From this line it can be seen that after 8 exchanged reactor volumes less than 15% of the catalyst has been washed out due to the lack of complete retention. So, this loss of catalyst cannot explain the entire loss of activity. Another deactivation process must be present.



Graph 7: Continuous allylic amination 3.

To investigate this deactivation in more detail, additional batch experiments were performed with H<sub>2</sub>O respectively air added into the reaction vessel. In the experiment with additional H<sub>2</sub>O, comparable activities were observed and the reaction went to completion (TON = 500). Furthermore, a catalytic run was performed with some membrane material added to the reaction vessel. Similar to the addition of H<sub>2</sub>O, no influence of this additional material could be observed and a similar activity was observed with complete conversion. In contrast to these experiments, no conversion could be observed when air was added to the reaction mixture. From this it can be concluded that the allylic amination reaction is not sensitive towards water or membrane material but, as expected, sensitive towards oxygen. Oxygen can oxidize the ligands leading to weaker coordination of the metal, which can be followed by leaching of the metal through the membrane.

### 4.3 Conclusions

The ligand system **XLtriPCP**, of which the synthesis and catalytic properties have been discussed in Chapters 2 and 3, is applied in continuous palladium-catalyzed allylic substitution reactions. In the continuous allylic alkylation reaction between cinnamyl acetate and dimethyl malonate maximum conversion of 25% was reached after 1.5 exchanged reactor volumes. After this maximum conversion a deactivation of the catalyst is observed causing the process to become inactive after 8 exchanged reactor volumes. A second continuous run

showed similar behavior despite the fact that the membrane was treated with trimethyl orthoformate.

In the allylic amination reaction maximum conversions of 80% were reached after 2 exchanged reactor volumes. After this maximum a constant conversion is observed for 1 h after which a deactivation was observed. The deactivation was investigated in batch catalysis. Catalysis with additional membrane material or H<sub>2</sub>O did not affect the conversion. Only catalysis in air showed no conversion. A total TON of 5000 was reached in batch catalysis showing that this catalyst is stable under catalytic conditions for longer periods. These observations point to deactivation of the catalyst in both continuous catalytic reactions, most likely via contamination with oxygen. The source of the oxygen in the system is still unknown.

## 4.4 Experimental

### General

All reactions were performed under an inert atmosphere of argon using standard Schlenk techniques. Chemicals were purchased from Aldrich Chemical Co., Acros or VWR. Solvents were purified using basic alumina columns after degassing. [(allyl)PdCl]<sub>2</sub><sup>25</sup> was synthesized according to literature procedures. Morpholine and decane were distilled from CaH<sub>2</sub>, cinnamyl acetate was degassed and stored over molecular sieves. Gas chromatographic analyses were performed on a Shimadzu GC-17A equipped with a 25 m ULTRA-2 column.

### Continuous allylic alkylation 1

Two stock solutions were prepared before starting the experiment. For solution A, 10.0 mL (51.8 mmol) decane (internal standard), 16.7 mL (106 mmol) cinnamyl acetate, and 41.8 mL (287 mmol) triethylamine were dissolved in 500 mL CH<sub>2</sub>Cl<sub>2</sub>. Solution B consists of 34.5 mL (295 mmol) dimethyl malonate and 72.7 mL (297 mmol) BSA in 500 mL CH<sub>2</sub>Cl<sub>2</sub>. The catalyst was prepared by stirring 8.1 mg (4.5 μmol) XLtriPCP ligand with 2.5 mg (6.7 μmol) [(allyl)PdCl]<sub>2</sub> in 3 mL dichlorobenzene for 0.5 h. The membrane (Koch MPF-50) was

immersed in MeOH overnight and for 1 h prior use in CH<sub>2</sub>Cl<sub>2</sub>. After cutting it to the correct size it was placed into the reactor. Next the reactor and membrane were flushed with 60 mL of both stock solutions at a flow of 1 mL/h. After adjusting both flows to 10 mL/h, 2 mL of catalyst solution (8.9 μmol [Pd]) were added using a HPLC injection valve. During catalysis, samples were taken, diluted with ether and analyzed by GC. After 5 h the flow of both pumps was decreased to 5 mL/h to increase the conversion. The catalytic run was stopped after 7 h. After opening of the reactor, the retentate was collected and together with combined filtrates analyzed for Pd using ICP-AAS measurements.

### **Continuous allylic alkylation 2**

Stock solutions of the previous experiment were used. This time the reactor was flushed with 100 mL CH<sub>2</sub>Cl<sub>2</sub> after placing the membrane and 2 mL (14.6 mmol) trimethyl orthoformate were added to dry and alter the surface of the membrane. After flushing the reactor overnight with CH<sub>2</sub>Cl<sub>2</sub> the reactor was filled and flushed with stock solutions both at 10 mL/h. Next, 8.6 μmol [Pd], in the form of preformed catalyst, were added. The reaction was stopped after 9.5 h of continuous operation. After opening of the reactor, the retentate was collected and together with combined filtrates analyzed for Pd using ICP-AAS measurements.

### **Continuous allylic amination 1**

Two stock solutions were prepared before starting the experiment. For solution A, 9.8 mL (48.6 mmol) decane (internal standard) and 16.7 mL (101 mmol) cinnamyl acetate were dissolved in CH<sub>2</sub>Cl<sub>2</sub> filled to a total volume of 250 mL. Solution B consists of 17.4 mL (197 mmol) in CH<sub>2</sub>Cl<sub>2</sub> with a total volume of 250 mL. The catalyst was prepared by stirring 3.6 mg (2.0 μmol) XLtriPCP ligand with 1.1 mg (3.0 μmol) [(allyl)PdCl]<sub>2</sub> in 3 mL dichlorobenzene for 0.5 h. The membrane was immersed in MeOH overnight and for 1 h prior use in CH<sub>2</sub>Cl<sub>2</sub>. After cutting it to the correct size it was placed into the reactor. Next the reactor and membrane were flushed with 60 mL of both stock solutions at a flow of 1 mL/h. After adjusting both flows to 4.1 mL/h, 2 mL of catalyst solution (4.0 μmol [Pd]) were added using a HPLC injection valve. During catalysis, samples were taken, diluted with MeOH and analyzed by GC. The catalytic run was stopped after 9 h. After opening the reactor, the



retentate was collected and together with combined filtrates analyzed upon Pd using ICP-AAS measurements.

### Continuous allylic amination 2

Two stock solutions were prepared before starting the experiment. For solution A, 6.4 mL (32.9 mmol) decane (internal standard) and 12.8 mL (66.9 mmol) cinnamyl acetate were dissolved in CH<sub>2</sub>Cl<sub>2</sub> filled to a total volume of 175 mL. Solution B consists of 14.7 mL (169 mmol) in CH<sub>2</sub>Cl<sub>2</sub> with a total volume of 230 mL. The catalyst was prepared by stirring 13.9 mg (7.7 μmol) XLtriPCP ligand with 11.3 mg (23.0 μmol) [(allyl)Pd(COD)] [SbF<sub>6</sub>] in 3 mL DMF for 0.5 h. Membrane and reactor were prepared in the same way as in previous experiments. 2 mL (15.3 μmol [Pd]) of catalyst solution were injected. Flow of both pumps is 7.5 mL/h. After 5 h a new substrate solution was used prepared by dissolving 1.5 mL (7.6 mmol) decane, 5.2 mL (31.1 mmol) cinnamyl acetate in CH<sub>2</sub>Cl<sub>2</sub> and filled to 80 mL. Samples were taken, diluted with MeOH and analyzed by GC. The reaction was stopped after 8.5 h.

### Continuous allylic amination 3

Similar reaction conditions as described in the previous experiment, but in this case only one stock solution was pumped into the reactor, at 15 mL/h, using only one pump. This stock solution was prepared by dissolving 5.0 mL (25.6 mmol) decane, 8.4 mL (50.7 mmol) cinnamyl acetate and 11.9 mL (99.5 mmol) morpholine. The catalyst was prepared by stirring 13.0 mg (7.2 μmol) XLtriPCP ligand with 10.6 mg (21.6 μmol) [(allyl)Pd(cod)] [SbF<sub>6</sub>] in 3 mL DMF for 0.5 h. The reaction was stopped after 11 h.

## 4.5 References and Notes

- <sup>1</sup> U. Kragl, T. Dwars, *Trends Biotechnol.* **2001**, *19*, 442.
- <sup>2</sup> N. J. Hovestad, E. B. Eggeling, H. J. Heidebüchel, J. T. B. H. Jastrzebski, U. Kragl, W. Keim, D. Vogt, G. van Koten, *Angew. Chem. Int. Ed.* **1999**, *38*, 1655.
- <sup>3</sup> D. J. Cole-Hamilton, *Science* **2003**, *299*, 1702.
- <sup>4</sup> K. K. Sirkar, P. V. Shanbhag, A. S. Kovvali, *Ind. Eng. Chem. Res.* **1999**, *38*, 3715.
- <sup>5</sup> U. Kragl, D. Vasic-Racki, C. Wandrey, *Chemie Ingenieur Technik* **1992**, *64*, 499.
- <sup>6</sup> U. Kragl, D. Gygax, O. Ghisalba, C. Wandrey, *Angew. Chem., Int. Ed. Engl.* **1991**, *30*, 827.
- <sup>7</sup> N. Brinkmann, D. Giebel, G. Lohmer, M. T. Reetz, U. Kragl, *J. Catal.*, **1999**, *183*, 163-168.

- <sup>8</sup> A. W. Kleij, R. A. Gossage, R. J. M. Klein Gebbink, N. Brinkmann, E. J. Reijerse, U. Kragl, M. Lutz, A.L. Spek, J. Boersma, G. van Koten, *J. Am. Chem. Soc.* **2000**, *122*, 12112.
- <sup>9</sup> M. Ohff, A. Ohff, E. van der Boom, D. Milstein, *J. Am. Chem. Soc.* **1997**, *119*, 11687.
- <sup>10</sup> E. B. Eggeling, N. J. Hovestad, J. T. B. H. Jastrzebski, D. Vogt, G. van Koten, *J. Org. Chem.* **2000**, *65*, 8857.
- <sup>11</sup> J. M. Longmire, X. Zhang, *Tetrahedron Lett.* **1997**, *38*, 1725.
- <sup>12</sup> S. Deerenberg, H. S. Schrekker, G. P. F. van Strijdonck, P. C. J. Kamer, P. W. N. M. van Leeuwen, J. Fraanje, K. Goubitz, *J. Org. Chem.* **2000**, *65*, 4810.
- <sup>13</sup> X. Hu, H. Chen, X. Hu, H. Dai, C. Bai, J. Wang, Z. Zheng, *Tetrahedron Lett.* **2002**, *43*, 9179.
- <sup>14</sup> S. Yasuike, S. Okajima, K. Yamaguchi, J. Kurita, *Tetrahedron Lett.* **2003** *44*, 6217.
- <sup>15</sup> T. Kanayama, K. Yoshida, H. Miyabe, T. Kimachi, Y. Takemoto, *J. Org. Chem.* **2003**, *68*, 6197.
- <sup>16</sup> T. Yamagishi, M. Ohnuki, T. Kiyooka, D. Masui, K. Sato, M. Yamaguchi, *Tetrahedron: Asymmetry* **2003**, *14*, 3275.
- <sup>17</sup> D. de Groot, J. N. H. Reek, P. C. J. Kamer, P. W. N. M. van Leeuwen, *Eur. J. Org. Chem.* **2002**, 1085.
- <sup>18</sup> O. Belda, C. Moberg, *Synthesis* **2002**, *11*, 1601.
- <sup>19</sup> G. E. Oosterom, S. Steffens, J. N. H. Reek, P. C. J. Kamer, P. W. N. M. van Leeuwen, *Topics in Catal.* **2002**, *19*, 61.
- <sup>20</sup> E. B. Eggeling, *Zur Codimerisierung von Styrol und Ethen*, Thesis, Rheinisch-Westfälischen Technischen Hochschule Aachen, Germany, **1999**.
- <sup>21</sup> D. de Groot, J. N. H. Reek, P. C. J. Kamer, P. W. N. M. van Leeuwen, *Eur. J. Org. Chem.* **2002**, 1085.
- <sup>22</sup> R. A. van Santen, P. W. M. N. van Leeuwen, J. A. Moulijn, B. A. Averill (Editors), *Catalysis: An Integrated Approach, Second, Revised and Enlarged Edition*, Elsevier, Amsterdam, **1999**, p 392.
- <sup>23</sup> Latek, Germany, <http://www.latek.de>.
- <sup>24</sup> Bischoff, Leonberg, Germany, <http://www.bischoff-chrom.de>.
- <sup>25</sup> Y. Tatsuno, T. Yoshida, Seiotsuka, *Inorg. Synthesis*, **XIX**, 220.



# 5

## Immobilization of Diphosphine Ligands via Amine Coupling

### Abstract

---

Molecular enlarged ligands were synthesized using palladium-catalyzed direct amination reactions. This strategy proved to be straightforward for the coupling of phenoxazine to small supports but turned out to be more difficult when the substrate contained phosphine functionalities. Protection of the phosphine groups, variation of the bases and longer reaction times, however, gave the desired products. With the rigid phenoxazine functionalized compound, two different nanofiltration membranes were compared using toluene and ethyl acetate as solvents. Attempts were made to convert the immobilized phenoxazine compound **8** to a Nixantphos derivative **9**. Whereas the standard procedure for this conversion gave mixtures of mono- and diphosphines, the desired product could be obtained by the coupling of protected Nixantphos. The direct amination reaction was also successfully used to immobilize Nixantphos and PPM on a second-generation polyphenylene dendrimer.

Nucleophilic substitution was applied in order to couple diphosphine ligands bearing secondary amine groups. With the molecular enlarged Nixantphos derivative **17** Rh-catalyzed hydroformylation reactions were performed. These enlarged catalysts showed comparable selectivities but slightly higher activities compared to the parent Nixantphos-Rh system.

---

## 5.1 Introduction

As already described in Chapter 2, the coupling reaction of ligands to supports is one of the key issues of the immobilization of homogenous catalysts. In this chapter, the immobilization of bidentate phosphorus ligands onto dendritic supports is described. The two ligands used in this investigation are 4,5-bis(diphenylphosphino)phenoxazine (Nixantphos **1**), and the chiral (2*S*,4*S*)-4-(diphenylphosphino)-2-[(diphenylphosphino)methyl]pyrrolidine (PPM **2**) ligand. The immobilization of these ligands is achieved via direct amination reactions of the secondary amine functionality.

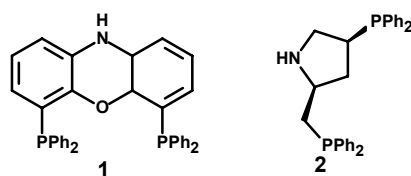


Figure 1: Nixantphos and PPM.

Nixantphos belongs to the xantphos ligand family used for a systematic study of the bite-angle effect in the rhodium-catalyzed hydroformylation of alkenes.<sup>1</sup> It was first reported by Van Leeuwen *et al.*<sup>2,3,4</sup> Recently, Nixantphos was covalently linked to a silica matrix via the sol-gel process and used in heterogeneous hydroformylation as well as hydrogenation reactions.<sup>5,6</sup> In 2000 it became commercially available.<sup>7</sup> To the best of our knowledge, no immobilization was performed on soluble dendritic supports yet.

PPM is a chiral, bidentate diphosphine ligand, which can be prepared in a six-step synthesis from relatively inexpensive, naturally occurring trans-4-hydroxy-L-proline. In 1976 Achiwa reported for the first time the catalytic performance of PPM in the asymmetric hydrogenation of cinnamic acid derivatives.<sup>8</sup> Achiwa reported later on the first non-soluble polymer-supported PPM ligand systems synthesized by co-polymerisation of 1-(4-vinylbenzoyl)-PPM with hydroxyethyl methacrylate.<sup>9</sup> Independently, Stille *et al.* reported similar polymer-supported ligands.<sup>10</sup> Both systems were used in the hydrogenation of acetamidocinnamic acid. While Achiwa's catalyst gave an enantiomeric excess (ee) of 23%, the polymer supported catalyst of Stille gave an ee of 91%.

In another immobilization approach, Oehme *et al* used sodium dodecyl-sulfate micelles functionalized with PPM.<sup>11</sup> These micelles were used in aqueous media for the hydrogenation of methyl- $\alpha$ -acetamidocinnamate giving ee's of 78 to 96 %. A rhodium-complex embedded in the interior of micelles was used by Kragl *et al*.<sup>12</sup>

N-tert-butoxycarbonyl-4-diphenylphosphino-2-diphenylphosphinomethylpyrrolidine (BPPM) **3** (Figure 1) has also been used as a ligand in heterogenized systems. Jamis *et al*. immobilized Rh-BPPM and Ru-BINAP into the pores of mesoporous silica and used this material for the enantioselective hydrogenation of acetamidocinnamic acid achieving ee's of 40-60%.<sup>13</sup> Pugin bound the chiral diphosphine PPM to silicagel with different loadings and used it as a model to detect effects of site isolation in the asymmetric hydrogenation of methylacetamidocinnamate. The enantiomeric excesses varied from 85 to 94%, which is extra-ordinary high for heterogeneous asymmetric catalysts.<sup>14</sup>

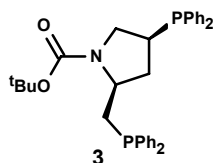
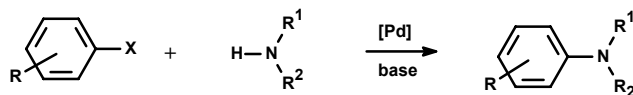


**Figure 2:** BPPM.

As mentioned before, no immobilization has been performed yet on dendritic soluble supports. In this chapter, the palladium-catalyzed direct amination reaction will be described, which allows coupling of the secondary nitrogen atoms of Nixantphos and PPM, to aryl bromide support molecules (Scheme 1).



**Scheme 1:** General direct aryl amination reaction.

The catalytic amination reaction has been studied extensively by the group of Buchwald, who applied a variety of phosphine, phosphine-amine ligands and palladacycle systems for this reaction.<sup>15,16,17,18</sup> Other groups also studying this type of reaction used Buchwalds ligand<sup>19</sup> **4** or the Xantphos ligand **5** (Figure 3).

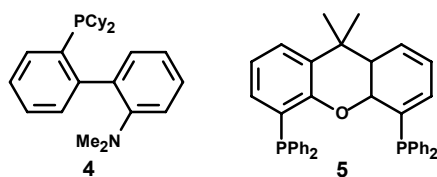


**Figure 3:** Buchwald's ligand and Xantphos.

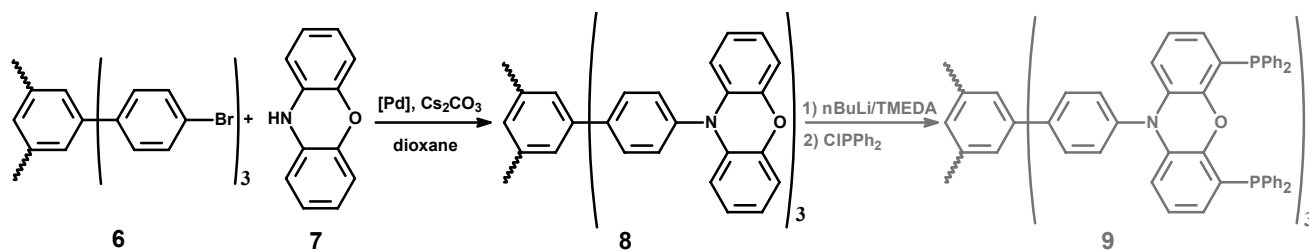
In most studies the best results were obtained with the solvent/base combination toluene/ $\text{Cs}_2\text{CO}_3$ , or dioxane/ $\text{NaO}^t\text{Bu}$ . In our approach both systems were tested and used for the coupling of PPM and Nixantphos to dendritic supports. In addition, the nucleophilic substitution reaction (discussed in Chapter 2) will be used for the coupling of PPM and Nixantphos to support molecules bearing benzylic bromide functionalities.

## 5.2 Results and Discussion

### *Attempt 1:*

#### 5.2.1 Coupling of Phenoxazine 7 to the Support 6 and Subsequent Conversion to the Bidentate Ligand

The palladium-catalyzed coupling reactions were first performed in dioxane, using  $\text{KO}^t\text{Bu}$  as the base. The catalyst was preformed by mixing Xantphos with the palladium precursor  $\text{Pd}_2(\text{dba})_3 \cdot \text{CHCl}_3$  in dioxane under inert conditions. This preformed catalyst was added to a mixture of 1,3,5-tris(4-bromophenyl)benzene **6**, and the secondary amine phenoxazine **7**. Phenoxazine is a common precursor for the bidentate phosphorus ligand Nixantphos, which is synthesized by protecting the free amine, followed by lithiation and reaction with chlorodiphenylphosphine.<sup>1</sup> With the same method, the tris(phenoxazine)-containing product **8** was synthesized, which was subsequently converted into the ligand system containing three Nixantphos units **9** on one support molecule (Scheme 2).



**Scheme 2:** Synthesis of tris(phenoxazine) and functionalization to tris(Nixantphos).

Using the Xantphos/Pd<sub>2</sub>(dba)<sub>3</sub> system as catalyst, the product was formed in almost quantitative yield as a light brown solid which could be recrystallized from hot toluene (*vide infra*).

The synthesis was also performed in toluene using Buchwalds ligand and Cs<sub>2</sub>CO<sub>3</sub> as base. The product was formed in reasonable yield, but no quantitative reactions were obtained as in the case of the Xantphos containing system, which was the system of choice for this reaction.

Other synthetic methods for this type of reaction have been reported in literature.<sup>20,21,22</sup> In these articles stoichiometric amounts of copper powder were used giving only low yields (<45%). Here we describe a method using catalytic amounts of palladium giving the product in near quantitative yields.

### 5.2.2 Concentration Dependent <sup>1</sup>H and <sup>13</sup>C NMR Spectroscopy

As will be discussed later in this chapter, the compound described above was used as a model compound for retention measurements with nanofiltration membranes. To ensure that monomeric compounds are present in solution and no aggregates are formed by e.g.  $\pi$ -stacking or the formation of hydrogen bridges, a concentration dependent NMR study was performed.<sup>23</sup> Aggregates will result in higher retentions than can be expected from the dimensions of a single molecule.



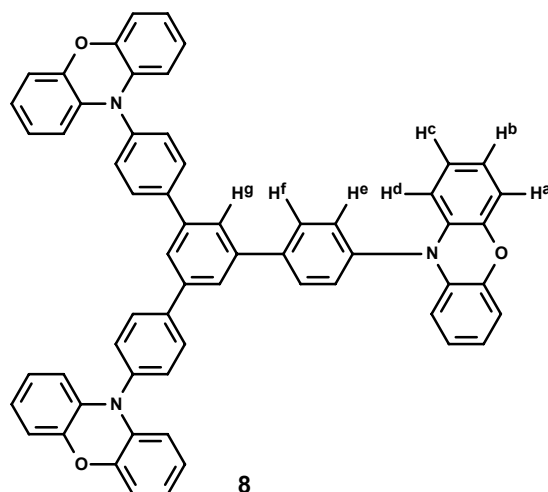


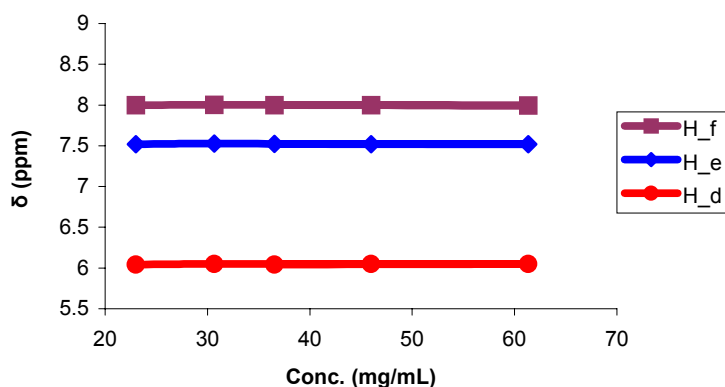
**Figure 4:** Proton labeling in tris(phenoxazine).

Tris(phenoxazine) **8** has seven different protons, of which 3 protons can be observed well separated from the others (chemical shifts shown in Table 1). These protons, d, e and f (Figure 4) were monitored by  $^1\text{H}$  NMR spectroscopy in  $\text{CDCl}_3$  varying the concentration of the compound.

**Table 1:** Protons in tris(phenoxazine).

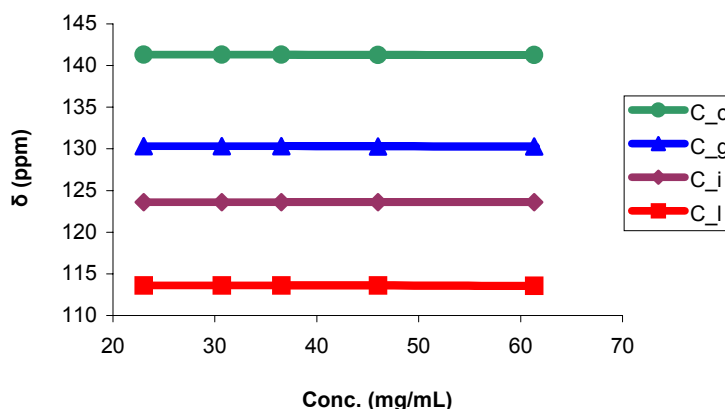
| Proton | Chem. shift (ppm) | Multiplicity | Coupling (Hz) |
|--------|-------------------|--------------|---------------|
| a-b    | 6.78-6.62         | m            |               |
| d      | 6.06              | dd           | 7.2, 2.1      |
| e      | 7.52              | d            | 8.4           |
| f      | 7.98              | s            |               |
| g      | 7.99              | d            | 7.8           |

As can be seen in Graph 1, none of the selected protons shows a change in chemical shift at different concentrations. It can be concluded that tris(phenoxazine) is not forming aggregates in  $\text{CDCl}_3$  in the concentration range of 20-65 mg/mL.



**Graph 1:** Chemical shifts of selected protons.

In the same concentration interval,  $^{13}\text{C}$  NMR spectra were recorded as well. The chemical shifts of four selected carbon atoms are plotted in Graph 2. Again, none of them showed any change in chemical shift and therefore no aggregates are expected under these conditions.



**Graph 2:** Chemical shifts of selected carbon atoms.

### 5.2.3 Crystal Structure Determination

Crystals of the tris(phenoxazine) **8** could be obtained by dissolving the compound in boiling toluene and slowly cooling the solution to room temperature. Big square blocks were formed (not suitable for X-ray analysis) among some smaller single crystals, which were analyzed by X-ray diffraction. The crystal structure of **8** is shown in Figure 5 and Figure 6.

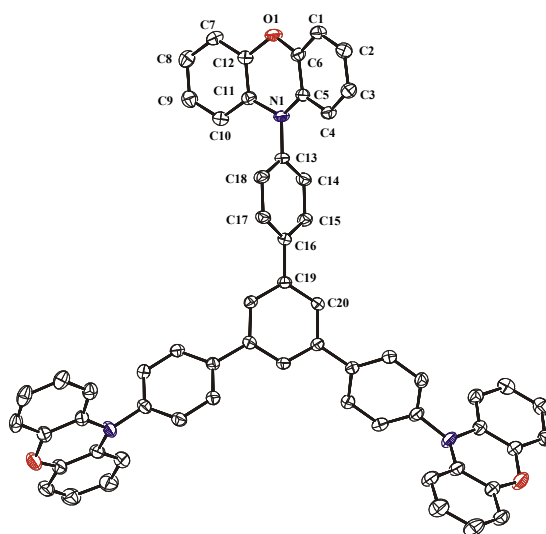


**Figure 5:** Crystal structure of **8**, top view, ORTEP 50 % displacement ellipsoids.  
Hydrogen atoms are omitted for clarity.

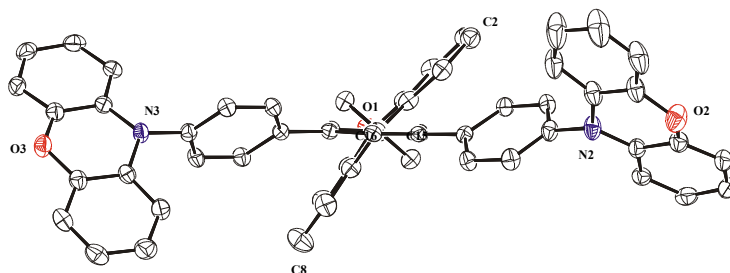


**Figure 6:** Crystal structure of **8**, side view, ORTEP 50 % displacement ellipsoids.  
Hydrogen atoms are omitted for clarity.

The molecular structure shows the central benzene ring substituted with three phenoxazine groups connected via a phenyl bridge. Each bridging phenyl ring forms a dihedral angle of  $36.4 - 43.1^\circ$  with the central benzene ring, while the phenoxazine groups are forming a dihedral angle of  $69.4 - 75.9^\circ$  with this bridging phenyl group.

For the separation by nanofiltrations, the overall dimensions of the molecular enlarged compounds are important to know in relation to the pore-size of the used membranes. From the crystal structure, the average O – O distance was determined to be  $17.0 \text{ \AA}$ . Using the rule of Pythagoras the length of the perpendicular was found to be  $14.7 \text{ \AA}$  (Figure 7). The thickness of this triangle was calculated using the C2 – C8 distance,  $7.3 \text{ \AA}$ , which was multiplied by the sinus of  $80^\circ$  (largest dihedral angle of phenoxazine with central benzene

ring) giving a thickness of 7.2 Å. However, all these calculation were performed on solid-state structures, while the structure in solution can alter significantly by rotation around the  $\sigma$ -bonds. This rotation does not alter the calculated perpendicular.

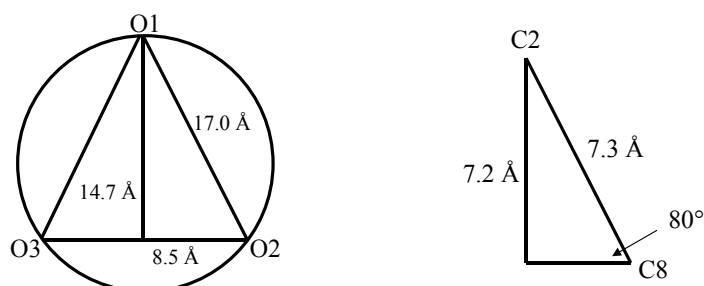
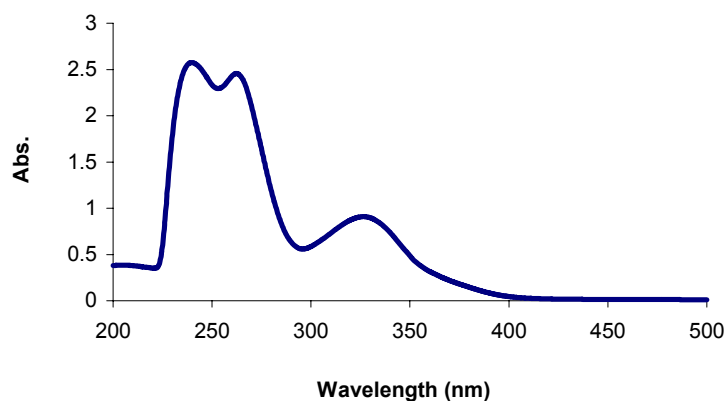


**Figure 7:** Calculation of perpendicular and thickness of **8**.

As shown by the calculation above, the synthesized molecule has dimensions well in the nanometer range providing a suitable test compound for the comparison of nanofiltration membranes with each other.

#### 5.2.4 Retention Tests

The tris(phenoxazine) substituted compound **8** is an ideal test compound to compare different nanofiltration membranes: As described above, its dimensions can be calculated from the solid-state structure, 1.5 nm times 0.7 nm, which falls in the nanofiltration scale (0.5-8 nm). Furthermore, the high extinction coefficient of various bands in the UV-region can be used to calculate concentrations very accurately. With these accurate concentrations, small variations in the retention can be observed. The UV/Vis spectrum shows 3 maxima at 239.6, 262.4 and 327.4 nm, respectively (Graph 3). As most solvents absorb in the region below 300 nm, which is the region of the first two maxima, the maximum at 327.4 was used to calculate the retention. The extinction coefficient ( $\epsilon$ ) of this maximum is  $1.8 \cdot 10^4 \text{ l} \cdot \text{mol}^{-1} \cdot \text{cm}^{-1}$ , which is quite high for this class of compounds.<sup>24</sup>



**Graph 3:** UV/Vis spectrum of tris(phenoxazine) **8**.

Additionally, due to its rigidity, tris(phenoxazine) **8** will probably not undergo shape changes in solution. Therefore the retention will not be influenced by the solvent used in retention measurements.

The membranes used are the MPF-50 manufactured by Koch International<sup>25</sup> and the STARMEM 120 and 228 manufactured by Membrane Extraction Technology.<sup>26</sup> Unfortunately the STARMEM membranes are not stable in THF or chlorinated solvents, which are commonly used in our reactions. For this reason retention tests were performed in toluene and ethyl acetate in order to investigate the influence of different solvents on the retention behavior for these membranes.

**Table 2:** Retention of tris(phenoxazine) **8** for three different membranes.

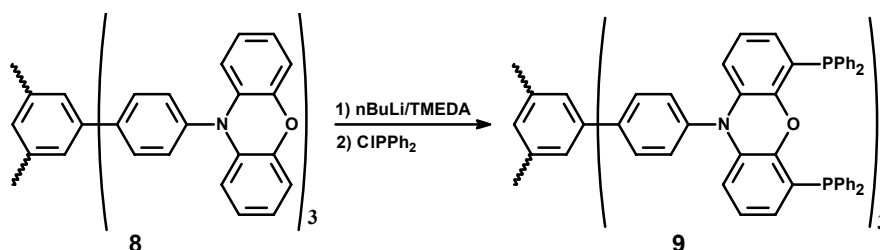
| Membrane    | MWCO | Retention EtOAc (%) | Retention Toluene (%) |
|-------------|------|---------------------|-----------------------|
| STARMEM 120 | 200  | 98.6                | 95.8                  |
| STARMEM 228 | 280  | 97.7                | 79.4                  |
| Koch MPF-50 | 700  | 55.4                | 62.1                  |

As can be seen in Table 2, the test compound has a poor retention using the MPF-50 membrane in ethyl acetate while the retentions using the two STARMEM membranes are much better due to the lower molecular weight cutoff (MWCO). When switching to toluene, the retention using the Koch membrane increased a little bit, while for the two STARMEM

membranes the retention dropped. Especially in the case of STARMEM 228 the retention dropped dramatically. According to the manufacture, this is most likely caused by the difference in membrane material used in both types of membranes.

### 5.2.5 Phosphinylation of Tris(phenoxazine)

To convert the phenoxazine backbone into the molecular enlarged diphosphine ligand a standard method was used,<sup>27</sup> which is lithiation in ether in the presence of TMEDA followed by the addition of chlorodiphenylphosphine. After workup, 2 signals were observed in the <sup>31</sup>P NMR spectrum at  $\delta = -15.69$  and  $-19.39$  ppm in an approximately 1:1 ratio, caused by either two inequivalent phosphorus atoms or by a mixture of mono- and disubstituted compounds. The second explanation was confirmed by a second lithiation and phosphinylation sequence yielding more of the desired product as indicated by an increased integral of the peak at  $-19.39$  ppm.



**Scheme 3:** Lithiation and phosphinylation of phenoxazine groups on support.

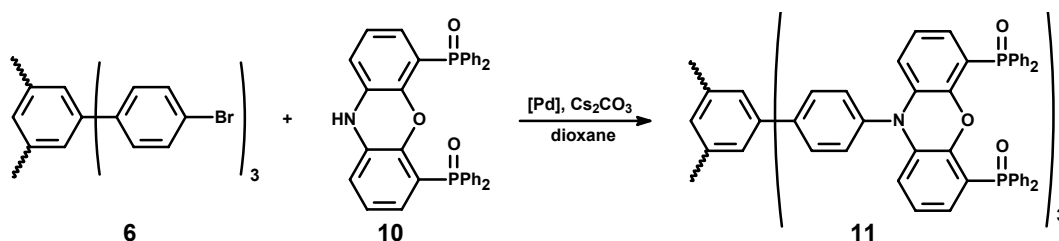
By several lithiation/phosphinylation sequences a fully functionalized system can probably be obtained in this case, but when going to higher generations this method will not lead to the desired diphosphine functionalized products in an acceptable yield and purity.

#### *Attempt 2:*

### 5.2.6 Coupling of Oxidized Nixantphos to Support 6

Because of the difficult functionalization of the phenoxazine groups, a second approach was followed to obtain bidentate phosphine systems. In this method, oxidized Nixantphos **10** was coupled to the support **6** by direct amination reactions (Scheme 4). The Nixantphos ligand

was protected by oxidation of the phosphine groups with  $\text{H}_2\text{O}_2$  in ethanol.<sup>28</sup> The reaction was performed on small scale and the products were analyzed by MALDI-TOF MS.

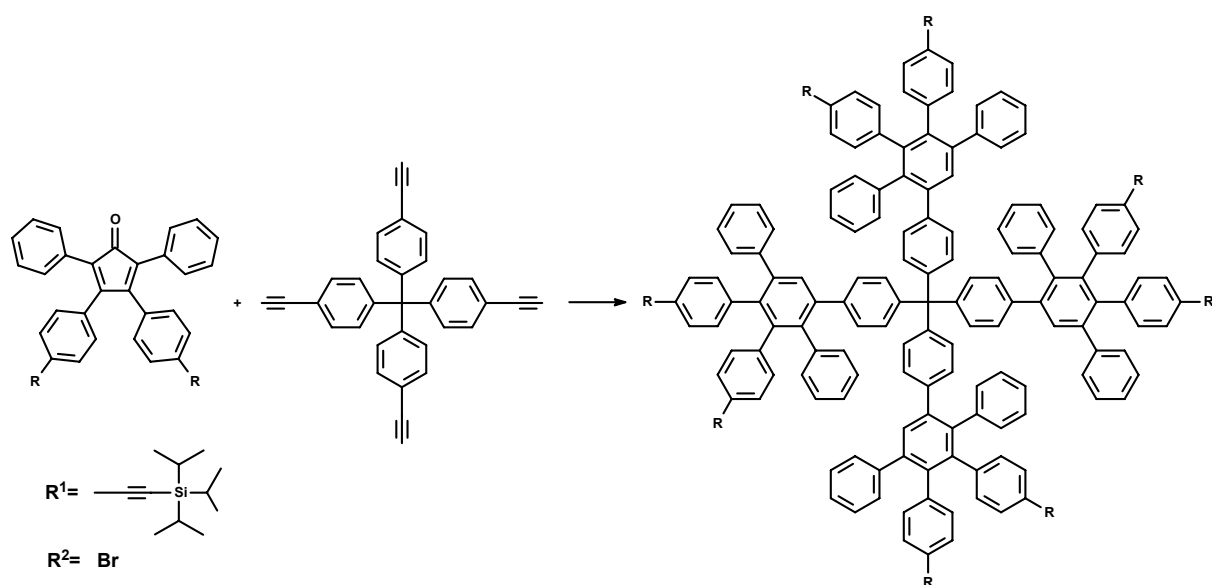


**Scheme 4:** Direct amination of oxidized Nixantphos (10) to the support 6.

The MALDI-TOF-MS spectrum showed peaks at  $m/z = 2051$ ,  $1549$  and  $584$  which correspond to tris- and bisubstituted products together with the unreacted, oxidized Nixantphos. Several reasons could account for the fact that the reaction did not go to completion: catalyst degradation, low solubility of the partially functionalized products in dioxane or an extremely slow reaction.

### 5.2.7 Coupling of Oxidized Nixantphos to a Polyphenylene Dendrimer

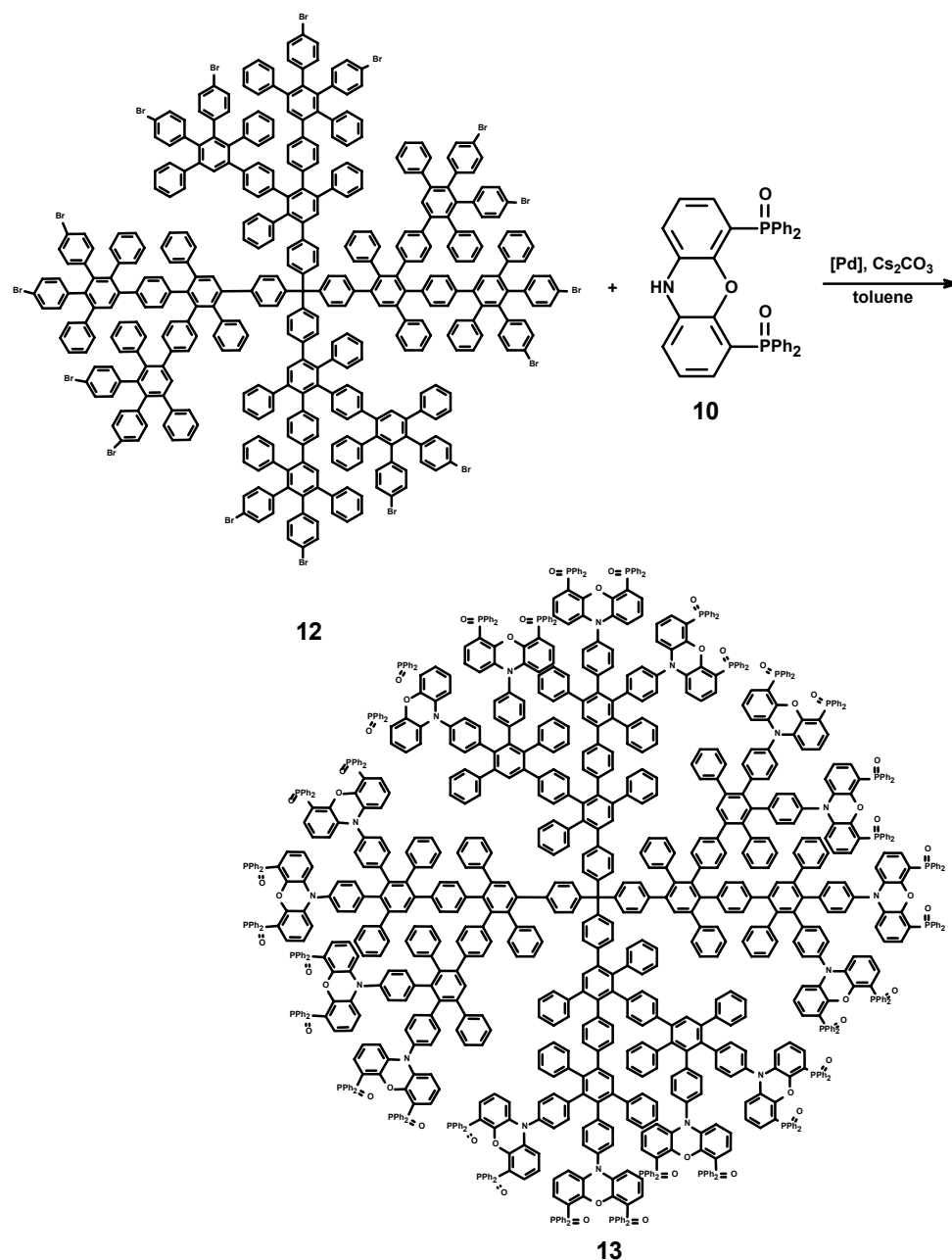
The palladium-catalyzed direct amination reaction was also applied to a second generation polyphenylene dendrimer. This dendrimer was synthesized in the group of Müllen (Max-Planck-Institute für Polymerforschung, Mainz, Germany). The synthesis involves a [2+4]cycloaddition of 3,4-bis[(4-triisopropylsilyl)ethynyl]phenyl-2,5-diphenylcyclopenta-2,4-dienon and a core such as 1-(ethynyl)-4-[tris(4-(ethynyl)phenyl)methyl]benzene (Scheme 5).<sup>29</sup> After cleavage of the triisopropylsilyl groups, the obtained dendrimer can undergo further Diels-Alder reactions. In the final step, the brominated building block is used yielding a dendrimer with sixteen bromide atoms on the periphery. These bromide groups can be used for further functionalization using, for example, Suzuki coupling or direct amination reactions.



**Scheme 5:** The key step in the synthesis of polyphenylene dendrimers.

The direct amination was carried out in toluene in which both reactants dissolve;  $\text{Cs}_2\text{CO}_3$  was used as the base and palladium in combination with the Buchwald ligand as catalyst. After a reaction time of 72 h, the solvent was replaced by dioxane because a lot of precipitate appeared while most solids are dissolved in dioxane. Next,  $\text{KO}^t\text{Bu}$  was added as base and Xantphos was used as ligand for palladium. After another 72 h of reaction time, water was added and the product (**8**) was extracted with dichloromethane.





**Scheme 6:** Direct amination of oxidized Nixantphos **10** on second generation polyphenylene dendrimer **12**.

<sup>31</sup>P NMR spectra of the obtained brown product showed three peaks, at  $\delta = 29.71$ , 29.23 and 27.60 ppm respectively. The different species are probably unreacted oxidized Nixantphos, [Pd]-Xantphos complex while the third peak has been assigned to the product formed. By washing with ethanol, two peaks originating from by-products, could be isolated from the compound with a peak at 29.23 ppm. Using MALDI-TOF-MS, this peak was assigned to the partially functionalized product. The MALDI-TOF spectrum shows a broad Gaussian curve

with a mean  $m/z$  of 11470. The shape of this curve shows a statistical functionalization with an average of eleven Nixantphos groups on the periphery of the dendrimer.

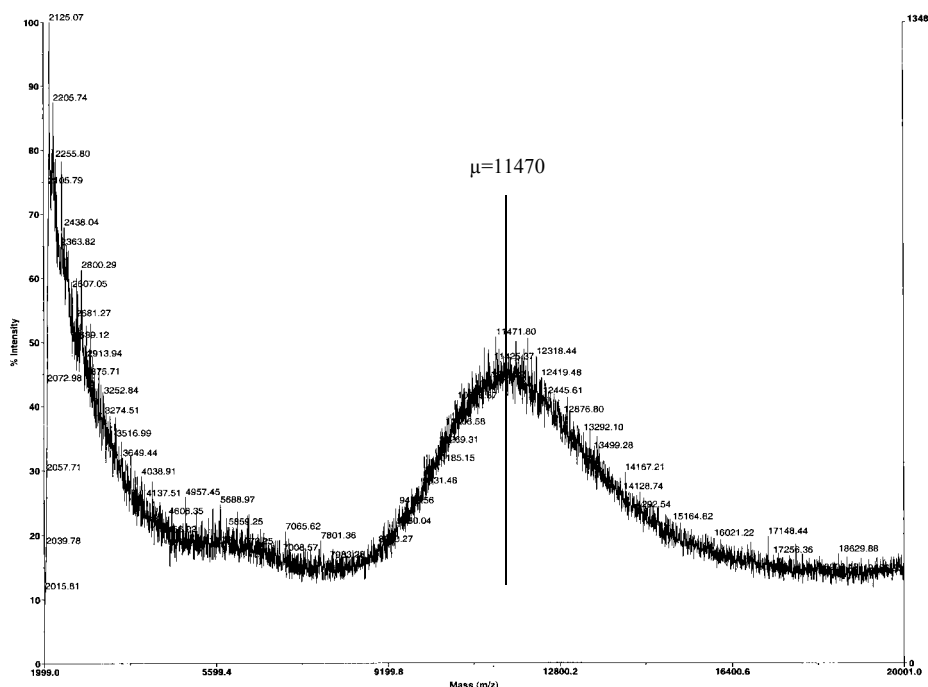


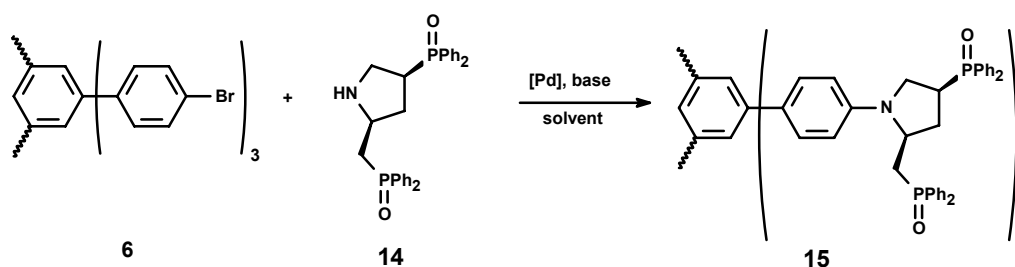
Figure 8: MALDI TOF spectrum of immobilized Nixantphos.

From the previous described experiment (Scheme 4) it was known that full functionalization of all aryl bromides is difficult. It was expected that in the case of higher functionalized systems this would lead to mixtures of polyfunctionalized products. By knowing the average number of ligands attached to the dendrimer, the metal loading should be corrected when the compound is used in catalysis.

The obtained protected Nixantphos system can be reduced using  $\text{HSiCl}_3$  in a high boiling solvent giving a free bidentate phosphine ligand system. It is known that Nixantphos is active in the rhodium-catalyzed hydroformylation<sup>1</sup> and palladium-catalyzed allylic amination,<sup>30</sup> which is the reaction of choice to test in a continuous operating nanofiltration membrane reactor.

### 5.2.8 The Synthesis of Tris(PPM(oxide)) 15

Many factors can influence the direct amination reaction. To investigate the reaction in detail, an optimization study was performed varying the base, the solvent and the ligand system in the reaction of support **6** and oxidized PPM **14**.



**Scheme 7:** Synthesis of tris[PPM(oxide)].

The first ligand used in this catalytic synthesis was PPM itself. The advantage of this attempt is that no additional diphenylphosphine ligand is introduced as a possible source of impurities. However, no activity was observed with two possible explanations for this observation:

1. Pd-PPM does not exhibit activity towards this amination reaction.
2. The very large PPM / Pd molar ratio of approximately 90 (which is caused by the fact that PPM is also the substrate in the reaction) results in inhibition. This is probably due to coordination of two equivalents of PPM to the metal blocking its coordination sphere.

The reaction was therefore performed using (+/-)-BINAP as a ligand. The resulting catalytic system is known for its activity in similar aminations,<sup>31</sup> but again no evidence of reaction could be observed. It was concluded that PPM inhibits the reaction by coordination to the metal as a result of the large excess of this ligand. Consequently the reaction is either inhibited by the inactivity of the coordinated ligand or by coordination of more than one equivalent of PPM to the metal. The exact reason was not determined as this was of secondary importance to the synthesis itself. It was concluded that the phosphine oxide of PPM would have to be used for the reaction.

**Table 3:** Optimization of the direct amination of **14** with support **6**.<sup>a</sup>

| Entry | Amine  | Ligand      | Base                            | Solvent | Results and observations   |
|-------|--------|-------------|---------------------------------|---------|--|
| 1     | PPM    | PPM         | NaO <sup>t</sup> Bu             | toluene | no reaction; excess of PPM apparently inhibits the reaction                            |
| 2     | PPM    | (+/-)-BINAP | NaO <sup>t</sup> Bu             | toluene | no reaction; use phosphine oxide <b>14</b>   |
| 3     | PPM(O) | (+/-)-BINAP | NaO <sup>t</sup> Bu             | toluene | reaction not complete; lots of byproducts  |
| 4     | PPM(O) | none        | NaO <sup>t</sup> Bu             | toluene | NaO <sup>t</sup> Bu reacts with <b>14</b> ; base too strong?                           |
| 5     | PPM(O) | (+/-)-BINAP | Cs <sub>2</sub> CO <sub>3</sub> | toluene | CsCO <sub>3</sub> is too weak as a base  |
| 6     | PPM(O) | (+/-)-BINAP | Et <sub>3</sub> N               | toluene | Et <sub>3</sub> N appears to be too weak; evidence not conclusive however <sup>b</sup> |
| 7     | PPM(O) | Xantphos    | NaO <sup>t</sup> Bu             | toluene | MW-enlarged ligand formed, easy separation of product/byproducts                       |
| 8     | PPM    | Xantphos    | NaO <sup>t</sup> Bu             | toluene | large amount of byproducts; no advantages over <b>14</b>                               |
| 9     | PPM(O) | Xantphos    | NaO <sup>t</sup> Bu             | DMF     | no reaction; catalyst does not appear to form in DMF                                   |
| 10    | PPM(O) | Xantphos    | NaO <sup>t</sup> Bu             | dioxane | conversion of aryl bromide +/- 60%   |
| 11    | PPM(O) | Xantphos    | NaO <sup>t</sup> Bu             | dioxane | adding <b>6</b> dropwise; no reaction  |
| 12    | None   | Xantphos    | NaO <sup>t</sup> Bu + 18-C-6    | dioxane | no significant monocoupling or dehalogenation of <b>6</b>                              |
| 13    | PPM(O) | Xantphos    | NaO <sup>t</sup> Bu + 18-C-6    | dioxane | conversion of aryl bromide +/- 90%   |

<sup>a</sup> Reaction conditions: ± 20 mL of solvent / mmol halide, 80-130 °C depending on the solvent (typically heating to reflux), Pd<sub>2</sub>(dba)<sub>3</sub> was used as the catalyst precursor, metal loading 5%, ligand / metal ratio 1.5, reaction continued until no further reaction could be observed (reaction times ranging from 1 hour to multiple days).

<sup>b</sup> Performed as a follow-up to entry 5; not separately tested.

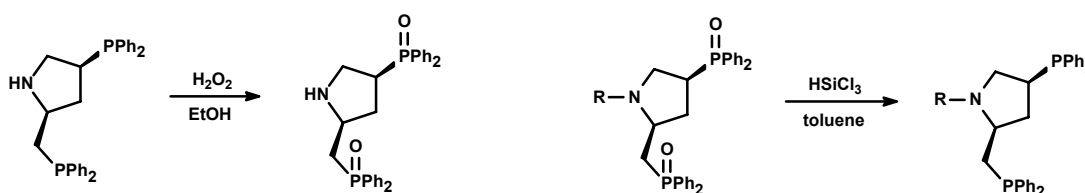
Using the phosphine oxide of PPM in the coupling reaction has three benefits:

1. The phosphine oxide cannot interfere with the Pd-catalyzed reaction. As explained before PPM itself can inhibit the reaction either by preferred coordination to the metal or by coordination of two equivalents of PPM to the metal.
2. The final step in the synthesis of the MW-enlarged ligand is the reduction of the phosphine oxides. This reaction should result in a near 100% conversion of the oxidized ligand in the MW-enlarged product. It would be difficult to achieve this purity after the

multiple step reaction from PPM to the eventual product without first reducing any formed phosphine oxides.

3. The product is not air-sensitive, facilitating the work-up procedure.

The reaction of PPM with  $\text{H}_2\text{O}_2$  is a straightforward reaction which produces the phosphine oxide in good yields (Scheme 8).<sup>28,32</sup> The same applies to the subsequent reduction of the phosphine oxides to form the diphosphine ligand using trichlorosilane in a high boiling solvent such as toluene.<sup>33</sup>



**Scheme 8:** Oxidation and reduction of PPM (derivatives).

Although the problem of inhibition by PPM could thus be solved by using the phosphine oxide, the reaction was still not performing to our expectations when using  $\text{Pd}/(+/-)\text{-BINAP}$  as the catalyst. Analysis of these earlier results in a later stage revealed that some MW-enlarged ligand was indeed formed. The problem was, however, that this was accompanied by an excessive amount of impurities, resulting in a very low yield and difficult, if not impossible, workup for the reaction. A test-reaction that involved stirring PPM oxide in the presence of  $\text{NaO}^t\text{Bu}$  at elevated temperature revealed that the base itself did react with PPM oxide and was probably too strong when using PPM oxide as a substrate. Using  $\text{Cs}_2\text{CO}_3$  or  $\text{Et}_3\text{N}$  (i.e. a weaker base) did not give satisfactory results, however, and the process of optimizing the applied base was abandoned because using Xantphos as a ligand and  $\text{NaO}^t\text{Bu}$  as a base ultimately resulted in a successful reaction.

A large amount of by-products is still formed using these reaction conditions, but the product is formed in decent yields after five days of reaction. The reaction is very slow compared to reported aminations of simple substrates that reach conversions of around 80-90% within a maximum of one day of reaction. More importantly, the starting products can still be detected.

The MW-enlarged product dissolves very poorly in toluene, which enables filtration as a simple way to remove most of the impurities. Subsequent precipitation from diethyl ether already yields a product of decent purity. It is, however, expected that the reaction is negatively affected by this poor solubility of the reaction product. Another result of this problem is the presence of mono-, bis- and tris-substituted compounds in the eventual reaction product rather than one distinct, quantitatively aminated product.

A range of different solvents was tested in an effort to overcome this problem. The reaction did not occur in DMF, and it was doubted if the reaction would occur in  $\text{CHCl}_3$  or  $\text{CH}_2\text{Cl}_2$  in which the product is soluble. The reaction product did dissolve in boiling 1,4-dioxane however, which has previously been reported as a solvent for similar aryl bromide aminations.<sup>34,35</sup>

Performing the reaction in refluxing 1,4-dioxane resulted in approximately 60% amination of the aryl bromide functional groups. Although this is a substantial improvement over the results obtained in toluene ( $\ll 50\%$ , actual conversion was not determined), this still results in mono-, bis- and tris-substituted products with on average two ligands linked to the support. While the low yield by itself is not a major problem in this study, the fact that the aryl bromides of the support are not quantitatively aminated is more problematic, since the actual amount of ligand in catalysis would be unknown and specific advantage of the dendrimer i.e. precisely defined structure and MW, would be lost.

A remarkable characteristic of the reaction in 1,4-dioxane is that it is much faster than in toluene. After 1 hour the reaction is complete and adding more of either of the reactants or the base does not result in any observable continued activity. This was not expected since the reactions ran for days in toluene and the catalyst once formed appeared to be stable in 1,4-dioxane for a number of days. This very limited period of reactivity also frustrated an attempt to add the aryl bromide dropwise to the reaction mixture. It was hoped that creating a large excess of the amine would result in quantitative substitution of the aryl bromide substrate, but apart from some negligible initial activity no improvement could be observed.

It became evident that preformation of the catalyst is important as well. Initially this was not taken into account, leading to several failed reactions and inconsistent results. Formation of

the catalyst by heating a mixture of the ligand and the palladium precursor in dioxane prior to the addition of the other reactants did indeed solve these problems. This observation is in contrast with the article published by Buchwald,<sup>31</sup> where it was reported that catalyst preformation was not necessary and at most led to a faster reaction rather than no reaction at all. In our case, this preformation led to a significantly better coupling reaction.

Since NaO<sup>t</sup>Bu appeared to be poorly soluble in 1,4-dioxane, it was hoped that the conversion could be improved using an alternative base with better solubility. Such a base could not immediately be found, but an alternative is the addition of a crown ether. This increases the activity of the base by solvation of the sodium cation as was reported earlier for the amination of an aryl iodide in THF.<sup>36</sup>

Application of these reaction conditions led to a conversion of 90% of the bromide sites in only 30 minutes. After this time no further improvement could be observed. The reaction was continued for 2 hours and stirred at room temperature overnight. This resulted the formation of a byproduct accounting to  $\pm 20\%$  of the intended product, with similar properties as the actual MW-enlarged ligand. This was also previously observed for a reaction in toluene after it was continued for more than 2 weeks. This byproduct could unfortunately not be separated from the desired product, but its formation can probably be prevented by termination of the reaction at an earlier stage (i.e. after 30 minutes or possibly even less).

An explanation for the fact that the amination stops at a certain conversion, might be due to side reactions like homocoupling or dehalogenation of the aryl bromide. Both are well known palladium catalyzed reactions for aryl halides although normally they do not occur under similar reaction conditions.<sup>37,38</sup> A test reaction was performed to see whether homocoupling or dehalogenation of the aryl bromide occurred indeed. Running the reaction for 24 hours did not result in significant formation of either the dehalogenated or the homocoupled product. It can therefore be concluded that both reactions are not a problem, in particular when the high rate of the amination reaction under the applied reaction conditions is taken into account.

In summary a successful synthetic route has been developed for the synthesis of immobilized PPM. While the reaction was definitely not straightforward as was initially expected, step-by-step progress has resulted in a conversion of 90% of the aryl bromide functional groups of the

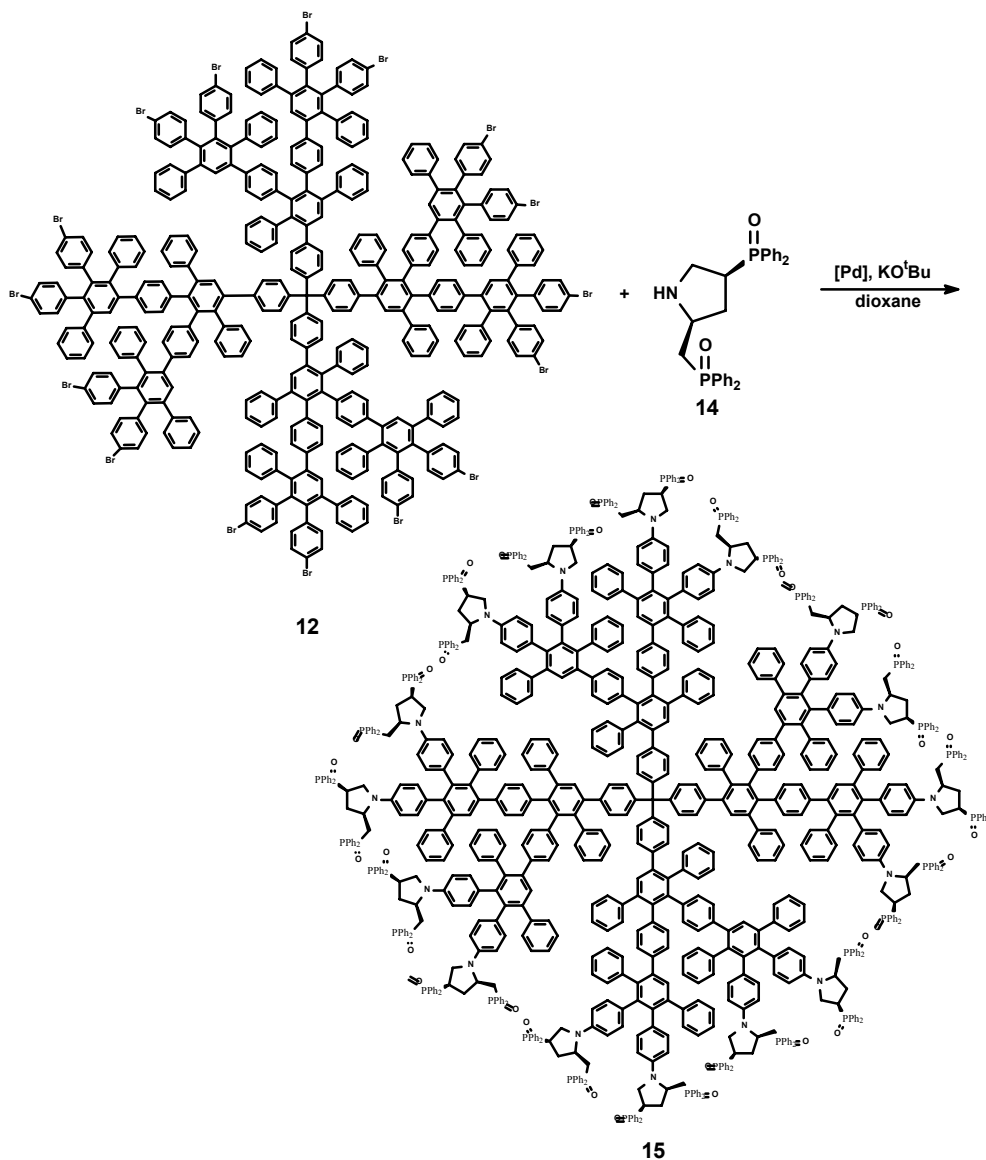
support. It is expected that a 100% pure product can be achieved, either by further improving the conversion or by application of purification methods, such as size-exclusion chromatography.

### **5.2.9 Coupling of Oxidized PPM to a Polyphenylene Dendrimer**

Using the optimized direct amination method, oxidized PPM (**14**) was coupled to a second-generation polyphenylene dendrimer (Scheme 9). From previous experiments and from the coupling of oxidized Nixantphos we did not expect full conversion of all bromide groups on the periphery of the dendrimer. As discussed before, when using the system in catalysis, the metal loading should be adjusted to the average number of ligands on one dendrimer.

The reaction was performed in dioxane, Pd-Xantphos was used as catalyst and KO<sup>t</sup>Bu as base with an amine/aryl bromide ratio of 2. After one night of reaction, five signals were observed in the <sup>31</sup>P NMR spectrum originating from unreacted PPM-oxide (2 peaks), coupled PPM oxide (2 peaks) and one peak which was assigned to the Pd-Xantphos complex. The integration of the peaks belonging to the unreacted PPM-oxide and of the product approached the ratio 1 : 1 which point to full conversion of the aryl bromide groups as the ratio amine/aryl bromide was 2. The reaction was continued for another 24 h but no further change in the integration ratio of the <sup>31</sup>P NMR peaks was observed. The solvent was evaporated, and the product dissolved in CH<sub>2</sub>Cl<sub>2</sub> and washed with aqueous NaHCO<sub>3</sub>. No characterization of this product or catalysis has been performed yet.

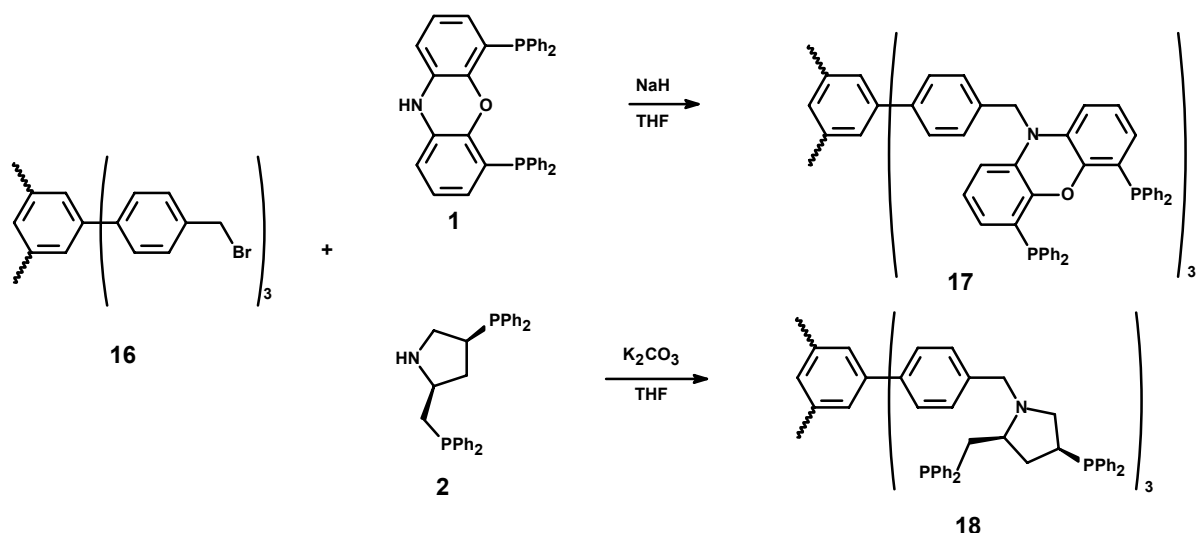




**Scheme 9:** Direct amination of oxidized PPM on a second generation polyphenylene dendrimer.

### 5.2.10 Synthesis of Supported Nixantphos and PPM Using Nucleophilic Substitution Reactions

As discussed in Chapter 2, the nucleophilic substitution on benzyl bromides is a useful and easy reaction to couple ligands to supports. In this section, Nixantphos is coupled to the support **16** containing three benzyl bromide functionalities (Scheme 10).



**Scheme 10:** Synthesis of supported Nixantphos and PPM via nucleophilic substitution.

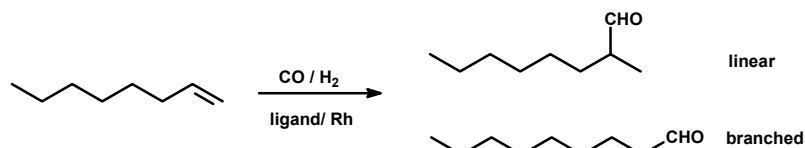
In a test reaction, phenoxazine was used as substrate in the nucleophilic substitution reaction. KOH and K<sub>2</sub>CO<sub>3</sub> were used as base to deprotonate the nitrogen, but according to NMR analysis the reaction failed. Next, NaH in DMF was used as the base as reported by Sandee for a similar reaction.<sup>39</sup> According to NMR the reaction of phenoxazine and 1,3,5-tris[4-(bromomethyl)phenyl]benzene using NaH as the base did indeed lead to the immobilized product. Van der Veen also reported a similar reaction in which he used benzyl chloride in the reaction with Nixantphos to obtain benzyl Nixantphos.<sup>40</sup> This reaction was carried out in THF using also NaH as the preferred base. Using this method, Nixantphos was coupled to the support in good yields. The product was characterized by NMR spectroscopy and MALDI-TOF MS.

One final remark about the substitution reactions should be made. Sandee and Van der Veen used the benzyl chlorides in the nucleophilic substitution reaction because in the reaction of benzyl bromide with Nixantphos, formation of phosphonium salts was observed. This salt formation was not observed in our reactions.

Using the same method, PPM was also immobilized on support **16**. In contrast to the necessity to use a very strong base in the case of Nixantphos, in this reaction K<sub>2</sub>CO<sub>3</sub> was sufficiently strong to facilitate the nucleophilic substitution. The use of a weak base was described by Jia *et al.*<sup>41</sup> who coupled PPM to a benzylic bromide containing cyclodextrines using K<sub>2</sub>CO<sub>3</sub> in DMF.

### 5.2.11 Hydroformylation of 1-octene Using Immobilized Nixantphos

The activity of immobilized Nixantphos and parent Nixantphos were compared in the Rh-catalyzed batch hydroformylation reaction of 1-octene.



**Scheme 11:** Hydroformylation of 1-octene.

The catalyst was prepared *in situ* by mixing the ligand with  $\text{Rh}(\text{CO})_2(\text{acac})$  and pressurizing with syngas to 20 bar at  $80^\circ\text{C}$  for 1.5 h. The hydroformylation reaction gives the linear and branched aldehyde as the two major products (Scheme 11). In the hydroformylation of 1-octene, the linear aldehydes are the desired products, which are commonly used as plasticizers and detergents. The results of these hydroformylation reactions are depicted in Table 4.

**Table 4:** Results of the hydroformylation of 1-octene<sup>a</sup>.

| Ligand  | Time (h) | Conv. (%) | TOF <sup>c</sup> | l:b | % lin. ald. |
|---|----------|-----------|------------------|-----|-------------|
| benzyl Nixantphos <sup>b</sup>                | 0.8      | 20        | 154              | 51  | 94          |
| Nixantphos <sup>b</sup>                       | 0.8      | 20        | 160              | 69  | 95          |
| Nixantphos                                    | 1        | 51        | 300              | 62  | >99         |
| immobilized Nixantphos <b>17</b>              | 1        | 36        | 641              | 59  | >99         |
| immobilized Nixantphos <b>17</b> <sup>d</sup> | 1        | 13        | 74               | 62  | >99         |

<sup>a</sup> Conditions:  $\text{CO}/\text{H}_2=1$ ,  $P(\text{CO}/\text{H}_2)=20$  bar,  $T=80^\circ\text{C}$ , ligand/Rh=5, substrate/Rh=588, toluene,  $\text{Rh}(\text{CO})_2\text{acac}$  precursor; <sup>b</sup> literature values<sup>40</sup>; <sup>c</sup> the TOF is given in  $(\text{mol aldehyde}) (\text{mol Rh})^{-1} (\text{h})^{-1}$ ; <sup>d</sup> without glass beaker, with internal temp. control.

As can be seen in Table 4, the conversion determined for the various ligands is in all cases higher than the reported literature values, resulting in higher TOFs. The l : b ratio lies in the same region as reported in literature. The selectivity towards the linear aldehyde is slightly higher than reported, which means that less hydrogenation or isomerization took place. It must be noted that the conversion determined in multiple experiments for each ligand showed some fluctuation. The reason for this is still unknown.

Continuous catalysis in the flat membrane reactor (discussed in Chapter 4) was not performed because the available membranes are not stable under hydroformylation reaction conditions. Furthermore, because of the poor solubility of syngas in the solvents used, hydroformylation reactions (and gas-liquid reactions in general) are difficult to perform in the dead-end reactor as described in Chapter 1. However, retention measurements of the immobilized ligand were performed. These retention tests were carried out in the aforementioned flat membrane reactor equipped with a Koch MPF-50 membrane and toluene as the solvent. The retention for the immobilized Nixantphos **17** was determined to be 95%. This retention is not high enough for large-scale application but should be sufficient for preliminary test reactions.

### **5.3 Conclusions**

The palladium-catalyzed direct amination reaction proved to be a useful reaction for the coupling of ligands bearing secondary amine groups. Especially in the coupling of phenoxazine high yields were obtained in short reaction times. The coupling of phosphine containing ligand systems to the support molecules was less straightforward. Protection of the phosphorus atoms was necessary, but still low yields were obtained and long reaction times were needed to come to high conversion. The nucleophilic substitution reaction again showed its benefit for the coupling of ligands to benzyl bromide containing supports, as was already demonstrated in Chapter 2. The Nixantphos ligands prepared by this reaction showed comparable 1 : b ratios in the hydroformylation of 1-octene, but a slightly higher selectivity towards the linear aldehyde was observed compared to the original ligands. The retention of the immobilized Nixantphos **17** was determined to be 95%.

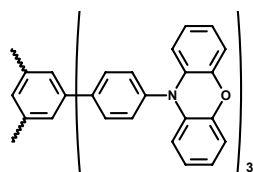
The rigid tris(phenoxazine) compound **8** proved to be a good test compound for the comparison of different nanofiltration membranes and was used to compare the Koch MPF-50 with the STARMEM membranes in two different solvents.

## 5.4 Experimental

### General

All reactions were performed under an inert atmosphere of argon using standard Schlenk techniques. Chemicals were purchased from Aldrich Chemical Co., Acros or VWR. Solvents were purified using basic alumina columns after degassing. NMR spectra were recorded on a Varian Mercury 400 spectrometer (400 MHz for  $^1\text{H}$ , 100 MHz for  $^{13}\text{C}$ , and 162 MHz for  $^{31}\text{P}$ ). GC analyses were performed on a Shimadzu GC-17A (HP Ultra 2 25 m\*0.25 mm column, FID detector).

### 1,3,5-Tris(4-phenyl-10-phenoxazine)benzene **8**



#### *Xantphos 5 / Pd-system*

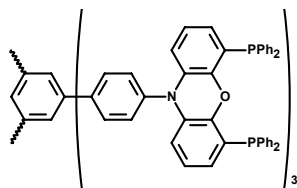
$\text{Pd}_2(\text{dba})_3 \cdot \text{CHCl}_3$  (36.4 mg, 0.04 mmol) and of Xantphos (58.6 mg, 0.10 mmol) were dissolved in 40 mL of dry 1,4-dioxane. This red solution was heated to 100 °C to form the catalyst, resulting in an orange solution. This solution was then added to a Schlenk flask charged with 0.59 g (1.09 mmol) of 1,3,5-tri(4-bromophenyl)benzene **6**, 0.72 g (3.9 mmol) of phenoxazine **7** and 0.45 g (4.68 mmol) of sodium *tert*-butoxide. The reaction mixture was stirred at 100 °C for 2 hours, after which NMR spectroscopy indicated complete reaction. The solvent was evaporated *in vacuo* and 50 mL of  $\text{CHCl}_3$  and 50 mL of hexanes were added to the residue. The resulting suspension was filtered and the product crystallized from the filtrate in the form of brown needles. Yield: 0.86 g (93%).

#### *Buchwald ligand 4 / Pd-system*

Ligand **4** (16.3 mg, 41.4  $\mu\text{mol}$ ) was added to a solution of  $\text{Pd}_2(\text{dba})_3 \cdot \text{CHCl}_3$  (28.6 mg, 27.6  $\mu\text{mol}$ ) in 5 mL of dioxane and stirred at room temperature for 10 minutes. The purple catalyst solution was added to a suspension of 3.0 g (5.5 mmol) 1,3,5-tri(4-bromophenyl)benzene **6**, 3.4 mg (18.2  $\mu\text{mol}$ ) phenoxazine **7** and 2.3 g (20.0 mmol)  $\text{KO}^t\text{Bu}$  in 50 mL of dioxane. The resulting mixture was refluxed overnight. Subsequently, the mixture was filtered and purified using column chromatography with a mixture of hexane and ethyl acetate 40:1. Crystals were

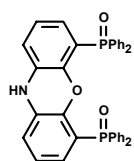
obtained by slowly cooling down a boiling toluene solution of the compound to room temperature.  $^1\text{H}$  NMR ( $\text{CDCl}_3$ , 300 MHz,  $\delta$  ppm): 7.99 (d,  $^3J_{\text{H-H}} = 8.1$  Hz, 6H), 7.98 (s, 3H), 7.51 (d,  $^3J_{\text{H-H}} = 8.1$  Hz, 6H), 6.76-6.62 (m, 18H), 6.04 (dd,  $^3J_{\text{H-H}} = 6.9$  Hz,  $^4J_{\text{H-H}} = 2.1$  Hz, 6H).  $^{13}\text{C}$  NMR ( $\text{CDCl}_3$ , 100 MHz,  $\delta$  ppm): 144.34, 142.04, 141.30, 138.98, 134.66, 131.72, 130.31, 125.96, 123.60, 121.79, 115.87, 113.60.

### 1,3,5-Tris[4-phenyl-10-[4,5-bis(diphenylphosphino)]phenoxazine]benzene **9**

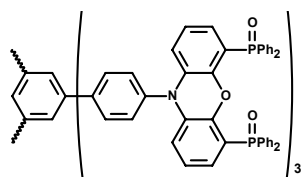


To a suspension of 1.0 g (1.2 mmol) tris(phenoxazine) **8** and 1.3 mL (8.4 mmol) TMEDA in 40 mL ether, 3.4 mL (8.4 mmol) *n*BuLi were added at 0 °C. This caused the solution to turn green. The suspension was stirred overnight at room temperature, cooled to 0 °C and 1.5 mL (8.4 mmol) ClPPh<sub>2</sub> were added and the color changed from green to colorless. After stirring for 24 h, 10 mL brine were added to hydrolyze the reaction mixture. The organic phase was separated, dried and concentrated giving a yellow solid (a combination of mono- and disubstituted product).  $^{31}\text{P}$  NMR ( $\text{CDCl}_3$ , 162 MHz,  $\delta$  ppm): -18.8 (s, PPh<sub>2</sub> disubstituted), -15.4 (s, PPh<sub>2</sub> monosubstituted).

### 4,5-Bis(diphenylphosphino)phenoxazine **10**



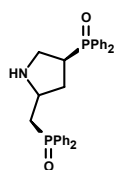
Nixantphos (2.0 g, 3.6 mmol) was suspended in ethanol and 0.4 mL (10 mmol) of a 30 wt% solution H<sub>2</sub>O<sub>2</sub> was added at 0°. This mixture was stirred for 1 h at room temperature after which the solvent was evaporated. The remaining solids were dissolved in CH<sub>2</sub>Cl<sub>2</sub> and washed with aqueous NaHCO<sub>3</sub>, dried with MgSO<sub>4</sub> and concentrated to dryness yielding 1.2 g (57 %) white solid.  $^{31}\text{P}$  NMR ( $\text{CDCl}_3$ , 162 MHz,  $\delta$  ppm): 26.86.

**1,3,5-Tris[4-phenyl-10-[4,5-bis(diphenylphosphinoyl)]phenoxazine]benzene 11**

Buchwald ligand **2** (4.7 mg, 12.0  $\mu\text{mol}$ ) were added to a solution of 6.2 mg (6.0  $\mu\text{mol}$ )  $\text{Pd}_2(\text{dba})_3 \cdot \text{CHCl}_3$  in 2 mL of dioxane and stirred at room temperature for 10 minutes. Next the purple catalyst solution was added to a suspension of 0.54 g (0.1 mmol) 1,3,5-tri(4-bromophenyl)benzene **6**, 0.2 g (0.34 mmol) Nixantphos oxide **10** and 0.14 g (0.42 mmol)  $\text{Cs}_2\text{CO}_3$  in 40 mL of dioxane. The resulting mixture was refluxed overnight. Subsequently, the mixture was concentrated to dryness and redissolved in  $\text{CH}_2\text{Cl}_2$ , washed with an aqueous  $\text{NaHCO}_3$  solution and dried with  $\text{MgSO}_4$ . Precipitation with ether yielded 0.14 g (68%) of a brown solid.  $^1\text{H}$  NMR ( $\text{CDCl}_3$ , 200 MHz,  $\delta$  ppm): 7.78 (s, 3H, Ar-H), 7.97-7.36 (m, 75H, Ar-H), 6.45-6.04 (m, 18H).  $^{31}\text{P}$  NMR ( $\text{CDCl}_3$ , 81 MHz,  $\delta$  ppm): 29.21 (s). MALDI-TOF-MS:  $m/z$  2051.6 ( $[\text{trisubstituted}+\text{H}]^+$ , calcd 2052.1), 1549.4 ( $[\text{disubstituted}+\text{H}]^+$ , calcd 1548.4).

**G<sub>2</sub>-Td-Nixantphos(oxide)<sub>1-16</sub> 13**

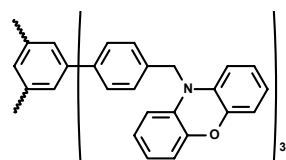
A mixture of 0.21 g (35  $\mu\text{mol}$ ) dendrimers **12**, 0.65 g (1.11 mmol) Nixantphos oxide **10**, and 0.46 g (1.4 mmol)  $\text{Cs}_2\text{CO}_3$  in 40 mL toluene was degassed using 3 cycles of vacuum/Argon. To this mixture, a solution of 22.0 mg (56.0  $\mu\text{mol}$ ) ligand and 14.5 (14.0  $\mu\text{mol}$ )  $\text{Pd}_2(\text{dba})_3 \cdot \text{CHCl}_3$  in 5 mL toluene was added. The obtained mixture was refluxed for 72 h after which the solvent was evaporated and replaced by dioxane. Next, a solution of 32 mg (56  $\mu\text{mol}$ ) xantphos and  $\text{Pd}_2(\text{dba})_3 \cdot \text{CHCl}_3$  14.5 mg (14.0  $\mu\text{mol}$ ) in 5 mL dioxane was added, after which the solution was refluxed for 48 h. 20 mL of a saturated  $\text{NaHCO}_3$  solution were added, filtered and extracted with  $\text{CH}_2\text{Cl}_2$ . Yield: 340 mg brown solid which was purified by precipitation from  $\text{CH}_2\text{Cl}_2$  with ethanol.  $^1\text{H}$  NMR ( $\text{CDCl}_3$ , 200 MHz,  $\delta$  ppm): 7.41 (br), 7.17 (br), 6.88 (br), 6.20 (br), 5.56 (br).  $^{31}\text{P}$  NMR ( $\text{CDCl}_3$ , 81 MHz,  $\delta$  ppm): 29.23. MALDI-TOF-MS:  $m/z$  11471.8 (br, min. 9000, max. 15000),  $[\text{monosubstituted}]^+$ , calcd. 6650.3,  $[\text{fully substituted}]^+$ , calcd. 14191.1.

**4-(Diphenylphosphinoyl)-2-[(diphenylphosphinoyl)methyl]pyrrolidine 14**

To a solution of 1.0 g (1.8 mmol) PPM in 20 mL ethanol, 0.5 mL (10 mmol) of a 30 wt% solution  $\text{H}_2\text{O}_2$  was added at room temperature. After stirring for 0.5 h, ethanol was evaporated, solids dissolved in  $\text{CH}_2\text{Cl}_2$  and washed with aqueous  $\text{NaHCO}_3$ . After drying and evaporation of the solvent, PPM(oxide) was obtained as a yellow oil, which solidified upon addition of ether. Yield: 1.0 g (quantitative).  $^1\text{H}$  NMR ( $\text{CDCl}_3$ , 300 MHz,  $\delta$  ppm): 7.73-7.57 (m, 8H), 7.38-7.35 (m, 12H), 4.15-3.70 (br, 1H, N-H), 3.56-3.47 (m, 1H), 3.35-3.26 (m, 1H), 3.04-2.88 (m, 2H), 2.85-2.74 (m, 1H), 2.51-2.40 (m, 1H), 2.19-2.13 (m, 1H), 1.78-1.62 (m, 1H).  $^{13}\text{C}$  NMR ( $\text{CDCl}_3$ , 100 MHz,  $\delta$  ppm): 133.90, 133.46, 132.08-131.96 (m), 131.071-130.88 (m), 129.07-128.76 (m), 55.42, 46.31, 37.95 (d,  $^2J_{P-C} = 10.0$  Hz), 35.11, 34.44.  $^{31}\text{P}$  NMR ( $\text{CDCl}_3$ , 81 MHz,  $\delta$  ppm): 33.96 ( $\text{CH}_2\text{POPh}_2$ ), 29.96 ( $\text{POPh}_2$ ).

**G<sub>2</sub>-Td-PPM(oxide)<sub>1-16</sub> 15**

PPM(oxide) **14** (0.55 g, 1.1 mmol) and 0.218 g (35.4  $\mu\text{mol}$ ) dendrimers **12** were dissolved in 15 mL dry dioxane. Upon addition of 0.150 g (1.3 mmol)  $\text{KO}^t\text{Bu}$ , the yellow solution turned red. A catalyst solution of 32.5 mg (56.0  $\mu\text{mol}$ ) Xantphos and 14.7 mg (14.2  $\mu\text{mol}$ )  $\text{Pd}_2(\text{dba})_3 \cdot \text{CHCl}_3$  was added. The resulting red solution was refluxed overnight. After evaporating the solvent, the product was redissolved in  $\text{CH}_2\text{Cl}_2$  and washed with aqueous  $\text{NaHCO}_3$ , dried and concentrated yielding 350 mg of brown solid.  $^{31}\text{P}$  NMR ( $\text{CDCl}_3$ , 162 MHz,  $\delta$  ppm): 36.00 ( $\text{CH}_2\text{POPh}_2$ ), 31.71 ( $\text{POPh}_2$ ).

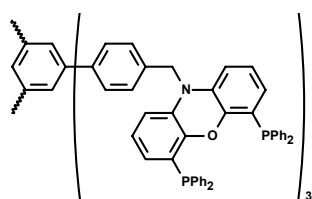
**1,3,5-Tris(4-phenyl-methyl-10-phenoxazine)benzene**

A solution of 550 mg (3.00 mmol) phenoxazine in 5 mL DMF was added to a suspension of 180 mg (4.50 mmol) of a 60 wt% suspension of NaH in mineral oil in 5 mL DMF under continuous stirring. This mixture was stirred during 2 h at 70  $^\circ\text{C}$ . 0.50 g (0.85 mmol) 1,3,5-



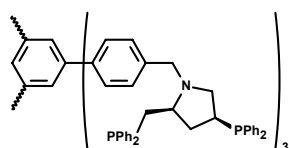
tris[(4-bromomethyl)phenyl]benzene **16** was added at room temperature. The mixture was stirred overnight at 70 °C followed by filtration and evaporation of the solvent. The mixture was dissolved in CH<sub>2</sub>Cl<sub>2</sub> and washed with water. The product was purified by size exclusion chromatography using CH<sub>2</sub>Cl<sub>2</sub> as eluent. <sup>1</sup>H NMR (CDCl<sub>3</sub>, 300 MHz, δ ppm): 4.84 (s, 6H), 6.39 (m, 6H), 6.71 (m, 18H), 7.41 (d, <sup>3</sup>J<sub>H-H</sub> = 8.4 Hz, 6H), 7.66 (d, <sup>3</sup>J<sub>H-H</sub> = 8.4 Hz, 6H), 7.74 (s, 3H). <sup>13</sup>C NMR (CDCl<sub>3</sub>, 75 MHz, δ ppm): 49.02 (-CH<sub>2</sub>N), 112.12, 115.23, 121.21, 123.65, 124.87, 126.50, 127.747, 133.73, 135.71, 139.93, 141.79, 145.09.

### 1,3,5-Tris[4-phenyl-methyl-10-[4,5-bis(diphenylphosphinoyl)]phenoxazine]benzene **17**



To a solution of 1.0 g (1.8 mmol) Nixantphos in 20 mL of THF was added 0.10 g (2.5 mmol) of a 60 wt% suspension of NaH in mineral oil and the reaction mixture was relaxed for 1 h. A solution of 0.30 g (0.50 mmol) 1,3,5-tris[(4-bromomethyl)phenyl]benzene **16** in 10 mL THF was added drop wise and the reaction mixture was refluxed for another 21 h. The purple reaction mixture was diluted with 40 mL of toluene and hydrolyzed with 40 mL of brine. The water layer was removed and the organic layer was dried over MgSO<sub>4</sub>. The mixture was concentrated and the residue was washed with hexane, dissolved in CH<sub>2</sub>Cl<sub>2</sub> and precipitated with EtOH (0.45 mmol, 90%). <sup>1</sup>H NMR (CDCl<sub>3</sub>, 400 MHz, δ ppm): 4.90 (s, 6H), 6.08 (dd, <sup>3</sup>J<sub>H-H</sub> = 6.0 Hz, <sup>4</sup>J<sub>H-H</sub> = 2.0 Hz, 6H), 6.38 (dd, <sup>3</sup>J<sub>H-H</sub> = 7.2 Hz, <sup>4</sup>J<sub>H-H</sub> = 0.8 Hz, 6H), 6.63 (t, <sup>3</sup>J<sub>H-H</sub> = 8.0 Hz, 6H), 7.27 (m, 60H), 7.45 (d, <sup>3</sup>J<sub>H-H</sub> = 8.0 Hz, 6H), 7.69 (d, <sup>3</sup>J<sub>H-H</sub> = 8.0 Hz, 6H), 7.77 (s, 3H). <sup>13</sup>C NMR (CDCl<sub>3</sub>, 100 MHz, δ ppm): 49.73 (-CH<sub>2</sub>N), 112.87, 123.90, 125.03, 125.76, 126.74, 128.28 (m), 133.91 (m), 135.56, 136.91, 140.10, 141.95, 147.51. <sup>31</sup>P NMR (CDCl<sub>3</sub>, 162 MHz, δ ppm): -19.00. MS (MALDI-TOF) m/z: 1997.77 (calcd for C<sub>135</sub>H<sub>99</sub>N<sub>3</sub>O<sub>3</sub>P<sub>6</sub>: 1997.13)

### 1,3,5-Tris[4-phenyl-methyl-1-{4-(diphenylphosphinoyl)-2-[(diphenylphosphinoyl)methyl]pyrrolidine}benzene **18**



1.5 g (3.3 mmol) PPM and 0.2 g (5 mmol)  $K_2CO_3$  were dissolved in 20 mL THF and stirred for 15 min at room temperature. Additionally, 0.5 g (0.85 mmol) 1,3,5-tris[(4-bromomethyl)phenyl]benzene **16** was added and stirring was continued for 16 h. After filtration of the reaction mixture, 5 mL toluene were added. After washing with degassed 4M NaOH, the solution was dried with  $MgSO_4$  and concentrated to dryness. Yield: 1.0 g (66%) white solid.  $^1H$  NMR ( $CDCl_3$ , 400 MHz,  $\delta$  ppm): 7.73 (s, 3H), 7.59-7.17 (m, H), 4.10 (d,  $^1J_{H-H} = 14.0$  Hz, 1H), 3.36 (d,  $^1J_{H-H} = 14.0$  Hz, 1H), 2.98 (m, 1H), 2.76-2.55 (m, 3H), 2.22-2.09 (m, 2H), 1.74-1.59 (m, 1H), 1.4 (m, 1H).  $^{31}P$  NMR ( $CDCl_3$ , 162 MHz,  $\delta$  ppm): -2.64 ( $-CH_2PPh_2$ ), -20.33 ( $PPh_2$ ).

### **Hydroformylation of 1-octene**

The hydroformylation reaction was carried out in a stainless steel autoclave (75 mL) equipped with a dropping funnel, an inner glass beaker and a magnetic stirring bar. It was heated by the use of an electric heating mantle. The autoclave was evacuated and heated to 80  $^{\circ}C$  overnight, flushed with argon and the catalyst solutions were added using a syringe. The autoclave was pressurized to 20 bar for 1.5 h. After preformation of the catalyst, the substrate solution was added using a dropping funnel. The reaction was stopped after 1 h by cooling on ice and the autoclave was depressurized. Samples were directly analyzed by GC. In a typical hydroformylation experiment, the catalyst solution consisted of 2.60 mg (10.0  $\mu$ mol) of the precursor  $Rh(CO)_2(acac)$  in 5 mL toluene and a ligand solution of 27.6 mg (50.0  $\mu$ mol) of Nixantphos in 10 mL toluene or 33.3 mg (16.7  $\mu$ mol) of MW-enlarged Nixantphos in 10 mL of toluene. Substrate solutions consisted of 1 mL of 1-octene (filtered over neutral activated alumina), 0.5 mL of n-decane (internal standard) and 5 mL of toluene. 0.5 mL of this solution was taken for GC analysis.

### **Retention measurements**

#### Retention measurement in toluene

The nanofiltration membranes, stored in water/ethanol mixture, were immersed in methanol overnight followed by a  $CH_2Cl_2$  bath for 1 h. Finally the membranes were immersed in a toluene bath prior to use. The membrane was cut and installed into the membrane reactor

followed by flushing the membrane with 25 mL of solvent. The test compound was dissolved in 3 mL of toluene of which 2 mL were injected into the reactor. Next 50 mL of solvent were flushed through the reactor with a flow of 20 mL/h at 20 bar and collected in a measuring flask. The retention was determined by UV/Vis spectrophotometry.

### Retention measurement in ethyl acetate

The retention was measured similar to the measurements in toluene, but the membranes were only immersed overnight in MeOH and for 1 h in ethyl acetate before use.

## 5.5 References and Notes

- <sup>1</sup> M. Kranenburg, Y. E. M. van der Burgt, P. C. J. Kamer, P. W. N. M. van Leeuwen, *Organometallics* **1995**, *14*, 3081.
- <sup>2</sup> P. W. N. M. van Leeuwen, P. C. J. Kamer, J. N. H. Reek, P. Dierkes, *Chem. Rev.* **2000**, *100*, 2741.
- <sup>3</sup> L. A. van der Veen, P. H. Keeven, G. C. Schoemaker, J. N. H. Reek, P. C. J. Kamer, P. W. N. M. van Leeuwen, M. Lutz, A. L. Spek, *Organometallics*, **2000**, *19*, 872.
- <sup>4</sup> P. W. N. M. van Leeuwen, P. C. J. Kamer, J. N. H. Reek, *Pure Appl. Chem.*, **1999**, *71*, 1443.
- <sup>5</sup> A. J. Sandee, J. N. H. Reek, P. C. J. Kamer, P. W. N. M. van Leeuwen, *J. Am. Chem. Soc.* **2001**, *123*, 8468.
- <sup>6</sup> P. W. N. M. van Leeuwen, A. J. Sandee, J. N. H. Reek, P. C. J. Kamer, *J. Mol. Cat. A: Chem.* **2002**, 107.
- <sup>7</sup> Strem Chemicals, Inc., Dexter Industrial Park 7, Mulliken Way, Newburyport, USA.
- <sup>8</sup> K. Achiwa, *J. Am. Chem. Soc.* **1976**, *98*, 8265.
- <sup>9</sup> K. Achiwa, *Chem. Lett.* **1978**, 905.
- <sup>10</sup> G. L. Baker, J. Fritschel, J. R. Stille, J. K. Stille, *J. Org. Chem.*, **1981**, *46*, 2954.
- <sup>11</sup> G. Oehme, I. Grassert, S. Ziegler, R. Meisel, H. Fuhrmann, *Catalysis Today* **1998**, *42*, 459.
- <sup>12</sup> T. Dwars, J. Haberland, I. Grassert, G. Oehme, U. Kragl, *J. Mol. Cat. A: Chem.* **2001**, *168*, 81.
- <sup>13</sup> J. Jamis, J. R. Anderson, R. S. Dickson, E. M. Campi, W. R. Jackson, *J. Organomet. Chem.* **2000**, *603*, 80.
- <sup>14</sup> B. Pugin, *J. Mol. Cat. A: Chem.*, **1996**, 107, 273.
- <sup>15</sup> D.W. Old, J.P. Wolfe, S.L. Buchwald, *J. Am. Chem. Soc.* **1998**, *120*, 9722.
- <sup>16</sup> A. R. Muci, S. L. Buchwald, *Topics in Current Chemistry* **2002**, *219*, 131.
- <sup>17</sup> B. H. Yang, S. L. Buchwald, *J. Organomet. Chem.* **1999**, *576*, 125.
- <sup>18</sup> D. Zim, S. L. Buchwald, *Org. Lett.* **2003**, *14*, 2413.
- <sup>19</sup> A. Ghosh, J. E. Sieser, M. Riou, W. Cai, L. Rivera-Ruiz, *Org. Lett.* **2003**, *13*, 2207.
- <sup>20</sup> H. J. Shine, S.-M. Wu, *J. Org. Chem.* **1979**, *19*, 3310.
- <sup>21</sup> Y. Shirota, H. Inada (to Bando Chem. Ind. Ltd.), *JP 6312982*, **1994**.
- <sup>22</sup> H. Gilman, L. O. Moore, *J. Am. Chem. Soc.* **1957**, *79*, 3485.
- <sup>23</sup> A. S. Shetty, J. Zhang, J. S. Moore, *J. Am. Chem. Soc.* **1996**, *118*, 1019.
- <sup>24</sup> H. P. Dijkstra, C. A. Kruithof, N. J. Ronde, R. van de Coevering, D. J. Ramón, D. Vogt, G. P. M. Klink, G. van Koten, *J. Org. Chem.* **2003**, *68*, 675.
- <sup>25</sup> Koch International B.V., Mechelaarstraat 14, 4903 RE Oosterhout (NB). [www.kochmembrane.com](http://www.kochmembrane.com).
- <sup>26</sup> Membrane Extraction Technology Ltd, c/o Department of Chemical Engineering, Imperial College, London [www.membrane-extraction-technology.com](http://www.membrane-extraction-technology.com)
- <sup>27</sup> L. A. van der Veen, P. H. Keeven, G. C. Schoemaker, J. N. H. Reek, P. C. J. Kamer, P. W. N. M. van Leeuwen, M. Lutz, A. L. Spek, *Organometallics* **2000**, *19*, 872.
- <sup>28</sup> C. Charrier, W. Chodkiewicz, P. Cadiot, *Bull. Soc. Chim. Fr.* **1966**, 1002.
- <sup>29</sup> F. Morgenroth, K. Müllen, *Tetrahedron* **1997**, *45*, 15349.
- <sup>30</sup> M. Kranenburg, P. C. J. Kamer, P. W. N. M. van Leeuwen, *Eur. J. Inorg. Chem.* **1998**, *1*, 25.

- <sup>31</sup> J. P. Wolfe, S. L. Buchwald, *J. Org. Chem.* **2000**, *65*, 1144.
- <sup>32</sup> R. J. P. Corriua, C. Guérina, B. J. L. Hennera, A. Joliveta, *J. Organomet. Chem.* **1997**, *530*, 39.
- <sup>33</sup> I. P. Beletskaya, A. V. Chuchurjukin, H. P. Dijkstra, G. P. M. van Klink, G. van Koten, *Tetrahedron Lett.* **2000**, *41*, 1081.
- <sup>34</sup> R. G. Browning, H. Hahmud, V. Badarinarayana, C. J. Lovely, *Tetrahedron Lett.* **2001**, *42*, 7155.
- <sup>35</sup> G. A. Grasa, M. S. Viciu, J. Huang, S. P. Nolan, *J. Org. Chem.* **2001**, *66*, 7729.
- <sup>36</sup> J. P. Wolfe, S. L. Buchwald, *J. Org. Chem.* **1997**, *62*, 6066.
- <sup>37</sup> J. Hassan, V. Penalva, L. Lavbenot, C. Gozzi, M. Lemaire, *Tetrahedron* **1998**, *54*, 13793.
- <sup>38</sup> M. S. Viciu, G. A. Grasa, S. P. Nolan, *Organometallics* **2001**, *20*, 3607.
- <sup>39</sup> A. J. Sandee, *Tailor-made catalysts immobilised on silica*, Thesis, University of Amsterdam, **2001**
- <sup>40</sup> L.A. van der Veen, *New ligands for selective hydroformylation*, Thesis, University of Amsterdam, **1999**
- <sup>41</sup> C. Yang, Y. T. Wong, Z. Li, J. J. Krepinsky, G. Jia, *Organometallics* **2001**, *20*, 5220.



# 6

## **Ligand Immobilization by Suzuki Coupling and Ullmann Diaryl Ether Synthesis**

### **Abstract**

---

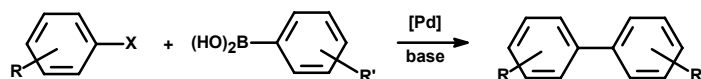
In this chapter, the Suzuki reaction was tested as a coupling reaction for the immobilization of pincer ligands. A series of molecular enlarged catalysts was synthesized with different size and shape. Their retention in a nanofiltration membrane reactor is investigated. Furthermore, the Ullmann diaryl ether synthesis was used to couple hydroxyl derivatives of the pincer ligand to different supports.

---

## 6.1 Introduction

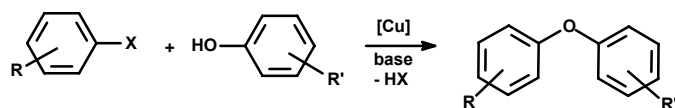
The development of efficient coupling methods, binding ligands known from their good performance in homogeneous catalysis to a support, is of utmost importance for the immobilization of homogeneous catalysts. Prerequisites for such coupling reactions are high conversions, high selectivities and preferably formation of rigid non-reactive bonds. Complete conversion of the anchoring point of the used support is important in order to avoid reactive sites left on the support. High selectivity is of importance to prevent unwanted reactions on the support molecules or ligands. When using small or lower generation dendrimers, rigid bonds can improve the retention behavior because shape changes are not possible.<sup>1</sup>

Polyphenylene dendrimers<sup>2</sup> have been used as soluble supports (see also chapter 4). These dendrimers bear halide groups on the periphery, which can be used for further functionalization. The most direct way of coupling aryl groups to these aryl halide groups on the supports is by C-C coupling. For the coupling of aryl groups the Suzuki coupling can be used which is a reaction of an aryl halide with a boronic acid or ester of a second aryl compound.<sup>3,4</sup> This coupling will give the most rigid link between ligand and support, which is an advantage for the separation of the catalyst by membrane filtration: Rigid structures will not undergo shape changes and thus leaching is diminished.



**Scheme 1:** General Suzuki coupling.

The availability of phenolic ligand precursors (see also chapter 1) for the Ullmann diaryl ether synthesis is another attractive coupling method to functionalize the aryl halide groups on the support molecules.<sup>5,6,7,8</sup> The Ullmann reaction is a reaction of an aryl halide and a phenol group catalyzed by copper salts under basic conditions giving diaryl ethers (Scheme 2). The classical Ullmann ether synthesis<sup>9</sup> remains an important tool in diaryl ether synthesis, despite its limitations such as elevated temperature (125-220°C), solvents like pyridine, collidine or DMF, enormous purification problems, generally low yields and the use of stoichiometric quantities of copper.



**Scheme 2:** General Ullmann diaryl ether synthesis.

Recently Buchwald *et al.* published a method using catalytic amounts of copper<sup>10</sup> instead of stoichiometric amounts. Studies were performed to find optimal reaction conditions. A variety of solvents were tested which showed that a combination of toluene with a small amount of ethyl acetate (5 mol%) was the most effective combination of solvents. The ethyl acetate is proposed to increase the solubility of the copper(I) complexes which results in higher activity. Screening of different bases confirmed that cesium carbonate was responsible for the improved activity. The choice of copper source proved to be less important. All sorts of copper(I) salts gave similar results except for  $(\text{CuOTf})_2 \cdot \text{C}_6\text{H}_6$ , which gave a slightly accelerated reaction, probably due to higher solubility.

In 2002 a paper was published by Reider *et al.* about the rate acceleration in the Ullmann diaryl ether synthesis by 2,2,6,6-tetramethylheptane-3,5-dione (TMHD).<sup>11</sup> Typical reaction conditions were: 1 eq. of aryl halide, 2 eq. of phenol, 0.1 eq. of TMHD and 2 eq. of cesium carbonate in NMP, to which 0.5 eq. of CuCl was added. Without TMHD this reaction was 10 to 15 times slower. Unfortunately large amounts of copper salts had to be used in this system.

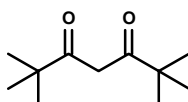


**Figure 1:** TMHD.

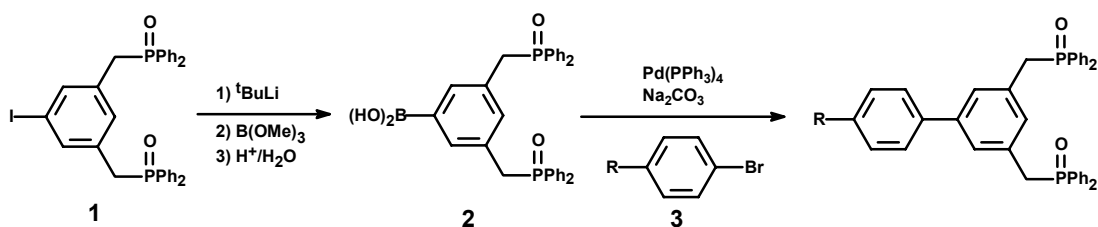
In this chapter the Suzuki coupling reaction and the Ullmann diaryl ether synthesis will be used to couple pincer ligands to model structures of the above-mentioned bromide containing polyphenylene dendritic supports (**9**, **10** and **11** Scheme 6).



## 6.2 Results and Discussion

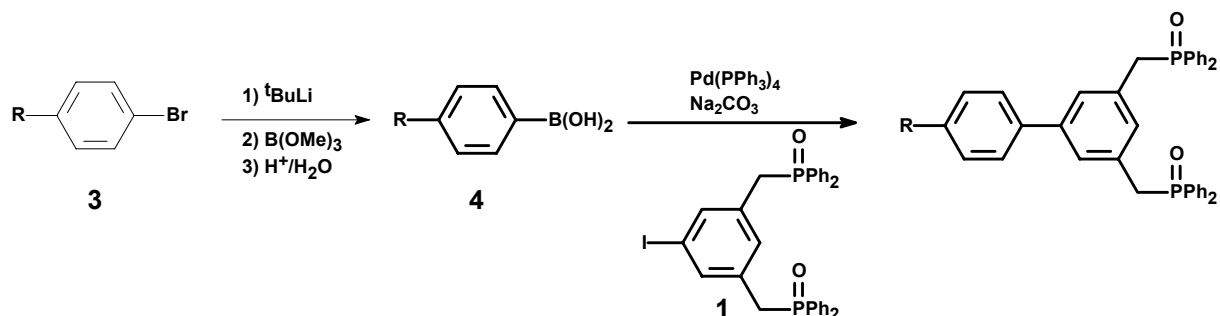
### 6.2.1 Suzuki Coupling

Two possible routes are available to perform the Suzuki reaction between ligand and support. The first route makes use of the boronic acid derivative of the ligand, which is coupled to the aryl bromides of the support molecule (Scheme 3). This boronic acid has to be synthesized from **1** by lithiation with 2 equivalents of  $t\text{BuLi}$ , followed by quenching in trimethylborate and hydrolysis to the boronic acid **2**.



Scheme 3: Suzuki coupling route 1.

The second route makes use of the boronic acid of the support **3** and the aryllic halide ligand **1** (Scheme 4). This route will work in the case of relatively small support molecules but not in the case of dendrimers. The reasons for this are, limitations in the lithiation step that has to be performed multiple times on the dendrimer: The lithiation reaction will lead to dramatic changes in solubility of the partially lithiated molecule causing precipitation preventing full conversion.



Scheme 4: Suzuki coupling route 2.

Because of the above-mentioned reasons the first route (the preferred route in the case of dendritic supports) was explored first. The boronic acid derivative of the pincer precursor **2** was synthesized starting from the iodine pincer derivative **1**, which was suspended in ether and lithiated with <sup>t</sup>BuLi at -78°C. The lithiated compound was quenched in trimethylborate. After hydrolysis the boronic acid could be obtained in quantitative yields. The Suzuki coupling was performed in a mixture of dimethoxyethane (DME) and water, containing 2 M Na<sub>2</sub>CO<sub>3</sub> using Pd(PPh<sub>3</sub>)<sub>4</sub> as catalyst. Unfortunately, no reaction occurred which was confirmed by <sup>31</sup>P NMR spectroscopy. Only the signal of the starting material was observed.

Therefore, the second route was tried using the boronic acid of support **4** which was reacted with iodine pincer derivative **1**. This route seemed to give better results. In overnight experiments a new signal was found in the <sup>31</sup>P NMR spectrum while the signal of the starting compound had decreased or even disappeared. Two signals are indicative for the change in chemical environment at the coupling point: The methylene protons connected to the phosphorus atom which can be observed by <sup>1</sup>H NMR and the phosphorus atoms themselves observed by <sup>31</sup>P NMR. By adding more starting material to the NMR tube, conclusions could be drawn on the position of signal of the starting compound and the products. In all cases the signals of the products were shifted to higher field meaning more electron density around the measured phosphorus atom. With this method three differently shaped molecules were synthesized (Figure 2, Figure 3, Figure 4). Compound **5** bears a central silicon atom surrounded by 4 wedges with pincer ligands. This molecule has a spherical structure, while compound **6**, built up from a central polyphenylene core, has a disk-like structure. The third compound in this series **7** is a kind of rod.

During the reaction, samples were taken and analyzed by <sup>1</sup>H and <sup>31</sup>P NMR spectroscopy. Using the integration of the different signals, the conversion could be determined. The difficulty in this analysis was the limited amount of signals, which can be observed well separated from each other. The signals, which are explicit for the product or the starting material, are the signals from the methylene protons which are connected to the phosphorus atoms. Other signals overlap each other in the aromatic region, which makes conclusive observations difficult. In <sup>31</sup>P NMR, the signal of the product could be assigned by addition of extra substrate, which increased the integral belonging to the starting material. This product characterization is unfortunately not appropriate in all cases (*vide infra*).

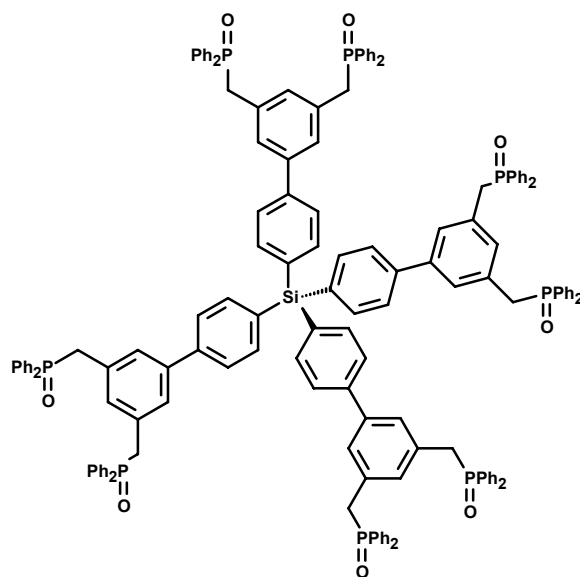


**Figure 2:** Suzuki coupling product 5.

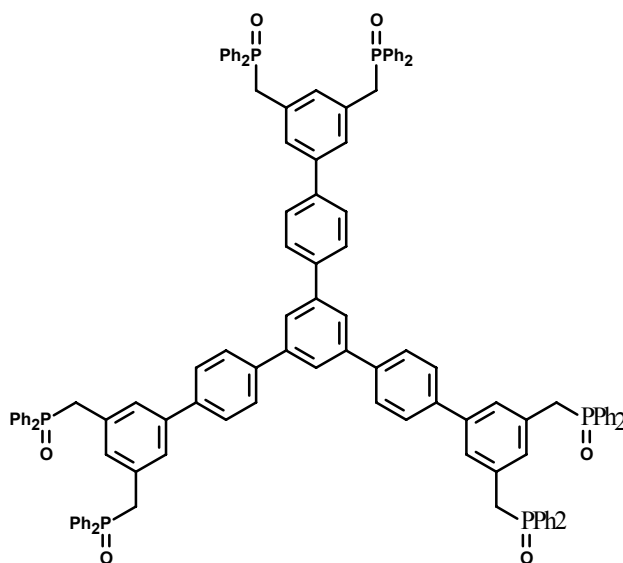


**Figure 3:** Suzuki coupling product 6.

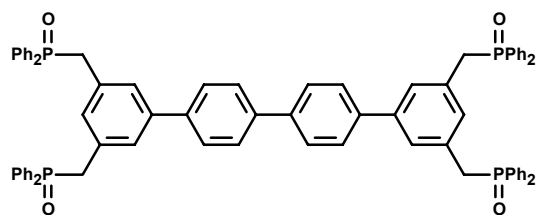


**Figure 4:** Suzuki coupling product 7.

### 6.2.2 Retention Tests with Ligands Synthesized via Suzuki Coupling.

With these differently shaped compounds retention tests in nanofiltration (Koch MPF-50) were performed (Table 1). A high retention was expected for **6** having the largest diameter. On the contrary **7**, with its long but small dimensions, was expected to cross the membrane faster.

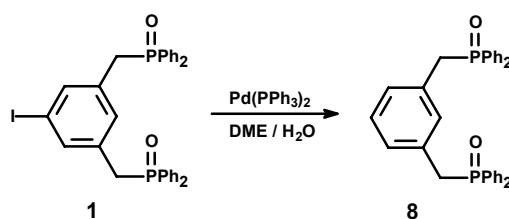
**Table 1:** Retention of Suzuki coupling products.

| Compound | Retention CH <sub>2</sub> Cl <sub>2</sub> (%) <sup>a</sup> | Retention DMF(%) <sup>b</sup> |
|----------|--|-------------------------------|
| <b>5</b> | 65.2   | 95.8                          |
| <b>6</b> | 62.0   | 96.9                          |
| <b>7</b> | 96.0   | 89.4                          |

<sup>a</sup>Average of 2 measurements; <sup>b</sup>Only 1 experiment performed.

Surprisingly, **5** and **6** showed low retention in CH<sub>2</sub>Cl<sub>2</sub> while the retention of **7** was reasonable. Changing the solvent from CH<sub>2</sub>Cl<sub>2</sub> to DMF had a huge effect on the retentions of **5** and **6** while that of **7** decreased only a little. These results questioned the purity of the compounds. It can be imagined that small impurities present in compounds **5** and **6** can be washed out during retention tests, suggesting low retentions.

Attempts were made to grow crystals from the three compounds in order to obtain X-ray crystal structures, which can prove the structure and dimensions of the synthesized compounds. From a solution containing **5**, crystals suitable for X-ray analysis could be obtained. However, the isolated material appeared to be the dehalogenated pincer derivative **8** (Scheme 5).



**Scheme 5:** Dehalogenation of iodopincer.

X-ray analysis showed that the dehalogenated compound was present in the product mixture. Size exclusion chromatography was performed to separate the by-products. It turned out that the desired compound is only a small portion of these mixtures whereas the rest consisted of **8**. In 2003 Zhang *et al.* reported about unusual dehalogenation reactions in the Suzuki and Stille coupling of bromopyrroles and aryls.<sup>12</sup> In some cases more than 50% of the starting material was dehalogenated instead of coupled to the boronic acid derivatives.

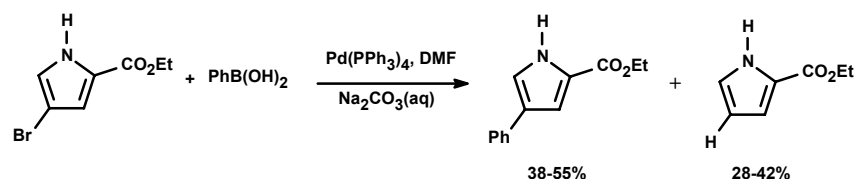


**Figure 5:** Dehalogenation in Suzuki coupling by Zhang *et al.*<sup>12</sup>

To circumvent this unwanted side-reaction, the free amine functionality was protected with a BOC group, leading to almost quantitative conversion to the desired product. From this result two possible causes can be proposed for the dehalogenation in our case. The solubility of the multiple boronic acids in the used solvent mixtures is low. The coupling reaction becomes very slow causing the dehalogenation reaction to be the major reaction pathway. Furthermore, highly polar groups like the amine in the reported article or phosphineoxide groups in the present case can interfere in the catalytic cycle of the Suzuki coupling. A solution for this problem can be the use of other protecting groups for the phosphorus atom like sulphur or the use of BH<sub>3</sub> adducts.

Knowing that most of the product of the Suzuki coupling was the dehalogenated pincer ligand, <sup>1</sup>H NMR signals of the dehalogenated starting compound can be assigned to the NMR spectra of the products. A coupled pincer ligand should only show 2 singlets in the area of 7.20-7.00 ppm in the ratio 1 : 2 which belong to the protons H<sup>a</sup> and H<sup>b</sup> (Figure 6).

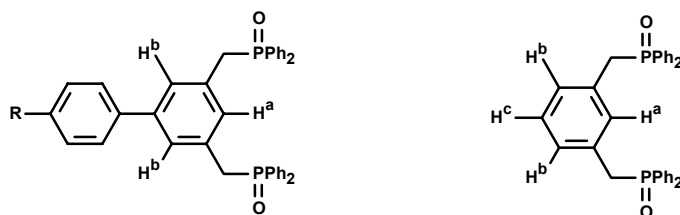


**Figure 6:** Characteristic <sup>1</sup>H NMR signals of coupled pincer vs. dehalogenated pincer ligand.

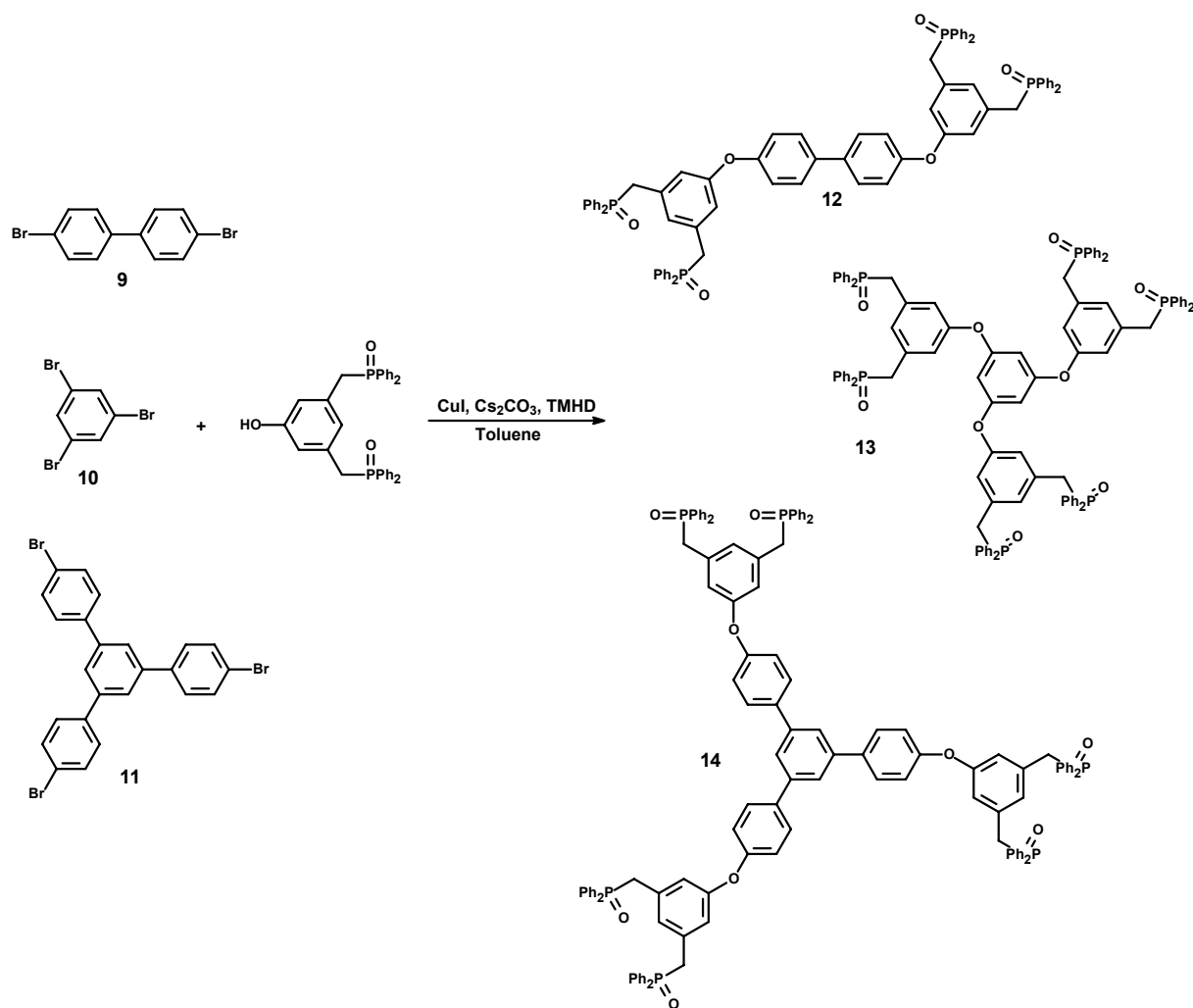
In some cases however, 3 signals were observed for protons of the unwanted product ( $H^a$  singlet,  $H^b$  multiplet and  $H^c$  multiplet).

This result made clear that full conversion of the aryl bromide groups on the support (*vide supra*) was not achieved, and the  $^{31}\text{P}$  NMR peak assigned to the product of the Suzuki coupling appeared to belong to the dehalogenated pincer.

### 6.2.3 Ullmann Diaryl Ether Synthesis

The second coupling method described in this chapter is the so-called Ullmann diaryl ether synthesis. We wanted to investigate this reaction because of the availability of the phenolic pincer ligand and the simplicity of this reaction. A combination of the two methods described in the introduction was used to perform the reaction. The typical reaction was performed in toluene, with cesium carbonate as base. To increase the solubility of the copper salt, TMHD or ethyl acetate was added as described by Buchwald and Reider.<sup>10,11</sup> The obtained mixture was degassed, after which copper(I) iodide was added. This reaction was usually performed for multiple days to drive the reaction to full conversion.

Again three differently shaped molecules were synthesized by this reaction starting from 4,4'-dibromobiphenyl **9**, 1,3,5-tribromobenzene **10** and 1,3,5-tris(4-bromophenyl)benzene **11**, respectively (Scheme 6). After workup, the compounds were purified by size exclusion chromatography to remove the excess of phenolic pincer compound. The products were analyzed using MALDI-TOF MS. The products were obtained as mixtures with the different intermediates (mono- and disubstituted in the case of compounds 2 and 3). The difference in weight between mono-, di- and tri-substituted compound (ca. 400 Da) is too small to separate the compounds using size exclusion chromatography. Preparative HPLC should be the method of choice.



**Scheme 6:** Synthesis of three ligand systems by the Ullmann reaction.

### 6.3 Conclusions

Suzuki coupling proved not to be a suitable reaction for the synthesis of molecular enlarged pincer systems. A dehalogenation process proved to be the major reaction instead of the desired C-C coupling. Selecting other protecting groups for the phosphines and further optimization of this reaction could possibly lead to better results. Unfortunately the Suzuki coupling has many parameters making simple optimization difficult. Examples are: solvent, co-solvent, base, catalyst, type of functional groups on the halide and on the boronic acid and the excess of reactants. However, optimization using high-throughput experimentation techniques could be the solution.<sup>13</sup>

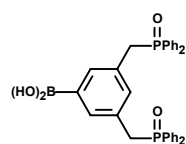
The Ullmann coupling reaction proved to be the method of choice in the coupling of a phenolic pincer ligand to different aryl bromide supports. Unfortunately, no full conversion of the bromide was obtained despite long reaction times and excess of phenol. Additional copper salt and/or co-solvent can possibly drive the reaction to completion.

## 6.4 Experimental

### General

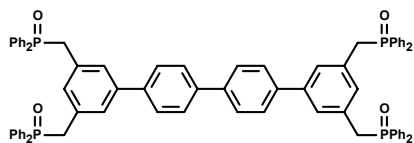
All reactions were performed under an inert atmosphere of argon using standard Schlenk techniques. Chemicals were purchased from Aldrich Chemical Co., Acros or VWR. Solvents were purified using basic alumina columns after degassing. NMR spectra were recorded on a Varian Mercury 400 spectrometer (400 MHz for  $^1\text{H}$ , 100 MHz for  $^{13}\text{C}$ , and 162 MHz for  $^{31}\text{P}$ ).

### 3,5-Bis[(diphenylphosphineoyl)methyl]benzene boronic acid **2**

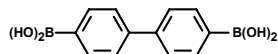


Iodopincer **1** (0.5 g, 0.81 mmol) was suspended in 30 mL ether and cooled to  $-78^\circ\text{C}$ . Next, 0.3 mL (2.0 mmol) of a 0.5 M  $t\text{BuLi}$  in hexane solution was added dropwise to this suspension. While stirring this mixture for 15 minutes the color changed from white to orange. Then, 0.4 mL (3.5 mmol) trimethylborate was added at once changing the color to white again. After warming the mixture to room temperature and stirring for another 15 min., 10 mL of 4 M HCl were added to hydrolyse the borate to boronic acid. The organic phase was separated and the aqueous phase extracted 3 times with  $\text{CH}_2\text{Cl}_2$ . The combined organic phases were dried with  $\text{MgSO}_4$  and concentrated *in vacuo* yielding 0.43 g (quantitative) of off white product.  $^1\text{H}$  NMR ( $\text{CDCl}_3$ , 200 MHz,  $\delta$  ppm): 7.67 (br, 20H, Ar-H), 7.11 (s, 2H), 7.04 (s, 1H), 4.90 (br, 1H,  $-\text{B}(\text{OH})_2$ ), 3.45 (d,  $^2J_{\text{P-H}} = 13.6$  Hz, 4H,  $-\text{CH}_2-$ ).  $^{31}\text{P}$  NMR ( $\text{CDCl}_3$ , 81 MHz,  $\delta$  ppm): 30.61.

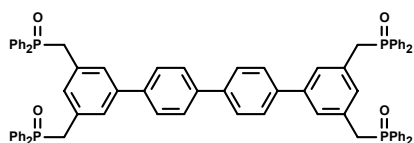


**3,5,3''',5'''-Tetrakis[(diphenylphosphinoyl)methyl]-[1,1',4',1'',4'',1''']quaterphenyl 7***Suzuki coupling of dibromobiphenyl 9 and PCP boronic acid 2*

A mixture of 0.68 g (1.3 mmol) boronic acid **2**, 0.18 g (1.0 mmol) 4,4'-dibromobiphenyl, 15 mL Na<sub>2</sub>CO<sub>2</sub> (aq) and 45 mL dimethoxyethane were degassed 6 times. After adding 5 mol% of Pd(PPh<sub>3</sub>)<sub>4</sub> the mixture was heated to reflux. The progress of the reaction was followed by -unlocked <sup>31</sup>P NMR. The reaction mixture was worked up by concentrating to a small volume and extracting the product with CH<sub>2</sub>Cl<sub>2</sub>. After characterization it was concluded that the desired product was not obtained, the synthesis was redone using Suzuki coupling route 2 (*vide infra*).

**Biphenyl-4, 4'-diboronic acid 15**

The experimental conditions are similar to those described for **2**. Product extracted with ether, washed with water and dried on MgSO<sub>4</sub>. Yield: 0.80 g (quantitative) white solid. <sup>1</sup>H NMR (CDCl<sub>3</sub>, 300 MHz, δ ppm): 7.56 (d, <sup>3</sup>J<sub>H-H</sub> = 6.6 Hz, 4H), 7.41 (d, <sup>3</sup>J<sub>H-H</sub> = 6.3 Hz, 4H).

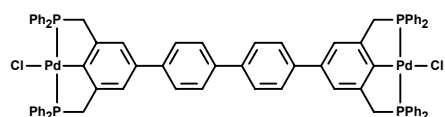
**3,5,3''',5'''-Tetrakis[(diphenylphosphinoyl)methyl]-[1,1',4',1'',4'',1''']quaterphenyl 7***Suzuki coupling of iodopincer 1 and biphenyl-4,4'-diboronic acid 15*

The experimental conditions are similar to those described for the previous Suzuki coupling. Yield: 2.5 g (53%) white solid. <sup>1</sup>H NMR (CDCl<sub>3</sub>, 400 MHz, δ ppm): 7.72-7.67 (m, 20H), 7.52-7.44 (m, 28H), 7.18-7.08 (m, 10H), 3.63 (d, <sup>2</sup>J<sub>P-H</sub> = 12.0 Hz, 8H) (*I-PCP*: 3.53). <sup>31</sup>P NMR (CDCl<sub>3</sub>, 162 MHz, δ ppm): 30.70 (*I-PCP*: 30.65). Anal. calcd for C<sub>76</sub>H<sub>62</sub>O<sub>4</sub>P<sub>4</sub>: C 79.20; H 5.32. Found: C 73.32; H 5.37.

## Reduction of phosphineoxides

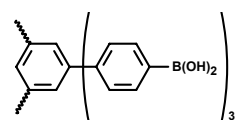
The phosphineoxides were dissolved or suspended in toluene. After degassing, 3 eq.  $\text{HSiCl}_3$  per phosphineoxide group were added. The mixture was refluxed for 1-4 h after which it was cooled to room temperature followed by hydrolysis with a thoroughly degassed 2 M NaOH solution. The mixture was concentrated *in vacuo* after which the product was extracted with dichloromethane. After drying and concentrating the products were obtained in almost quantitative yields.

## Metallated dipincer 16

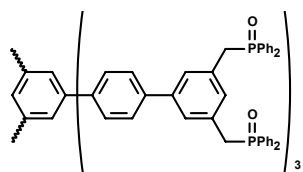


This complex was synthesized according to a literature procedure from the starting phosphinoyde-protected compound **15**.<sup>14</sup> Yield: 0.64 g (88%) yellow solid.  $^1\text{H}$  NMR ( $\text{CDCl}_3$ , 400 MHz,  $\delta$  ppm): 7.91-7.42 (m, 67H), 4.05 (t,  $^4J_{\text{P-H}} = 4.4$  Hz, 8H).  $^{31}\text{P}$  NMR ( $\text{CDCl}_3$ , 162 MHz,  $\delta$  ppm): 34.27. Anal. calcd for  $\text{C}_{76}\text{H}_{60}\text{Cl}_2\text{P}_4\text{Pd}_2$ : C 66.10; H 4.38. Found: C 61.48; H 4.10

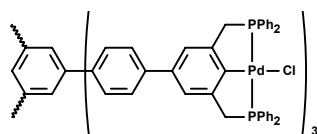
## 1,3,5-Tri(*p*-phenylboronic acid)benzene 17



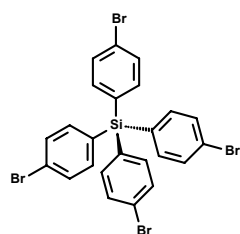
The experimental conditions are similar to those described for **2**. During lithiation, the color turned from white to gray. Upon addition of  $\text{B}(\text{OMe})_3$  the color changed to white again. Product was extracted with  $\text{CH}_2\text{Cl}_2$ , washed with hexane and dried on  $\text{MgSO}_4$ . Yield: 0.57 g (50%) light pink solid.  $^1\text{H}$  NMR ( $\text{CDCl}_3$ , 200 MHz,  $\delta$  ppm): 7.71 (s, 3H), 7.63 (d,  $^3J_{\text{H-H}} = 5.6$  Hz, 6H), 7.55 (d,  $^3J_{\text{H-H}} = 5.6$  Hz, 6H).

**Tris[3,5-bis(diphosphinoylmethyl)phenyl]-1,3,5-triphenylbenzene 6***Suzuki coupling of iodopincer 1 and 1,3,5-tri(phenylboronic acid)benzene 17*

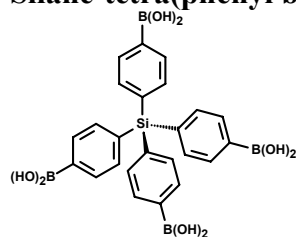
Triboronic acid **17** (1.5 g, 3.4 mmol) and 7.0 g (12.4 mmol) I-PCP **1** was suspended in a mixture of 15 mL 2M Na<sub>2</sub>CO<sub>3</sub> and 45 mL ethyleneglycol. After degassing 3 times, 5 mol% Pd(PPh<sub>3</sub>)<sub>4</sub> was added and the mixture was heated to 120°C for 2 days. The mixture was neutralized with 2 M HCl (aq) and extracted with CH<sub>2</sub>Cl<sub>2</sub>. After drying, 6.2 g (96%) of light brown product was obtained. <sup>1</sup>H NMR (CDCl<sub>3</sub>, 200 MHz, δ ppm): 7.78-7.41 (br, 75H, Ar-H), 6.95 (s, 6H, Ar-H), 6.80 (s, 12H, Ar-H), 3.53 (d, <sup>2</sup>J<sub>P-H</sub> = 14.0 Hz, 12H, -CH<sub>2</sub>-) (*I-PCP*: 3.45). <sup>31</sup>P NMR (CDCl<sub>3</sub>, 81 MHz, δ ppm): 30.50 (*I-PCP*: 30.13). Anal. calcd for C<sub>120</sub>H<sub>96</sub>O<sub>6</sub>P<sub>6</sub>: C 79.20; H 5.32. Found: C 71.06; H 5.11.

**Metallated triPCP 18**

Synthesized according to literature procedure starting from the phosphinoyl-protected compound.<sup>14</sup> <sup>1</sup>H NMR (CDCl<sub>3</sub>, 400 MHz, δ ppm): 7.91-7.42 (m, 67H), 4.05 (t, <sup>4</sup>J<sub>P-H</sub> = 4.4 Hz, 8H). <sup>31</sup>P NMR (CDCl<sub>3</sub>, 162 MHz, δ ppm): 34.27. Anal. calcd for C<sub>76</sub>H<sub>60</sub>Cl<sub>2</sub>P<sub>4</sub>Pd<sub>2</sub>: C 66.10; H 4.38. Found: C 61.48; H 4.10.

**Tetrakis(4-bromophenyl)silane 19**

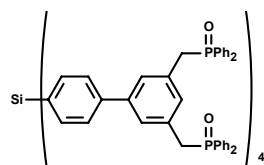
Synthesis according to literature procedure.<sup>15</sup>

**Silane-tetra(phenyl boronic acid) 20**

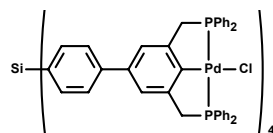
The experimental conditions are similar to those described for **2**. THF was used as solvent instead of ether.

**Tris[3,5-bis(diphosphinoylmethyl)phenyl]-tetraphenylsilane 5**

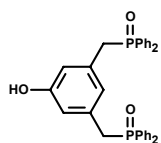
*Suzuki coupling of iodopincer 1 and silane-tetra(phenyl boronic acid) 20*



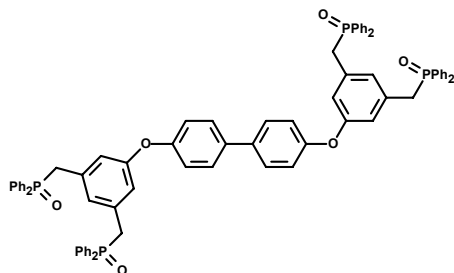
The experimental conditions are similar to those described for the previous Suzuki coupling. Purified by column chromatography using a mixture of MeOH and CH<sub>2</sub>Cl<sub>2</sub> (1:9) as eluent. <sup>1</sup>H NMR (CDCl<sub>3</sub>, 400 MHz, δ ppm): 7.66-7.61 (m, 40H), 7.51-7.40 (m, 48H), 7.03-6.89 (m, 18H), 3.54 (d, <sup>2</sup>J<sub>P-H</sub> = 13.6 Hz, 16H). <sup>13</sup>C NMR (CDCl<sub>3</sub>, 100 MHz, δ ppm): 171.34, 132.97, 132.34 (t, <sup>4</sup>J<sub>P-C</sub> = 5.3 Hz), 131.98, 131.58, 131.48, 131.32 (d, <sup>2</sup>J<sub>P-C</sub> = 9.1 Hz), 128.82, 128.71 (d, <sup>2</sup>J<sub>P-C</sub> = 12.1 Hz), 128.61, 128.59, 38.08 (d, <sup>1</sup>J<sub>P-C</sub> = 65.9 Hz); <sup>31</sup>P NMR (CDCl<sub>3</sub>, 162 MHz, δ ppm): 30.77 (*I-PCP*: 31.78). Anal. calcd for C<sub>152</sub>H<sub>124</sub>O<sub>8</sub>P<sub>8</sub>Si: C 77.54; H 5.31. Found: C 73.32; H 5.40.

**Metallated Si-tetrapincer 21**

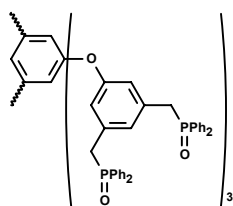
Synthesized according to literature procedure starting from the phosphinoyl protected compound **20**.<sup>14</sup> <sup>1</sup>H NMR (CDCl<sub>3</sub>, 400 MHz, δ ppm): 7.90-7.85 (m, 30H), 7.42-7.39 (m, 47H), 7.13-7.11 (m, 13H), 3.96 (t, <sup>4</sup>J<sub>P-H</sub> = 4.8 Hz, 16H, -CH<sub>2</sub>-). <sup>31</sup>P NMR (CDCl<sub>3</sub>, 162 MHz, δ ppm): 34.50.

**3,5-Bis[(diphenylphosphinoyl)methyl]phenol**

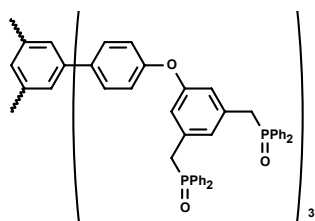
Synthesized as described in chapter 2.

**4,4'-Bis[3,5-bis[(diphenylphosphinoyl)methyl]phenoxy]biphenyl 12**

3,5-Bis[(diphenylphosphinoyl)methyl]phenol (1.5 g, 2.3 mmol), 0.30 g (1.0 mmol) 4,4'-bisbromobiphenyl, 37 mg (0.2 mmol) TMHD and  $\text{Cs}_2\text{CO}_3$  were suspended in dry toluene. After degassing the suspension three times, 190 mg (1 mmol)  $\text{CuI}$  were added and the suspension was subsequently degassed. Upon heating everything dissolved yielding an orange solution, which was refluxed for 4 days. Water was added, the organic phase was separated and the aqueous phase was extracted three times with toluene yielding a green solid. The product was purified by size exclusion chromatography using Biobeads X-1 as stationary and  $\text{CH}_2\text{Cl}_2$  as the mobile phase. 0.32 g (27%) off white solid.  $^1\text{H}$  NMR ( $\text{CDCl}_3$ , 400 MHz,  $\delta$  ppm): 7.67-7.36 (m, 52H), 6.88 (s, 2H), 6.72-6.68 (m, 4H), 6.59 (s, 4H), 3.53 (d,  $^3J_{P-H} = 13.6$  Hz, 8H).  $^{13}\text{C}$  NMR ( $\text{CDCl}_3$ , 100 MHz,  $\delta$  ppm): 157.05, 156.77, 139.80, 135.77, 135.00, 133.46, 132.97, 132.18, 132.12, 132.00, 131.39 (d, 9.1 Hz), 128.86 (d, 11.4 Hz), 128.71, 128.37, 128.25, 127.88, 121.49, 119.60, 119.22, 119.17, 38.16 (d,  $^1J_{P-C} = 66.0$  Hz).  $^{31}\text{P}$  NMR ( $\text{CDCl}_3$ , 162 MHz,  $\delta$  ppm): 29.23. MALDI-TOF-MS:  $m/z$  1195.4 ( $[\text{M} + \text{H}]^+$ , calcd. 1195.4), 1217.4 ( $[\text{M} + \text{Na}]^+$ , calcd. 1217.3), 1233.4 ( $[\text{M} + \text{K}]^+$ , calcd. 1233.4); mono couplings product:  $m/z$  753.2 ( $[\text{M} + ^{79}\text{Br} + \text{H}]^+$ , calcd. 753.1), 755.2 ( $[\text{M} + ^{81}\text{Br} + \text{H}]^+$ , calcd. 755.1), 775.1 ( $[\text{M} + ^{79}\text{Br} + \text{Na}]^+$ , calcd. 775.1), 777.1 ( $[\text{M} + ^{81}\text{Br} + \text{Na}]^+$ , calcd. 777.1).

**1,3,5-Tris[3,5-bis[(diphenylphosphinoyl)methyl]phenoxy]benzene 13**

The experimental conditions were similar to those described for **12**. After purification by SEC, 0.8 g (49%) of the product was obtained.  $^1\text{H}$  NMR ( $\text{CDCl}_3$ , 400 MHz,  $\delta$  ppm): 7.64-7.60 (m, 26H), 7.41-7.34 (m, 36H), 6.96 (s, 33H), 6.60 (6H), 3.55 (d,  $^2J_{P-H} = 13.2\text{Hz}$ ,  $-\text{CH}_2-$ ).  $^{13}\text{C}$  NMR ( $\text{CDCl}_3$ , 100 MHz,  $\delta$  ppm): 158.85, 156.12, 133.74, 132.60, 132.20, 131.61, 131.26 (d,  $^2J_{P-C} = 9.1\text{ Hz}$ ), 128.84 (d,  $^2J_{P-C} = 11.4\text{ Hz}$ ), 128.14, 119.68, 103.84, 38.00 (d,  $^1J_{P-C} = 65.9\text{ Hz}$ ).  $^{31}\text{P}$  NMR ( $\text{CDCl}_3$ , 162 MHz,  $\delta$  ppm): 29.79. MALDI-TOF-MS:  $m/z$  1640.4 ( $[\text{M} + \text{H}]^+$ , calcd. 1640.6), 1662.3 ( $[\text{M} + \text{Na}]^+$ , calcd. 1662.6).

**Tris-*p*-[3,5-bis[(diphenylphosphinoyl)methyl]phenoxy]-1,3,5-triphenylbenzene 14**

The experimental conditions were similar to those described for **12**. After purification by SEC, 0.5 g (27%) of the product was obtained.  $^1\text{H}$  NMR ( $\text{CDCl}_3$ , 400 MHz,  $\delta$  ppm): 7.71-7.40 (m, 77H), 6.86 (s, 3H), 6.78-6.77 (m, 6H), 6.63 (s, 6H), 3.54 (d, 13.6 Hz, 12H).  $^{13}\text{C}$  NMR ( $\text{CDCl}_3$ , 100 MHz,  $\delta$  ppm): 157.11, 142.31, 136.06, 133.57, 133.01, 132.34, 132.16, 131.43 (d,  $^2J_{P-C} = 9.1\text{ Hz}$ ), 129.25, 128.88 (d,  $^2J_{P-C} = 12.1\text{ Hz}$ ), 127.85, 125.32, 124.74, 119.62, 119.28, 38.23 (d,  $^1J_{P-C} = 65.2\text{ Hz}$ ).  $^{31}\text{P}$  NMR ( $\text{CDCl}_3$ , 162 MHz,  $\delta$  ppm): 29.19. MALDI-TOF-MS:  $m/z$  1868.3 ( $[\text{M} + \text{H}]^+$ , calcd. 1868.9), 1890.23 ( $[\text{M} + \text{Na}]^+$ , calcd. 1890.9); di-couplings product:  $m/z$  1427.1 ( $[\text{M} + \text{H}]^+$ , calcd. 1427.3), 1449.1 ( $[\text{M} + \text{Na}]^+$ , calcd. 1449.3); mono couplings product:  $m/z$  985.0 ( $[\text{M}]^+$ , calcd. 984.7), 1006.9 ( $[\text{M} + \text{Na}]^+$ , calcd. 1007.7).

## 6.5 References and Notes

- <sup>1</sup> H. P. Dijkstra, C. A. Kruithof, N. J. Ronde, R. van de Coevering, D.J. Ramón, D. Vogt, G. P. M. van Klink, G. van Koten, *J. Org. Chem.* **2003**, *68*, 675.
- <sup>2</sup> F. Morgenroth, K. Müllen, *Tetrahedron* **1997**, *45*, 15349.
- <sup>3</sup> A. Suzuki, *Pure & Appl. Chem.* **1994**, *66*, 213.
- <sup>4</sup> N. Miyaura, A. Suzuki, *Chem. Rev.* **1995**, *95*, 2457.
- <sup>5</sup> J. S. Sawyer, *Tetrahedron* **2002**, *56*, 5045.
- <sup>6</sup> F. Theil, *Angew. Chem. Int. Ed.* **1999**, *38*, 2345.
- <sup>7</sup> J. Lindley, *Tetrahedron* **1984**, *40*, 1433.
- <sup>8</sup> J. Hassan, M. Sevignon, C. Gozzi, E. Schulz, M. Lemaire, *Chem. Rev.* **2002**, *102*, 1359.
- <sup>9</sup> F. Ullmann, *Chem. Ber.* **1904**, *37*, 853.
- <sup>10</sup> J.-F. Marcou, S. Doye, S. L. Buchwald, *J. Am. Chem. Soc.* **1997**, *119*, 10539.
- <sup>11</sup> E. Buck, Z. J. Song, D. Tschäen, P. G. Dormer, R. P. Volante, P. J. Reider, *Org. Lett.* **2002**, *4*, 1623.
- <sup>12</sup> S. T. Handy, H. Bregman, J. Lewis, X. Zhang, Y. Zhang, *Tetrahedron Lett.* **2003**, *44*, 427.
- <sup>13</sup> E. G. IJpeij, F. H. Beijer, H. J. Arts, C. Newton, J. G. de Vries, G.-J. M. Gruter, *J. Org. Chem.* **2002**, *67*, 169.
- <sup>14</sup> I. P. Beletskaya, A. V. Chuchurjukin, H. P. Dijkstra, G. P. M. van Klink, G. van Koten, *Tetrahedron Lett.*, **2000**, *41*, 1081.
- <sup>15</sup> B. Kirste, W. Harrer, H. Kurreck, *Angew. Chem.* **1981**, 912.

## Summary

For the development of supported or immobilized homogeneous catalysts, the stability of the catalyst is a key factor determining the success of an approach. In the work described in this thesis, the stable tridentate PCP-ligand system was used, leading to very stable coordination to transition metals. The supports used consisted of polyphenylene molecules, resulting in shape persistent, rigid catalyst systems. This rigidity favors high retention in membrane filtration and minimizes possible cooperative (most of the time negative) dendritic effects. The aim of this thesis was to synthesize rigid molecular enlarged catalyst systems able to perform continuous catalysis with high TON. Dendritic catalysts as well as smaller, non-dendritic systems were compared in order to obtain information about the required size and shape for these catalysts.

**Chapter one** gave an overview of the techniques used to separate homogeneous catalysts from the reaction mixture by means of membrane filtration. Dendrimer-supported homogeneous catalysts together with molecular enlarged systems were discussed together with the applied reactors and membranes. Furthermore, dendritic effects observed in catalysis were discussed.

The synthesis of rigid supported PCP-pincer ligand systems was described in **Chapter two**. The ligands were coupled to three different support molecules using nucleophilic substitution reactions of phenolic ligand precursors and support molecules functionalized with benzyl bromide groups. The support molecules differed in size and shape, which made it possible to investigate the influences of these parameters on catalytic performance and retention behavior using nanofiltration. Retention tests in  $\text{CH}_2\text{Cl}_2$  and THF in a nanofiltration membrane (Koch MPF-50) reactor, showed moderate to good retentions. The influence of the solvent was negligible. Furthermore, catalytic tests were performed with all ligand systems in the palladium-catalyzed allylic substitution reactions showing constant, high selectivities and slightly variable activities.

The kinetics of the allylic amination reaction catalyzed by PCP-pincer-Pd systems was investigated in **Chapter three**. The reaction orders were determined and the rate constant was measured. For the reaction of morpholine with cinnamyl acetate, a zeroth order in cinnamyl acetate and a first order in both morpholine and catalyst were found; The rate constant was determined to be  $6.68 \cdot 10^{-2} \text{ h}^{-1}$  under standard conditions. These values were used to predict conversions when the pincer ligand systems were applied in a continuous stirred tank reactor.



**Chapter four** describes the application of the largest pincer system in continuous homogeneous catalysis. Both the allylic alkylation and the allylic amination reactions were performed in a continuously operated nanofiltration membrane reactor. Reactions were performed for more than 10 h. During these experiments a drop in activity was observed. The lack of complete retention of the catalyst only could not explain this drop in activity, which points to a deactivation process. Investigations of this deactivation showed that the performance of catalyst is not influenced by added water or membrane material. Catalysis under air gave no conversion. From this, contamination with oxygen was expected to cause the deactivation. The source of oxygen in the system is unknown yet.

In **Chapter five**, a side project was performed in which diphosphine ligands, bearing secondary amine groups, are coupled to different supports. The actual coupling reaction was a palladium-catalyzed amine coupling to support molecules functionalized with aryl bromide groups. Using this coupling method, Nixantphos and PPM were immobilized on a model support and on a second-generation polyphenylene dendrimers. Furthermore, the nucleophilic substitution reaction, explored in chapter two, was used for the coupling of these ligands to rigid supports. Comparison of the parent Nixantphos to the immobilized Nixantphos derivative showed constant, high selectivities in the rhodium-catalyzed hydroformylation of 1-octene, but a slightly higher activity was observed.

Alternative coupling methods were tested in **Chapter six**. Here the Suzuki coupling is tested in the reaction of boronic acid derivatives of the pincer ligand with aryl halide groups on the support and *vice versa*. Precise analysis of the products showed that the desired coupling was not the major reaction but this was a palladium-catalyzed dehalogenation process. Furthermore, a coupling reaction between phenolic pincer ligand derivatives and support molecules containing aryl halide groups was investigated, the so-called Ullmann diaryl ether synthesis. Using this reaction, three different pincer ligand systems were synthesized. Characterization by MALDI-TOF showed the desired product together with incompletely functionalized intermediate compounds. It was impossible to separate the product from this mixture by size-exclusion chromatography.

## Samenvatting

Bij de ontwikkeling van gedragen of geïmmobiliseerde homogene katalysatoren, is de stabiliteit van het katalysatorsysteem een van de belangrijkste factoren die bepalend zijn voor het succes van de gekozen methode. In het werk, beschreven in dit proefschrift, werd gebruik gemaakt van tridentate PCP-liganden, die zeer stabiele complexen kunnen vormen met overgangsmetalen. De dragermoleculen die werden gebruikt, bestaan uit polyfenyleen moleculen, die vormvaste, rigide katalysatorsystemen opleveren. Deze rigiditeit geeft bij toepassing in membraanfiltratie een vergrootte kans op hoge retentie en minimaliseert mogelijke coöperatieve (meestal negatieve), dendritische effecten. Het doel van dit onderzoek was de synthese van rigide, moleculair-vergrootte katalysator systemen die, met hoge productiviteit, kunnen worden toegepast in continue katalyse. Dendritische katalysatoren en kleinere modelsystemen werden vergeleken om informatie te krijgen over de benodigde grootte en de gewenste vorm van dergelijke katalysatoren.

In **Hoofdstuk een** werd een overzicht gegeven van de mogelijkheden voor de scheiding van homogene katalysatoren van het reactiemengsel door middel van membraanfiltratie. Dendriemergedragen homogene katalysatoren en moleculair-vergrootte systemen werden hier besproken samen met de gebruikte reactoren en membranen. Vervolgens werd het “dendrimeer effect”, wat in sommige katalyses voorkomt, besproken.

De synthese van rigide, gedragen PCP-ligand systemen werd beschreven in **Hoofdstuk twee**. De liganden werden gekoppeld aan drie verschillende dragermoleculen met behulp van een nucleofiele substitutie reactie tussen een fenolische ligandprecursor en de benzyl-bromide groepen op het dragermolecuul. De zo verkregen moleculen verschillen in grootte en vorm, waardoor het mogelijk werd de invloed van deze parameters op de katalytische prestatie en op het gedrag in nanofiltratie te onderzoeken. De retenties werden getest in  $\text{CH}_2\text{Cl}_2$  en THF in een nanofiltratiemembraan (Koch MPF-50) reactor, waarbij middelmatige tot goede retenties werden gevonden. De invloed van het oplosmiddel was verwaarloosbaar. Daarnaast werden er katalytische testen uitgevoerd op de allylische substituties reactie, constante, hoge selectiviteiten werden gevonden met een kleine variatie in de activiteit van de katalysator.

De kinetiek van de allylische aminerings reactie gekatalyseerd door PCP-palladium systemen werd onderzocht in **Hoofdstuk drie**. De reactieorders werden bepaald en de snelheidsconstante werd gemeten. Voor de reactie van morfoline met cinnamylacetaat werd een nulde orde in cinnamylacetaat gevonden en een eerste orde afhankelijkheid in morfoline en in de katalysator; De snelheidsconstante

werd bepaald op  $6.68 \cdot 10^{-2} \text{ h}^{-1}$  bij standaard condities. Deze waarden werden gebruikt om voorspellingen te doen van de te verwachten omzettingen bij de toepassing van deze PCP-palladium systemen in een continue, geroerde reactor.

**Hoofdstuk vier** beschreef de toepassing van het grootste PCP systeem in continue homogene katalyse. De allylische alkylering alsmede de allylische aminering werden uitgevoerd in een continu werkende membraanreactor. De reactie werd gedurende meer dan 10 uur uitgevoerd. Tijdens deze experimenten werd een afname van de activiteit waargenomen. Deze afname in activiteit kan niet alleen verklaard worden door onvolledige retentie, wat wijst in de richting van deactivering. Onderzoek van deze deactivering liet zien dat de prestaties van de katalysator niet worden beïnvloed door het toevoegen van water of membraanmateriaal. Bij katalyse in een zuurstofrijke omgeving werd geen conversie gevonden. Door deze vinding werd contaminatie met zuurstof beschouwd als waarschijnlijke oorzaak voor de deactivering. De bron van deze contaminatie is tot nu toe nog niet gevonden.

In **Hoofdstuk vijf** werd een bijproject uitgevoerd waarin difosfine liganden, die een secundaire amine groep bevatten, gekoppeld werden aan diverse dragermoleculen. De gebruikte koppelmethode was een palladium-gekatalyseerde aminekoppeling aan de drager moleculen die waren gefunctionaliseerd met aryl bromide groepen. Met deze methode werden Nixantphos en PPM gekoppeld aan een model dragermolecuul en aan een tweede-generatie polyfenyleen dendrimeer. Daarnaast werd ook de nucleofiele substitutie reactie gebruikt, beschreven in hoofdstuk twee, om de genoemde liganden te immobiliseren. Vergelijking van het oorspronkelijk Nixantphos ligand met de geïmmobiliseerde versie in rhodium-gekatalyseerde hydroformylings reactie gaf constant, hoge selectiviteiten maar liet een kleine variatie in activiteit zien.

Alternatieve koppelmethoden werden getest in **Hoofdstuk zes**. De Suzuki koppeling werd getest in de koppeling van boorzuur derivaten van de PCP-liganden met aryl halide groepen op de dragermoleculen en *vice versa*. Nauwkeurige analyse van de producten liet zien dat niet de bedoelde koppeling de hoofdreactie was, maar een palladium-gekatalyseerde dehalogeneringsproces. Vervolgens werd de koppelingsreactie van een fenolisch PCP-ligand met de aryl halide groepen op het drager molecuul onderzocht, dit is de zogenaamde Ullmann diaryl ether synthese. Met behulp van deze reactie werden drie verschillende PCP-ligandsystemen gesynthetiseerd. Bij karakterisering van de producten met behulp van MALDI-TOF, bleek dat er naast de gewenste producten ook nog onvolledig gefunctionaliseerde intermediairen in het reactiemengsel aanwezig waren. Het was onmogelijk het product te scheiden van het mengsel door middel van "size-exclusion" chromatografie.

## Curriculum Vitae

De schrijver van dit proefschrift werd geboren op 4 september 1976 te Harderwijk. De middelbare school werd afgesloten in 1991 aan de HAVO “Groevenbeek” te Ermelo. In 1997 behaalde hij zijn diploma (hoofdrichting organische chemie) van het Hoger Laboratorium Onderwijs (HLO) in Arnhem na een stageperiode bij Akzo Nobel in Deventer. Tijdens dit onderzoek werd de metaalverdeling van “Bi-supported Ziegler-Natta katalysatoren” verbeterd. Na het HLO startte hij een studie scheikunde aan de Katholieke Universiteit van Nijmegen waar hij een afstudeerstage heeft gedaan onder supervisie van prof.dr. B. Zwanenburg, in de organische chemie. Diverse varianten van bis-oxazoline liganden werden gesynthetiseerd en getest in koper-gekatalyseerde asymmetrische cyclopropaneringsreacties. Eind 1999 ontving hij zijn bul. Aan het begin van het nieuwe millennium begon de schrijver zijn promotieonderzoek aan de Technische Universiteit van Eindhoven bij prof.dr. D. Vogt. Tijdens dit onderzoek werden de mogelijkheden van continu uitgevoerde homogene katalyse onderzocht. Op 21 april 2004 werd dit onderzoek afgesloten met een promotie.

The writer of this thesis was born on September 4, 1976, in Harderwijk (The Netherlands). He finished the secondary school at the HAVO “Groevenbeek” in Ermelo in 1991. In 1997 he graduated at the HLO (higher vocational education) of Arnhem after an internship at Akzo Nobel Deventer. During this practical period he improved the metal distribution of “Bi-supported Ziegler-Natta Catalysts”. After the HLO he started to study chemistry on the Catholic University of Nijmegen. The writer performed his undergraduate project in organic chemistry in the group of prof.dr. B. Zwanenburg. During this project, a variety of bis-oxazoline ligands were synthesized and tested in copper-catalyzed asymmetric cyclopropanation reactions. At the end of 1999 he received his Master of Science degree. At the start of the new millennium the writer started his doctoral research on the Eindhoven University of Technology in the group of prof.dr. D. Vogt. During this investigation the possibilities of continuous homogeneous catalysis were explored. On April 21, 2004, this research will be closed with a promotion ceremony.